

The Role of Heparan Sulfate Proteoglycans and Heparanase in the Control of Vascular Remodeling

by

Aaron B. Baker

B.S.E. Bioengineering
University of Washington (1999)

M.S.E. Bioengineering
University of Washington (2000)

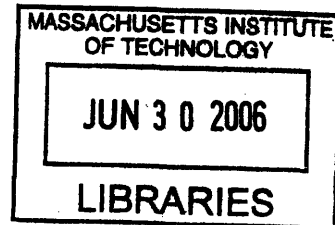
S.M. Biological Engineering
Massachusetts Institute of Technology (2002)

Submitted to the division of Health Sciences and Technology in
Partial Fulfillment of the Requirements for the Degree of

Doctor of Philosophy in Biomedical Engineering
at the
MASSACHUSETTS INSTITUTE OF TECHNOLOGY

May 2006

[June 2006]



©2006 Massachusetts Institute of Technology. All rights reserved.

ARCHIVES

The author hereby grants to MIT permission to reproduce and to distribute
publicly paper and electronic copies of this thesis document in whole or in part.

Signature of Author

[Handwritten signature]

Division of Health Science and Technology

Certified by

[Handwritten signature]

Elazer R. Edelman

Thomas D. and Virginia W. Cabot Professor
Division of Health Sciences and Technology

Accepted by

[Handwritten signature]
Martha L. Gray, Ph.D.
Edward Hood Taplin Professor of Medical and Electrical Engineering
Director, Harvard-MIT Division of Health Sciences and Technology

The Role of Heparan Sulfate Proteoglycans and Heparanase in the Control of Vascular Remodeling

By

Aaron B. Baker

Submitted to the Division of Health Science and Technology
on May 25, 2006 in Partial Fulfillment of the Requirements for the Degree of
Doctor of Philosophy in Biomedical Engineering

ABSTRACT

Arterial remodeling is a major pathophysiological mechanism underlying clinical cardiovascular disorders such as hypertension, atherosclerosis and restenosis. We examined heparan sulfate proteoglycan homeostasis as a mechanism of regulation of arterial vascular remodeling in response to altered mechanical environments such as hypertension and injury. We first studied the effect of in-vitro mechanical strain on the ability of endothelial cells to inhibit vascular smooth muscle cell proliferation. Under these conditions we found mechanical strain increased endothelial inhibition of smooth muscle cell proliferation through increased production of heparan sulfate proteoglycans. Using inhibitors to p38 MAPK and ERK, we showed that activation of both of these pathways was essential for load-induced heparan sulfate production, TGF- β 1 activation, smad-2 activation and increased FGF-2 uptake. Further, we exposed cells to strain in the presence of a neutralizing antibody to TGF- β 1 and demonstrated that autocrine TGF- β 1 signaling was essential for load-induced HSPG production and sustained p38 MAPK and ERK activation. We also examined the endothelium of spontaneously hypertensive rats using immunohistochemical staining for heparan sulfate proteoglycan core proteins, TGF- β 1 and phosphorylated signaling intermediates and found results that correlated well with our in-vitro experiments. Taken together these results imply a novel paradigm of vascular remodeling to mechanical stimuli in which net arterial remodeling is controlled by the dynamic interplay between pro-growth signals from vascular smooth muscle cells and anti-growth signals from endothelial cells.

In a second portion of this work, we examined the role of heparanase in vascular remodeling. Using siRNA gene silencing and overexpression techniques, we showed that alterations in heparanase expression lead to a profound modulation in endothelial inhibition of vascular smooth muscle cell proliferation. In vivo, we quantified heparanase expression in animal models of hypertension, vascular disease and injury. Immunohistochemical analysis of the aortae of hypertensive rats revealed an increase in endothelial production of heparanase that strongly correlated with increased aortic structural remodeling. Studies of vascular injury with stenting in the Zucker rat model of diabetes showed a relationship between neointimal heparanase expression and lesion thickness. Our results define a new role for heparanase as a key molecular controller of vascular remodeling in diverse disease states.

Thesis Supervisor: Elazer R. Edelman

Title: Thomas D. and Virginia W. Cabot Professor, Division of Health Sciences and Technology

Acknowledgements

The author would like to thank the many people who made this thesis possible. I am, first and foremost, heavily indebted to Elazer for his understanding, support and guidance throughout my thesis. One goes through many low points in the long course of a graduate education and our discussions about life and science have always renewed and sustained my enthusiasm for an academic career. Elazer's dedication to his students and his family has truly set him apart as a great role model and mentor for me.

I would also like to thank the many members of the Edelman lab for creating a great environment in which to do research. In particular I would like to thank David Ettenson for his help teaching me the basics of practical cell biology and for providing a sounding board for my ideas. I would like to thank David Wu for first getting me interested in heparan sulfate proteoglycans and for broadening my scientific horizons. To the histology crew, Phil, Gee, and Leslie I would like to thank you for all your hard work and help. I am indebted to Michael Jonas and Adam Groothuis for taking my thesis into other models of vascular remodeling—without their help this work not have been possible. To my many friends in the Edelman lab, I would like to express my gratitude to all of you for providing entertainment and comradery through the years.

One could not imagine a more ideal thesis committee for this work. In particular I would like to thank both Professors Ram Sasisekharan and Matt Nugent for their expertise and enthusiasm for my work as well as Professor Martha Gray for always asking the tough fundamental question and for the loan of the mechanical loading device.

I would especially like to thank my friends and family who have helped to make this thesis possible. Your support and belief in me has helped me make it through and remain young in the process. Most of all, I would like to express my gratitude to my parents for their unconditional love and support throughout every phase of my life.

To My Mother...

Table of Contents

LIST OF FIGURES	7
LIST OF TABLES	12
CHAPTER 1: INTRODUCTION	13
CHAPTER 2: BACKGROUND	15
VASCULAR WALL MECHANICS AND REMODELING	15
VASCULAR CELL MECHANOTRANSDUCTION	19
TGF- β IN THE VASCULAR SYSTEM	21
HEPARAN SULFATE PROTEOGLYCANS IN THE ENDOTHELIAL CONTROL OF VASCULAR SMOOTH MUSCLE CELL BIOLOGY	23
<i>Heparan Sulfate Proteoglycans</i>	24
<i>Heparanase in Cancer, Angiogenesis and Vascular Disease</i>	28
CHAPTER 3: REGULATION OF HEPARAN SULFATE PROTEOGLYCANS BY MECHANICAL STRAIN	31
METHODS	32
RESULTS	43
<i>Mechanical strains of 5% Maximal Strain are Not Cytotoxic to Endothelial Cells in Culture</i>	43
<i>Mechanical Strain Increases Endothelial Inhibition of Vascular Smooth Muscle Cell Proliferation</i>	45
<i>Mechanical Strain Increases Production of Heparan Sulfate Proteoglycans</i>	48
<i>Mechanical Strain Activates TGF-β1 through p38 and ERK1/2 Dependant Pathway</i>	63
<i>Mechanical Strain Alters Extracellular Matrix Bound FGF-2 through p38, ERK1/2, and TGF-β1 Mediated Mechanism</i>	66
<i>Mechanotransduction Pathway Controlling Load-Induced Heparan Sulfate Proteoglycans Involves p38/ERK activation and Autocrine TGF-β1 signaling</i>	71
<i>Promoter Analysis of Heparan Sulfate Proteoglycan Core Proteins and Heparanase</i>	76
<i>Inhibition of Transcription Factor Sp1 Leads to Maladaption of Endothelial Cells to Mechanical Strain</i>	76
DISCUSSION	79
CONCLUSION.....	85
CHAPTER 4: ROLE OF HEPARAN SULFATE PROTEOGLYCANS AND HEPARANASE IN SPONTANEOUSLY HYPERTENSIVE RATS	86
INTRODUCTION	86
MATERIALS AND METHODS	87
RESULTS	89
<i>Hypertension Increases Heparan Sulfate Proteoglycan and Heparanase Expression in the Endothelium of Spontaneously Hypertensive Rats</i>	89

<i>Hypertension Alters Transforming Growth Factor-Beta Expression and Phosphorylation State of Intracellular Signaling Intermediates</i>	<i>95</i>
<i>Correlation Analysis of Immunocytochemical Staining</i>	<i>101</i>
DISCUSSION	106
CONCLUSION.....	108
CHAPTER 5: ROLE OF HEPARANASE IN VASCULAR REMODELING	109
INTRODUCTION	109
MATERIALS AND METHODS	109
RESULTS	113
DISCUSSION	129
CONCLUSIONS.....	133
CHAPTER 6: CONCLUSIONS AND FUTURE DIRECTIONS.....	134
REFERENCES.....	136

List of Figures

Figure 1. Histologic slide of typical arterial structure [12].	15
Figure 2. Shear stress in the vascular system A) simplified view of the arterial shear stress profile. B) Magnitude of shear stress in various vascular conduits [12].	16
Figure 3. Types of vascular remodeling (adapted from [14]).	17
Figure 4. Molecular mechanisms of mechanotransduction [15].	19
Figure 5. Molecular components of a focal adhesion complex [20].	20
Figure 6. TGF- β Signaling Pathway [60].	23
Figure 7. Molecular structure of heparan sulfate glycosaminoglycan chain [76].	24
Figure 8. The biosynthesis of heparan sulfate [77].	25
Figure 9. Structural domains of perlecan [3].	26
Figure 10. Heparanase cleavage site within heparan sulfate and associated molecules released by heparan sulfate degradation [100].	28
Figure 11. Diagram of mechanical device for applying strain to cells in-vivo [127].	34
Figure 12. Photograph of mechanical device for applying strain to cultured cells.	35
Figure 13. Flow diagram for analysis of glycosaminoglycans. C.ase = Chondroitinase. Size Excl. Chrom. = Size Exclusion Chromatography. Ion Exchange Chrom. = Ion Exchange Chromatography.	39
Figure 14. Lactate dehydrogenase (LDH) release relative to static cultures in response to mechanical strain.	44
Figure 15. Inhibition of vascular smooth muscle cell proliferation by human umbilical endothelial cell conditioned media. “Control media” has not been exposed to endothelial cell. “No strain” is conditioned medium from endothelial cells that are under static conditions. “Five percent strain” is conditioned medium from endothelial cells exposed to mechanical load for 24 hrs. Results are mean + standard deviation, * $p < 0.05$ versus 5% control media; ** $p < 0.05$ versus no strain and control media; $n = 5-12$.	46
Figure 16. Inhibition of vascular smooth muscle cell proliferation by bovine aortic endothelial cell conditioned media. Five percent calf serum is control media that has not been exposed to endothelial cells. No strain is endothelial cell conditioned medium (ECCM) from endothelial cells that are under static conditions. Three or five percent strain is conditioned medium from endothelial cells exposed to mechanical load for 24 hrs at either 3% or 5% maximal strain. All comparisons have $p < 0.05$.	47
Figure 17. Western blot for HSPG core proteins, heparanase and the transcription factor Sp1 from endothelial cells exposed to 5% cyclic strain for 24 hrs. β -actin are from cell lysate samples. Perlecan is from conditioned medium. Results are mean + standard deviation, * $p < 0.05$ versus 5% control media; $n = 3-4$.	49
Figure 18. Real time PCR analysis of alterations in syndecan gene expression. Values are normalized to No Strain controls. HPA = Heparanase.	51
Figure 19. Total proteoglycans in endothelial cell conditioned media labeled with ^3H -glucosamine and separated by ion exchange chromatography. Samples treated with	

5% strain (dashed line) and no strain (solid line) are shown with the applied salt gradient (dotted line) on the second axis.	53
Figure 20. Heparan sulfate proteoglycans in the endothelial conditioned media labeled with ³ H-glucosamine and separated by ion exchange chromatography. Samples treated with 5% strain (solid line) and no strain (dashed line) are shown with the applied salt gradient (dotted line) on the second axis.	54
Figure 21. Total proteoglycans on the endothelial cell surface labeled with ³ H-glucosamine and separated by ion exchange chromatography. Samples treated with 5% strain (dashed line) and no strain (solid line) are shown with the applied salt gradient (dotted line) on the second axis.	55
Figure 22. Heparan sulfate proteoglycans on the endothelial cell surface labeled with ³ H-glucosamine and separated by ion exchange chromatography. Samples treated with 5% strain (dashed line) and no strain (solid line) are shown with the applied salt gradient (dotted line) on the second axis.	56
Figure 23. Total and isolated heparan sulfate proteoglycans in the endothelial conditioned media labeled with ³ H-glucosamine and separated by ion exchange chromatography (normalized to no strain, * comparison of p < 0.05).	57
Figure 24. Total proteoglycans in the endothelial conditioned media labeled with ³ H-glucosamine separated by size exclusion chromatography. Representative samples treated with 5% strain (dashed line) and no strain (solid line) are shown.	59
Figure 25. Heparan sulfate proteoglycans in the endothelial conditioned media labeled with ³ H-glucosamine separated by size exclusion chromatography. Representative samples treated with 5% strain (dashed line) and no strain (solid line) are shown. .	60
Figure 26. Cell surface total proteoglycans on the endothelial cell surface labeled with ³ H-glucosamine separated by size exclusion chromatography. Representative samples treated with 5% strain (dashed line) and no strain (solid line) are shown. .	61
Figure 27. Cell surface heparan sulfate proteoglycans on the endothelial cell surface labeled with ³ H-glucosamine and separated by size exclusion chromatography. Representative samples treated with 5% strain (dashed line) and no strain (solid line) are shown.	62
Figure 28. Active TGF-β in endothelial cell conditioned media after 24 hrs of mechanical strain or static conditions measured by ELISA assay.	64
Figure 29. Total TGF-β in endothelial cell conditioned media after 24 hrs of mechanical strain or static conditions measured by ELISA assay. Total TGF-b was activated by treatment with acid pH prior to ELISA assay.	65
Figure 30. Fibroblast growth factor-2 (FGF-2) extracted from the extracellular matrix of endothelial cultures pretreated for 1 hr with U0126 or SB 293063 and exposed to 24 hrs of static or strain conditions.	67
Figure 31. Fibroblast growth factor-2 (FGF-2) in the conditioned media of culture pretreated with U0126 or SB 293063 for 1 hr and exposed to static or strain conditions for 24 hrs.	68
Figure 32. A neutralizing antibody to TGF-β reduces blocks the load induced decrease in extracellular matrix (ECM) bound FGF-2. Endothelial cells were treated with a neutralizing antibody for 1 hr prior to exposure to 24 hrs of 5% mechanical strain.	69

Figure 33. The content of the conditioned media is unaffected by mechanical strain or a TGF- β neutralizing antibody. Endothelial cells were treated with a neutralizing antibody for 1 hr prior to exposure to 24 hrs of 5% mechanical strain.	70
Figure 34. Western blot analysis of intracellular signaling intermediates of the TGF- β , MAPK, and p38 MAPK pathways. Cells were pretreated with the indicated inhibitors for 1 hr prior and during exposure to static or mechanical strain conditions for 24 hrs.	73
Figure 35. Western blot analysis of intracellular signaling intermediates of the TGF- β , MAPK, and p38 MAPK pathways. Cells were pretreated with the neutralizing antibody for 1 hr prior and during exposure to static or mechanical strain conditions for 24 hrs.	74
Figure 36. Western blot analysis of heparan sulfate core proteins and heparanase. Cells were pretreated with the indicated inhibitors or neutralizing antibody for 1 hr prior and during exposure to static or mechanical strain conditions for 24 hrs.	75
Figure 37. Mithramycin and mechanical load together cause cell detachment and lactate dehydrogenase (LDH) release. (a) Phase contrast microscopy of cells treated with combinations of load and mithramycin. (b) Total LDH release into culture media of treated cell cultures (normalized to no strain controls).....	77
Figure 38. Control of perlecan and heparanase (HPA) expression by mechanical strain in mithramycin treated cells.	78
Figure 39. Overall mechanistic scheme of endothelial control of vascular remodeling to mechanical stimuli. This study supports the signaling network outlined underneath the endothelial cell portion of this scheme.	84
Figure 40. Hematoxylin and eosin staining of Wistar-Kyoto (WKY) and spontaneously hypertensive (SHR) rat aortae.	91
Figure 41. Immunohistochemical staining for heparan sulfate epitopes in Wistar-Kyoto (WKY) and spontaneously hypertensive (SHR) rat aortae. *Statistically significant comparison ($p < 0.05$).	92
Figure 42. Immunohistochemical staining for heparanase in Wistar-Kyoto (WKY) and spontaneously hypertensive (SHR) rat aortae. *Statistically significant comparison ($p < 0.05$).	93
Figure 43. Quantitative morphometry of vessel remodeling in SHR and WKY rats. Correlation between medial thickening and endothelial heparanase expression in SHR (■) and WKY (□) rats.	94
Figure 44. Immunohistochemical staining for TGF- β in Wistar-Kyoto (WKY) and spontaneously hypertensive (SHR) rat aortae (* $p < 0.05$, $n = 4$).	96
Figure 45. Immunohistochemical staining for phosphorylated Smad-2 in Wistar-Kyoto (WKY) and spontaneously hypertensive (SHR) rat aortae (* $p < 0.05$, $n = 4$).	97
Figure 46. Immunohistochemical staining for phosphorylated p38 in Wistar-Kyoto (WKY) and spontaneously hypertensive (SHR) rat aortae (* $p < 0.05$, $n = 4$).	98
Figure 47. Immunohistochemical staining for phosphorylated ERK in Wistar-Kyoto (WKY) and spontaneously hypertensive (SHR) rat aortae (* $p < 0.05$, $n = 4$).	99
Figure 48. Immunohistochemical staining for transcription factor Sp1 in Wistar-Kyoto (WKY) and spontaneously hypertensive (SHR) rat aortae (* $p < 0.05$, $n = 4$). No counterstain was used in this staining.	100

Figure 49. Correlation scatterplots for statistically significant correlations on the immunohistochemical staining of the endothelium on Wistar-Kyoto and spontaneously hypertensive rats. 103

Figure 50. Correlation scatterplots for statistically significant correlations on the immunohistochemical staining of the endothelium on Wistar-Kyoto and spontaneously hypertensive rats. 104

Figure 51. Photographs of the stenting procedure. A) The femoral arteriotomy prior to catheter insertion and stent placement. B) The stent in the abdominal aorta at time of harvest..... 112

Figure 52. Immunocytochemical staining for heparanase in endothelial cells transfected with a control vector (siCON), a heparanase targeted siRNA vector (siHPA) or a heparanase expression vector (pHPA). Cells were transfected with the various vector, incubated for 48 hrs and then stained using antibody to heparanase and a fluorescently labeled secondary antibody..... 115

Figure 53. Western blot for heparanase in endothelial cells transfected with a control vector (siCON), a heparanase targeted siRNA vector (siHPA) or a heparanase expression vector (pHPA). Cells were transfected with the various vector, incubated for 48 hrs, lysed and subjected to Western blot analysis..... 116

Figure 54. Vascular smooth muscle cell proliferation when exposed to endothelial cell conditioned medium from cells transfected with a control vector (siCON), a heparanase targeted siRNA vector (siHPA) or a heparanase expression vector (pHPA)..... 118

Figure 55. Total proteoglycans in endothelial cell conditioned media separated by ion exchange chromatography. Cells transfected with a control vector (black line), a heparanase targeted siRNA vector (blue line) or a heparanase expression vector (red line). The applied salt gradient (dotted line) on the second axis. 120

Figure 56. Heparan sulfate proteoglycans in endothelial cell conditioned media separated by ion exchange chromatography. Cells transfected with a control vector (black line), a heparanase targeted siRNA vector (blue line) or a heparanase expression vector (red line). The applied salt gradient (dotted line) on the second axis. 121

Figure 57. Total proteoglycans on the endothelial cell surface separated by ion exchange chromatography. Cells transfected with a control vector (black line), a heparanase targeted siRNA vector (blue line) or a heparanase expression vector (red line). The applied salt gradient (dotted line) on the second axis..... 122

Figure 58. Heparan sulfate proteoglycans on the endothelial cell surface separated by ion exchange chromatography. Cells transfected with a control vector (black line), a heparanase targeted siRNA vector (blue line) or a heparanase expression vector (red line). The applied salt gradient (dotted line) on the second axis. 123

Figure 59. Hematoxylin and eosin staining of histological sections of the stented abdominal aorta..... 125

Figure 60. Elastic fiber (Verhoff Van Geisen) staining of histological sections of the stented abdominal aorta. 126

Figure 61. Immunohistochemical staining for heparanase of histological sections of the stented abdominal aorta. 127

Figure 62. Correlation analysis comparing lesion thickness with heparanase staining.
Correlation between medial thickening and endothelial heparanase expression in
SHR (■) and WKY (□) rats. 128

List of Tables

Table 1. Classification of Blood Pressure in Adults..... 86
Table 2. Correlation Analysis of Immunohistochemical Staining of the Endothelium.. 102
Table 3. Correlation Analysis of Immunohistochemical Staining of the arterial media. 105

Chapter 1: Introduction

The vascular endothelium is comprised of a single layer of cells situated between the blood and the solid tissues of the body. In recent years, this thin layer of cells has been shown to be a dynamic constituent of the vascular system, exerting remarkable control over such diverse process as hemostasis, inflammation, and regulation of vascular tone. As a consequence of its unique location, the vascular endothelium is exposed to a distinct mechanical environment consisting of hemodynamic shear stress and mechanical stretch from blood pressure. Vascular homeostasis requires that endothelial cells must respond to their mechanical environment and regulate appropriate changes in arterial structure. In this work, we examine the role of heparan sulfate proteoglycans in the control of vascular remodeling.

Previous work has found that heparan sulfate proteoglycans are powerful, ubiquitous sensors of cardiovascular injury and mediators of cardiovascular health. These complex molecules are composed of a core protein covalently coupled to one or more heparan sulfate glycosaminoglycan chains. The heparan sulfate chains consist of a linear polymer of alternating disaccharide units heterogeneously modified by epimerization, deacetylation, and sulfation[1] to create an intricate molecular structure with an information capacity far exceeding that of nucleic acids [2]. Heparan sulfate is known to interact with a wide variety of proteins ranging from growth factors and cytokines to various enzymes and extracellular matrix molecules [3, 4].

Endothelial cells are known to be the major source of extracellular HSPG in arteries. The large extracellular proteoglycan perlecan has been shown to be a potent inhibitor of vascular smooth muscle cell proliferation [5] and a key component in

endothelial control of vSMC proliferation[6]. In addition to perlecan, endothelial cells and vSMCs express several cell surface HSPG including transmembrane proteoglycans syndecan-1, -2, and -4 as well as glypican-1[7]. The syndecans have been shown to be important in stabilizing the binding of FGF-2 to the FGFR and serve as a low affinity receptor for FGF capable of independent signaling[8-10]. In addition, the syndecans also have an emerging role in cell adhesion, cytoskeletal arrangement, and intracellular signaling [11].

In this thesis, we examined heparan sulfate proteoglycan homeostasis as major mechanism of endothelial regulation of arterial vascular remodeling. We first examined the role of mechanical forces in regulating the endothelial inhibition of vSMC proliferation and explored two potential mechanisms including the regulation of heparan sulfate proteoglycans and activation of TGF- β 1 under mechanical strain conditions. Through these studies we discovered that autocrine TGF- β 1, ERK1/2 and p38 MAPK were required for the increased production of perlecan induced by mechanical strain. Further we examine the aortae of hypertensive animals and immunostained for various components suggested by our in-vitro work.

While heparanase has received much attention as an enzyme involved in angiogenesis and cancer metastasis, its role in macrovascular disease and remodeling is relatively unexplored. To examine the role of heparanase expression in the vascular system we developed methods to knock-down and overexpress heparanase in endothelial cells. Further we examined heparanase expression in several models of vascular disease and injury. Our results supports the hypothesis that heparanase represent a key control point of vascular remodeling in diverse disease states.

Chapter 2: Background

Vascular Wall Mechanics and Remodeling

A short review of vascular anatomy is essential in understanding the mechanics of large vessels. The aorta is an elastic artery consisting of three major layers: the tunica intima, the tunica media and the tunica adventitia (shown in Figure 1 [12]). In non-injured, non-diseased arteries the intima consists of the endothelium and its underlying basement membrane. In injury and disease, vascular smooth muscle cells and immune cells migrate to form the neointima. The media

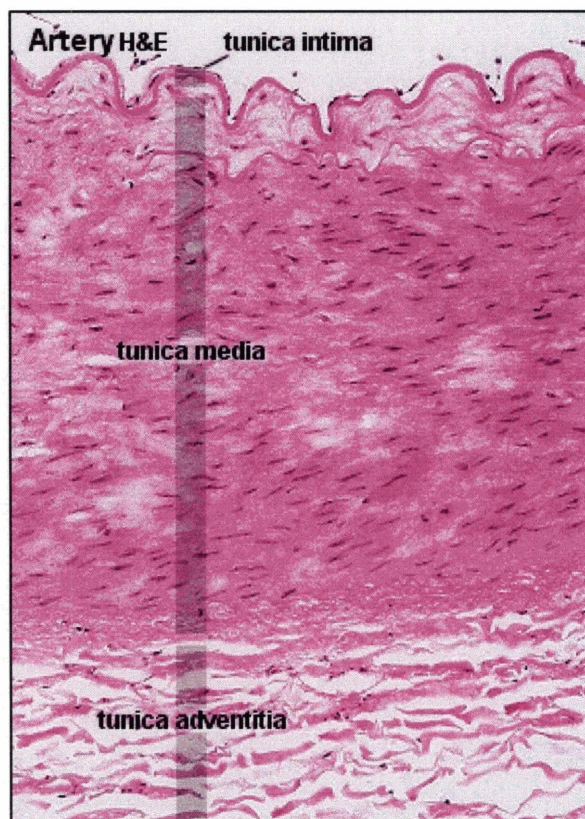


Figure 1. Histologic slide of typical arterial structure [12].

consists of vascular smooth muscle cells and organized layers of elastin known as the elastic laminae. These laminae give the aorta its characteristic elastic properties. The adventitia is composed of collagen and elastin with the appearance of loose connective tissue.

The vascular system is unique in its function of maintaining the regulated separation of blood components from the solid tissue of the body. As a consequence of this unique location, blood vessels are exposed to hemodynamic stresses from blood flow

and pressure. On the simplest level the artery can be considered an isotropic thin-walled vessel, leading to the familiar constitutive relationship:

$$\epsilon_h = \frac{\sigma_h}{E} = \frac{pr}{Et}$$

where ϵ_h is hoop (circumferential) strain, σ_h is hoop stress, p is transmural pressure, E is Young's modulus, r is vessel radius, and t is vessel thickness. In actuality, the stress-strain relation in arteries must account for the vessel anisotropy, vascular smooth muscle tone, and nonlinear elastic relations of vessel components [13]. Vascular cells are also subjected to wall shear stresses resulting from fluid flow. The simplest model of vascular flow would be to assume laminar, steady fluid flow governed by Poiseuille's Law (shown in Figure 2 below) with a parabolic fluid velocity regime. Actual fluid flow in arteries is made more complex by pulsatility, alterations in viscosity with fluid velocity, and the elasticity of the arterial wall.

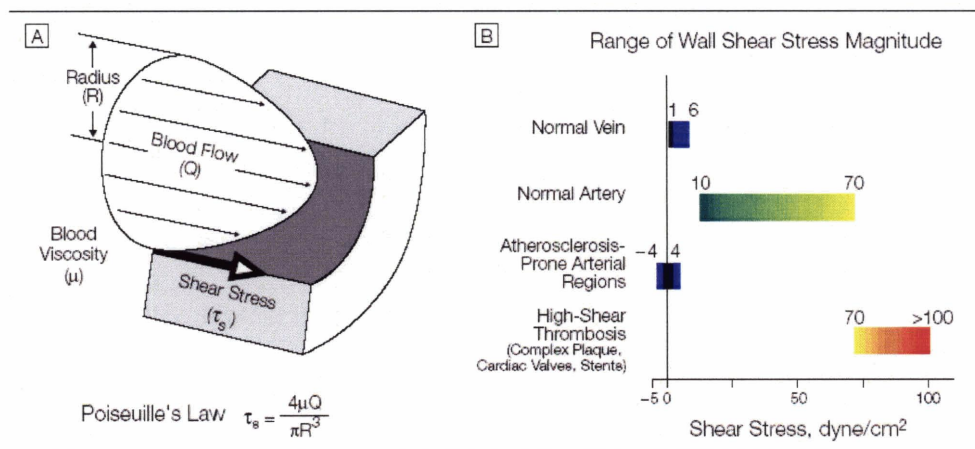


Figure 2. Shear stress in the vascular system A) simplified view of the arterial shear stress profile. B) Magnitude of shear stress in various vascular conduits [12].

Vascular remodeling represents both a normal healthy response to the body's changing hemodynamic needs and an underlying mechanism fundamental to most vascular disorders. There is a spectrum of vascular response depending on the stimulus and underlying disease processes (illustrated in Figure 3). While various cell types can participate in the remodeling process, endothelial cells are particularly well positioned to control these processes. Endothelial cells are able to control vascular tone, smooth muscle cell growth, immune cell adhesion and invasion, and are directly exposed to the hemodynamic and chemical milieu of the blood. Thus these cells are optimally situated as both sensors and effectors of the vascular remodeling process [14].

Shear stress from fluid flow is a powerful modulator of arterial remodeling. The vascular system normally maintains a shear stress of about 10-15 dynes cm^{-2} on the vascular wall regardless of location within the vascular tree [15]. One model used to

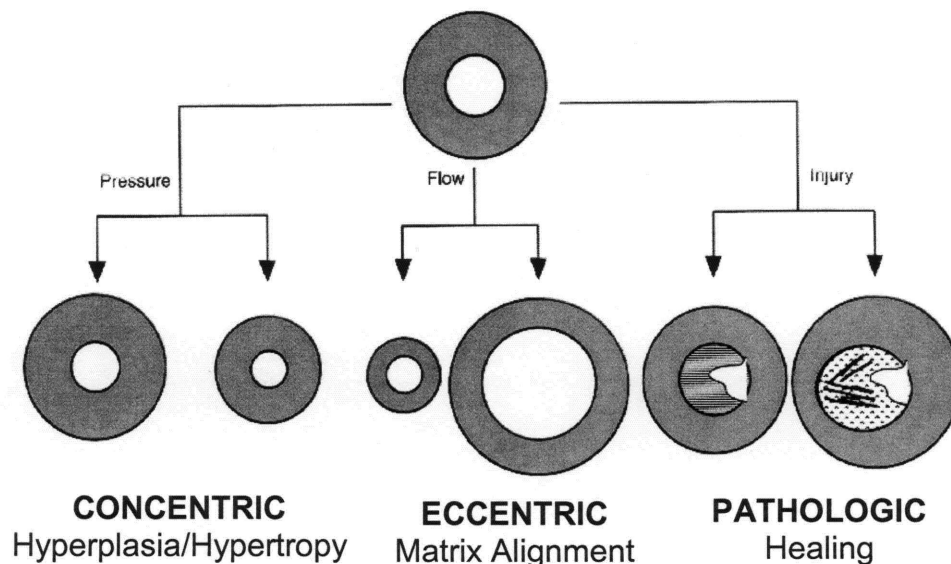


Figure 3. Types of vascular remodeling (adapted from [14]).

study this phenomema is the arteriovenous fistula which allows the flow rate to be increased by a factor of 8 within an artery. In response to this stimulus the vessel remodels by increasing its diameter, both through vascular smooth muscle cell relaxation and matrix remodeling involving matrix metalloproteases (MMPs) [16]. Blood pressure causes circumferential stress on the artery and likewise has a strong influence on arterial remodeling. Similar to shear stress, the physiology of the body maintains an approximately constant value (around $2 \cdot 10^6$ dynes cm^{-1}) of circumferential stress independent of location in the arterial tree. The vessel maintains this stress by regulating the thickness of the artery through vascular smooth muscle hypertrophy, proliferation and matrix synthesis [15].

Clinically, arterial stiffness increases with age and various disease states. These disease states themselves are associated with increased cardiovascular risk, so a fundamental question is whether stiffness is a marker or a direct causal agent in the development of vascular disease [17]. Recent studies have shown that components of the extracellular matrix can directly affect the development of hypertension, supporting a direct role for arterial stiffness in modulation of blood pressure [18].

Vascular Cell Mechanotransduction

Underlying the vascular response to mechanical stimuli is the fundamental biochemical mechanisms that govern the ability of cells to sense and respond to mechanical stimuli. Molecular mechanisms of cell signaling in response to mechanical stimuli have been the subject of an extensive amount of research (reviewed in [19] and [15]). Many receptors have been found to be responsive to mechanical stimuli in vascular cells (shown in Figure 4). One of the receptor types that has become synonymous with cell adhesion and mechanotransduction is the integrin family of receptors. These cell surface molecules exist as a dimer of an α and β subunit. Each of these pairings has a binding target in the extracellular matrix (e.g. $\alpha_5\beta_1$ for fibronectin). Integrins can become activated by binding their respective ligand and clustering. When activated, integrins bind into a focal adhesion complex consisting of several proteins

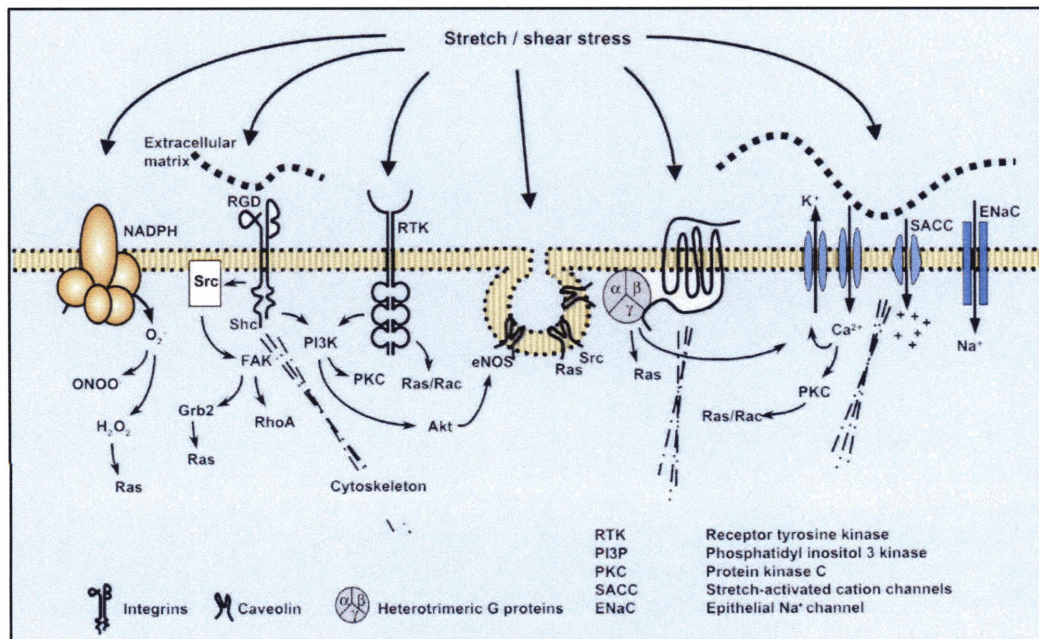


Figure 4. Molecular mechanisms of mechanotransduction [15].

including vinculin, talin and α -actinin (Figure 5) [20]. When cells are stimulated with mechanical force, integrin clustering leads to activation of focal adhesion kinase (FAK) [21-23] through c-Src [24] and possibly Rho A [25, 26]. Many studies support the involvement of mitogen-activated protein (MAP) kinase cascades in the mechanotransduction process. Cyclic stretch has been shown to activate ERK1/2 and JNK pathways in vascular smooth muscle cells both in-vitro [27] and in-vivo [28]. The p38 MAPK has also been implicated in the response to cyclic stress [29] and fluid shear stress [30]. The mechanistic step between FAK activation and MAPK or other cell signaling pathways remains elusive. Many pathways have been implicated but are highly dependent on the model of mechanical load being used. These include activation of G

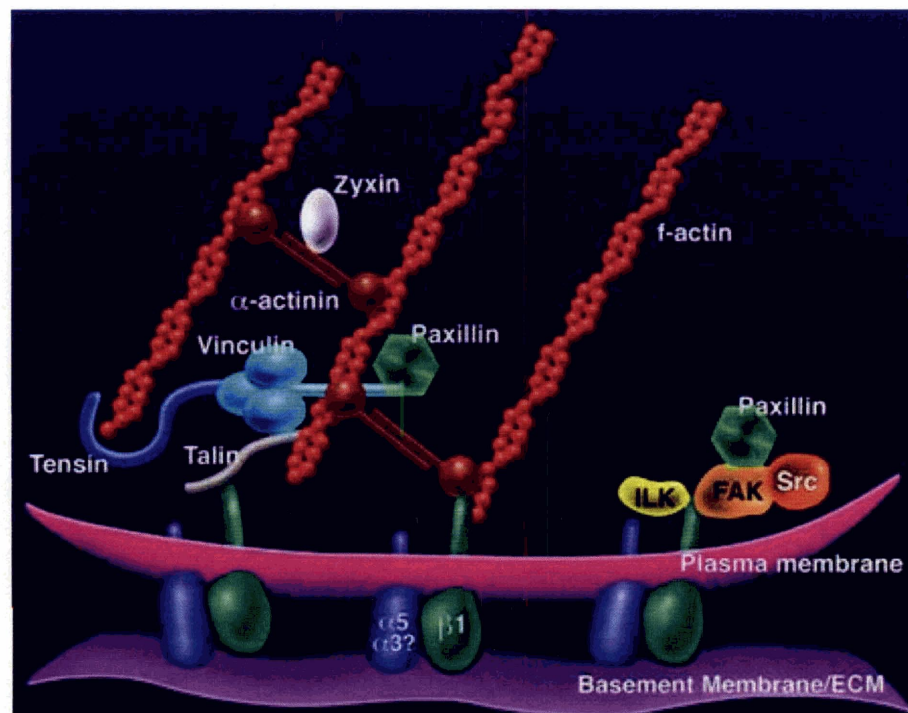


Figure 5. Molecular components of a focal adhesion complex [20].

proteins [19, 31], receptor tyrosine kinases [32], epidermal growth factor receptor [33] and generation of reactive oxygen species [29].

Multiple transcription factors have been implicated in the response of vascular cells to stretch and shear stresses. Elevated activity of NF- κ B and associated genes has been found in-vitro and in regions of disturbed flow in-vivo [34, 35]. The transcription factor KLF2 has also been implicated in flow response and proinflammatory activation [36, 37]. Depending on the load conformation and cell type, other transcription factors have been found to be involved in the regulation of mechanosensitive genes including Egr-1, Sp1 [38-40], and members of the AP-1 family [41].

TGF- β in the Vascular System

In this thesis we examine the role of transforming growth factor beta (TGF- β) in the mechanotransduction process and the control of heparan sulfate proteoglycan production. Transforming growth factor beta (TGF- β) is a cytokine with diverse functions including the regulation of proliferation, differentiation and survival of many cell types [42]. Specifically, TGF- β has been shown to play an essential role as a modulator of angiogenesis [43, 44], tumor growth [45, 46], and many diseases [47, 48]. A defect in TGF- β signaling has been linked to a hereditary vascular disorder known as Hereditary Hemorrhagic Telangiectasia or HTT [49, 50].

TGF- β is disulfide linked homodimeric protein that is made in latent form and activated by cleavage of a C-terminal polypeptide. This cleavage can occur through multiple mechanisms including proteolytic cleavage by MMPs or plasmin [51, 52], interaction with thrombospondin [53], integrins [54], reactive oxygen species [55], low

pH [56] or heparan sulfate [57]. TGF- β signaling occurs through a heteromeric complex of transmembrane serine/threonine receptors (shown in Figure 6). This complex consists of a high affinity type II receptor which binds to TGF- β and then recruits a type I receptor leading to autophosphorylation of the type I receptor and Smad proteins [58, 59]. Smads are the classical downstream effectors of TGF- β signaling and the question of how these molecules regulate specific genes is the subject of active research [60]. Smads alter transcription through several mechanisms. Firstly, Smads can form a heterotrimeric complex which can translocate to the nucleus and serve directly as a transcription factor [58, 61]. Smads can also affect transcription through Smad interacting transcription factors. These transcription factors have high affinity to a specific sequence of DNA in the gene regulatory region. Smad 2 through 4 have been shown to bind DNA with a less stringent sequence requirement than typical transcription factor and can consequently serve to enhance gene transcription if an appropriate Smad-binding region is in proximity to the binding sequence of the interacting transcription factor [58, 59] (for a summary of interacting transcription factors see [60]). Of particular interest to this work is the fact that when Smad 3 interacts with Sp1 and c-Jun the binding affinity of these factors increases [62, 63]. Smad-Sp1 interactions have been shown to activate TGF- β induced genes including PAI-1, collagen, integrin β 5, and Smad 7 [60].

Other signaling pathways have also been implicated in TGF- β signaling. Specifically, TGF- β has been shown to activate ERK [58, 59] and p38 MAPK [64]. Cross talk occurs through a signaling intermediate interaction with the Smads in the MAPK, Akt, JNK, and cyclin dependent kinase signaling networks (reviewed in [60]).

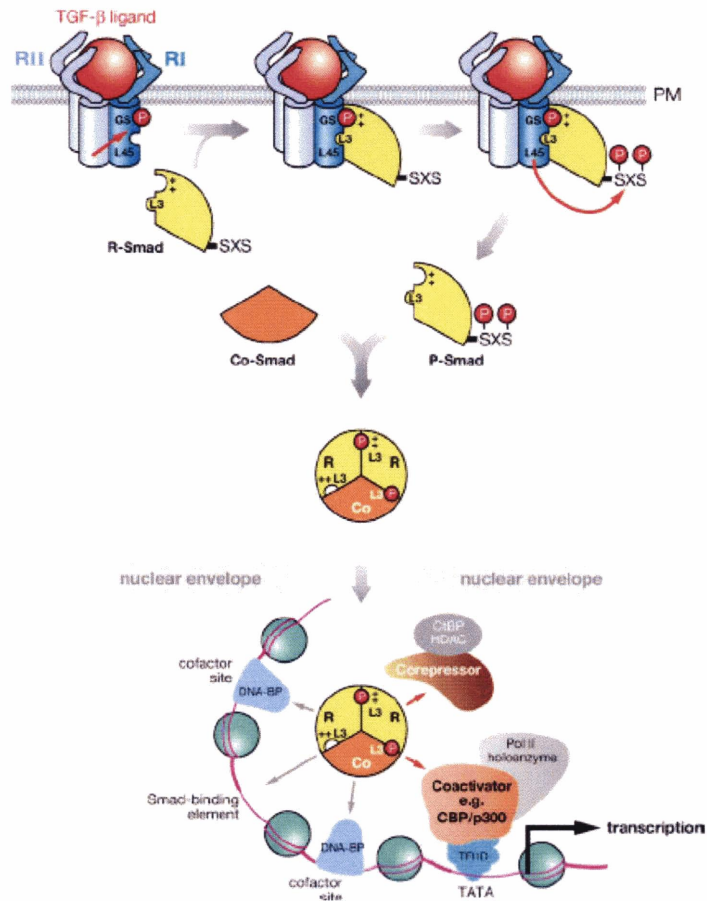


Figure 6. TGF- β Signaling Pathway [60].

Heparan Sulfate Proteoglycans in the Endothelial Control of Vascular Smooth Muscle Cell Biology

In order to control vascular remodeling, endothelial cells secrete a number of compounds that modulate smooth muscle cell growth and proliferation. In this work we examined heparan sulfate proteoglycans and TGF- β , two potent modulators of vascular smooth muscle that have been shown to interact and underlie endothelial inhibition of

smooth muscle cell proliferation. In culture, postconfluent endothelial cells inhibit vascular smooth muscle proliferation whereas subconfluent cultures do not [65-69]. Heparin and heparan sulfate have been shown to inhibit neointimal proliferation in animal models of vascular injury and disease [70-75]. This inhibition is dependant on heparan sulfate proteoglycans but also requires a protein component [6]. In this section we review the relevant aspects of heparan sulfate proteoglycans and their role in the vascular system.

Heparan Sulfate Proteoglycans

Heparan sulfate proteoglycans consist of a core protein covalently linked to one or more heparan sulfate glycosaminoglycan chains. The heparan sulfate chains consist of a linear polymer of alternating disaccharide units heterogenously modified by epimerization, deacetylation, and

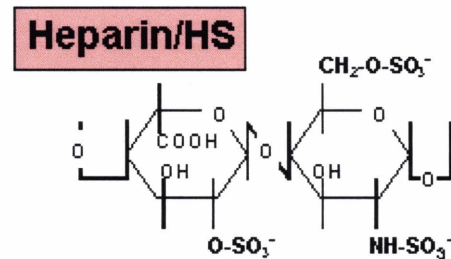


Figure 7. Molecular structure of heparan sulfate glycosaminoglycan chain [76].

sulfation [1] to create an intricate molecular structure (shown in Figure 7) with an information capacity far exceeding that of nucleic acids [2]. Heparan sulfate is known to interact with a wide variety of proteins ranging from growth factors and cytokines to various enzymes and extracellular matrix molecules [3, 4]. In particular, its structure is similar to that of the common anticoagulate drug heparin, but is less modified by sulfation.

The synthesis of HSPGs is complex and not fully understood. Proteins are targeted for glycosylation in the transgolgi by having a particular amino acid sequence Ser-Gly (Ala)-X-Gly (Ala). This site accepts an initial tetrasaccharide synthesized by four

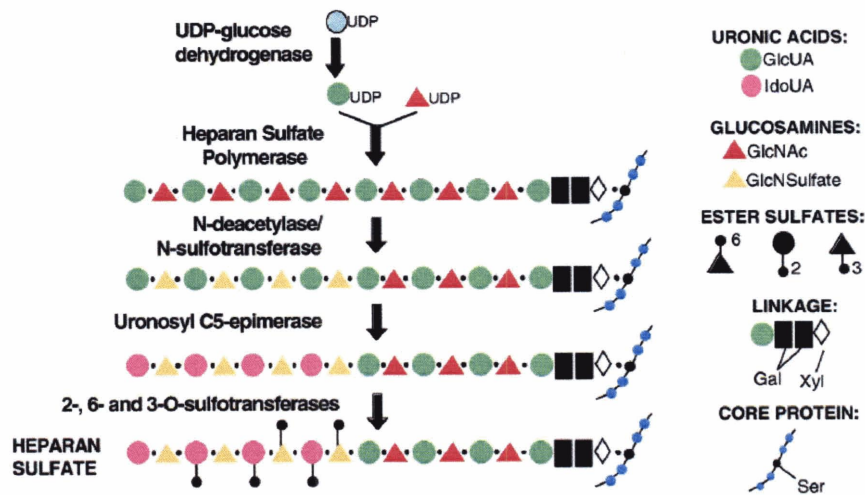


Figure 8. The biosynthesis of heparan sulfate [77].

enzymes [78]. Heparan sulfate synthesis is initiated by the heparan sulfate copolymerase that adds glucuronic acid and *N*-acetylglucosamine to produce the initial heparan sulfate structure (Figure 8). This initial chain is then heterogeneously modified by deacetylation, epimerization and sulfation to create an intricate fine structure [79].

In the vascular system heparan sulfate is found on several core proteins including the perlecans, glypicans, and syndecans. Perlecan is a large heparan sulfate proteoglycan found in the basement membrane. In humans it is the product of the *HSPG2* gene with a molecular weight of 470 kDa and approximately 800 kDa after post-translational glycosylation [3]. It has a modular structure possessing a myriad of interactions with growth factors, extracellular matrix molecules and adhesion molecules (Figure 9). Its name is derived from its “pearls on string” appearance under rotary shadowing electron microscopy [80]. In the vascular system perlecan has been shown to have a role in angiogenesis, atherosclerosis and vascular injury [5, 81].

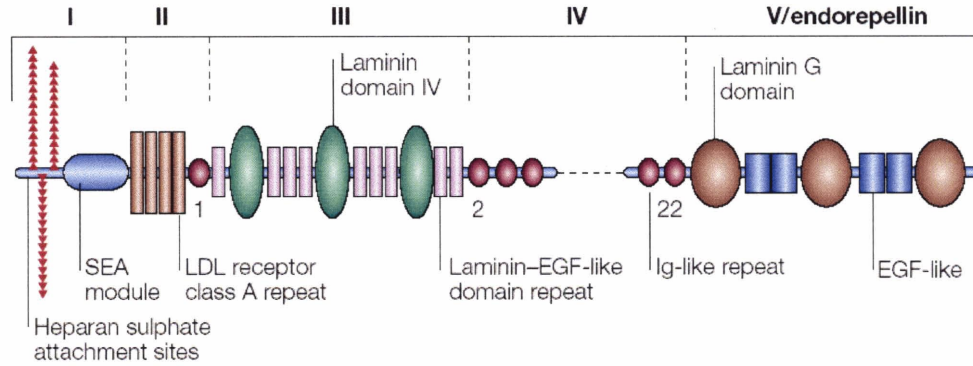


Figure 9. Structural domains of perlecan [3].

The syndecans are a family of transmembrane heparan sulfate proteoglycans found on the cell surface and shed in a soluble form (reviewed in [77]). Each syndecan consists of an extracellular domain that contains glycosaminoglycan attachment sites, a single pass transmembrane domain, and a short cytoplasmic domain with multiple phosphorylation sites. The heparan sulfate and chondroitin sulfate glycosaminoglycan chains allow syndecans to interact with a large number of ligands including FGF-2, VEGF, PDGF and TGF- β [11]. The interaction of syndecans with FGF-2 is probably the most characterized of these interactions. Syndecans and the attached heparan sulfate proteoglycan are essential for effective binding and signaling of the FGF receptor [82]. On the cell surface syndecans stabilize the FGF-2/FGFR complex and are essential for effective signaling [82]. When shed from the surface, syndecan-1 can inhibit FGF-2 induced cell proliferation [83]. However, physiologic degradation of syndecan by heparanase may lead to heparan sulfate fragments that enhance FGF-2 signaling [84]. Syndecan-4 has also been shown to interact with FGF-2 and promote FGF-2 signaling [9]. Recent work has also found that syndecans can act independently of the FGF receptor to act as a transmembrane receptor of FGF [8].

Transforming growth factor- β (TGF- β) has been shown to interact with the heparan sulfate chains on syndecans. Syndecan-2, in particular, has been shown to interact with TGF- β via a protein-protein interaction [85]. The exact nature and role of this interaction is complex and still remains to be elucidated. The presence of syndecan-2 may serve to compete with betaglycan (TGF receptor type III) for the binding of syndectin. Syndectin stabilizes betaglycan on the cell surface and, consequently, syndecan-2 may serve to reduce signaling in the TGF pathway [11, 85].

The syndecans have an intricate role in orchestrating development and are known to be involved in cell-cell and cell-matrix adhesion. Syndecan-1 has been shown to be important for cell adherence to type-I collagen [86]. In addition, syndecan-1 stabilizes the interactions of vitronectin with $\alpha v \beta 3$ integrin [87]. During migration syndecan-1, syndecan-4 and calveolin are directed to the region of cell contraction [88-90]. Syndecan-4 has also been shown to be an essential component for the activation of focal adhesion kinase and is known to bind fibronectin with its heparan sulfate chains [91-93]. In vascular smooth muscle cells exposed to shear stress syndecan-4 has been shown to dissociate from focal adhesions [94].

Several studies have revealed differential regulation of syndecans by various growth factors and cytokines. Fibroblast growth factor-2 (FGF-2) has been shown to increase syndecan-4 expression in vascular smooth muscle cells [95]. Arterial injury and myocardial infarction have also been shown to increase syndecan-4 expression [94, 96, 97]. Stimulation with tumor necrosis factor- α (TNF- α) increases syndecan-2 expression and decreases syndecan-1 in endothelial cells [98]. Transforming growth factor $\beta 2$ increases syndecan-4 and decreases syndecan-1 in epithelial cells [99].

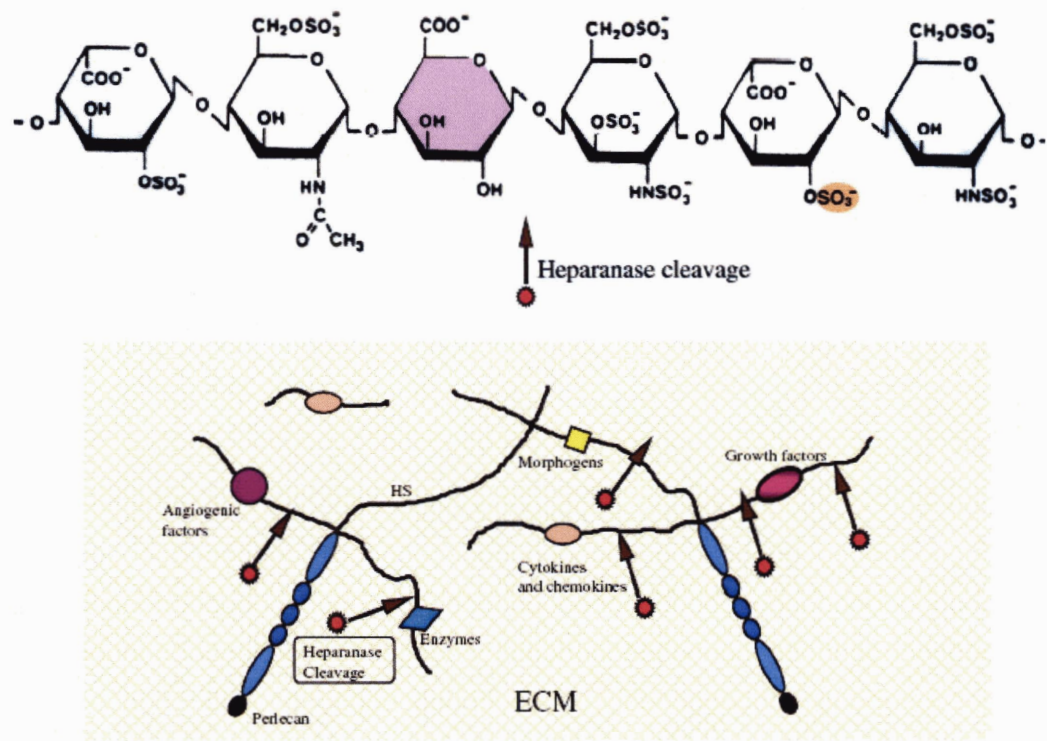


Figure 10. Heparanase cleavage site within heparan sulfate and associated molecules released by heparan sulfate degradation [100].

Heparanase in Cancer, Angiogenesis and Vascular Disease

A major goal of this thesis is to examine the role of heparanase in vascular remodeling. Heparanase is an endo-beta-D-glucuronidase that cleaves at a particular site in heparan sulfate to create fragments that are 10-20 sugar units long and still biologically active [84, 101-103] (Figure 10). While the presence of heparanase-like activity has been known for decades, the gene for heparanase was cloned independently by two groups in 1999 [104, 105]. Tight regulation of heparanase activity is essentially due to the potential

tissue damage that could result from widespread HSPG degradation. The enzyme is synthesized as a 65 kDa zymogen which is cleaved into the active 50 kDa form [105]. The exact regulator of this process is unknown but may potentially include cytokines, local pH, cellular localization and a membrane bound protease [106].

Heparanase is known to be involved in the metastasis of cancer [100].

Degradation of heparan sulfate is an essential step in the extravagation of cells in the blood [107-113]. Heparanase expression correlates strongly with metastasis of cancers cells [102, 104, 110, 114] and heparanase inhibitors significantly reduce the metastatic potential of cells in experimental models [109, 110, 115]. A recent paper has shown that inhibiting heparanase expression using gene silencing techniques reduced metastatic potential of cancer cells and inhibited tumor angiogenesis [116]. Sulfated polysaccharides have been shown to inhibit heparanase (as well as having other activities) and have also been shown to inhibit cancer metastasis [110].

Heparan sulfate and heparanase are also known to play an essential role in angiogenesis. Heparanase expression increases during endothelial cells undergoing angiogenesis versus mature vessels [102]. Further, wound vascularity is enhanced with the topical administration of heparanase [102]. The mechanism behind this relation is though to be the release and induction of angiogenic growth factors by heparanase [102].

While there exists a large body of work examining the role of heparanase in cancer, there are only a limited number of studies that have addressed the role of heparanase in macrovascular biology. Specifically, it has been shown that heparanase-like activity in combination with matrix metalloprotease-9 (MMP-9) is important for a phenotypic change in vascular smooth muscle cells induced by macrophages [117].

Other studies have shown that platelet-derived heparanase can release FGF-2 from the extracellular matrix and lead to vSMC proliferation and migration both in-vivo and in-vitro [118, 119].

Chapter 3: Regulation of Heparan Sulfate Proteoglycans by Mechanical Strain

It is the goal of this portion of the thesis to understand some of the basic mechanisms that control the vascular response to hemodynamic stimuli. Mechanical stress has both positive and negative effects on the artery. The negative effects are illustrated by the clinical outcomes of hypertension including increased risk of stroke and myocardial infarction. Hypertension induces the production of reactive oxygen species and pro-inflammatory factors and has increased plaque formation in animal models [120]. In contrast, mechanical stress also has beneficial effects in terms of atherosclerotic disease. Atherosclerotic plaques are found to form more frequently in arterial regions of disturbed flow or low shear stress when compared to arterial regions of steady laminar flow [121]. High shear stress is known to be a key mediator of this effect by inducing NO synthesis [122] and attenuating VCAM expression [123]. In contrast, oscillatory shear stress causes endothelial cells to express cell surface adhesion molecules and soluble factors that enhance leukocyte recruitment [124].

The specific aim of this section is to identify the role of mechanical stimuli in the endothelial production of inhibitory factors towards vascular smooth muscle cells. This aims to give insight into the fundamental mechanisms by which vascular remodeling is orchestrated by endothelial cells. This work was begun with a simple experiment directed at finding whether mechanical strain served to increase or decrease endothelial inhibition of vascular smooth muscle cells. After identifying two inhibitory molecules

that were modulated by mechanical load we then examined several potential mechanotransduction pathway that were responsible for regulating these alterations.

Methods

Cell Culture. Rat vascular smooth muscle cells (RVSMCs) and bovine aortic endothelial cells (BAECs) were isolated from fresh bovine or rat aortae. These cells were cultured in Dulbecco's Modified Eagle's Medium (DMEM; Invitrogen, Carlsbad, CA) supplemented with 5% calf serum (Hyclone, Logan UT) and 100 units per ml of penicillin, 100 μ g per ml streptomycin sulfate, and 2 mM L-glutamine. Human umbilical vascular endothelial cells (HUVECs, Cambrex, Walkersville, MD) were grown in DMEM with 5% fetal bovine serum (Hyclone) and EGM-2 supplements (Cambrex). All smooth muscle cells were used at passages 4 to 5 and all endothelial cultures were used at passages 3 to 5. All cells were incubated at 37°C in a humidified atmosphere containing 5% CO₂.

Mechanical Strain Application to Cultured Cells. The device to apply mechanical strain to cells has been described previously (shown in Figure 11 and Figure 12) [125]. This device was kindly loaned to us by Professor Martha Gray at MIT. Essentially, this device applies load by pushing a piston through the bottom of a custom culture plate with a flexible silastic membrane as a culture surface. A major advantage of this system over the commercially available Flexcell system is it creates a uniform strain field across most of the silastic membrane [126]. The Flexcell, however creates a heterogeneous strain field with both compressive and tensile regions. The maximal strains from studies using

this device are actually averages of this entire field. Consequently, a 20% maximal strain reported from this device represents a range of actual strains on cells.

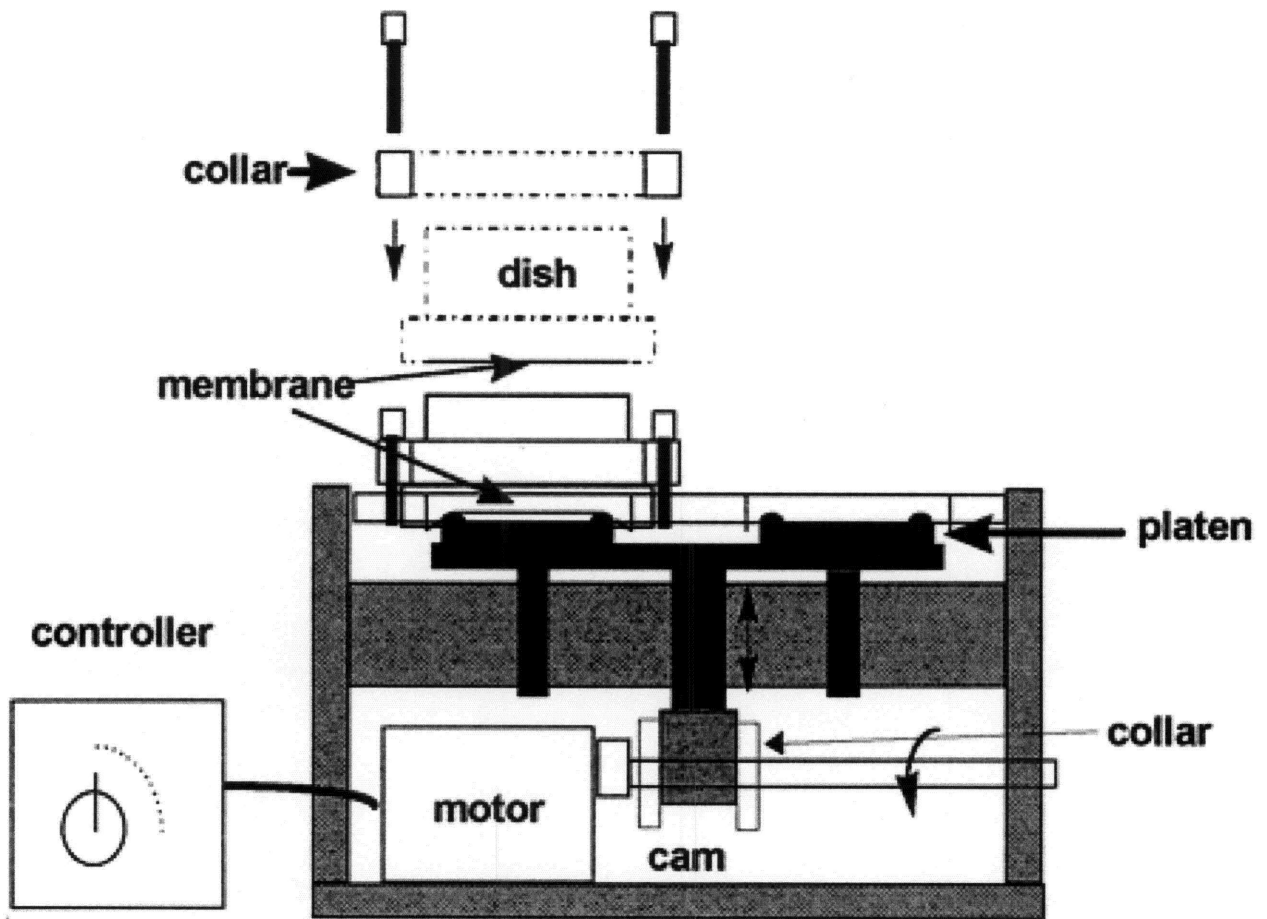


Figure 11. Diagram of mechanical device for applying strain to cells in-vivo [127].

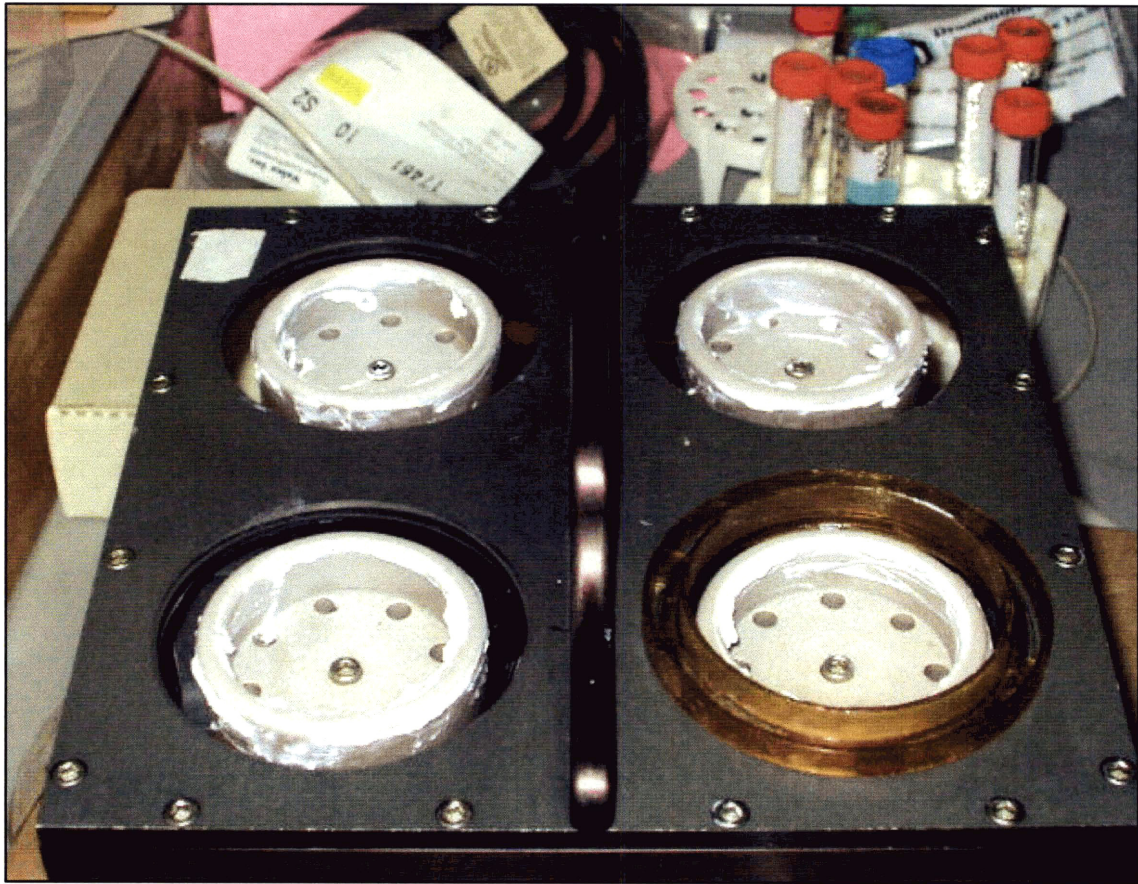


Figure 12. Photograph of mechanical device for applying strain to cultured cells.

We developed a notable addition to the use of this device by creating a manufacturing process for creating disposable cell culture inserts with silastic membrane culture surfaces. This allowed us to create many culture inserts and enabled simultaneous preparation of cell culture plates to allow faster serial runs with the mechanical loading device. The original culture inserts were sprayed with silicone mold release and molded using silicone rubber (Smooth Sil 950, Smooth-On, Inc., Easton, PA). The mold was cured overnight and the original part cut free of the mold. The culture inserts were then cast using Smooth-Cast 300 polyurethane plastic and post-cured overnight at 50°C. O-rings were created using 3/32" Buna-N o-ring cord (part #ORBK-015, Small Parts, Miami Lakes, FL) to match the original o-rings. The silicon membranes (0.005" nonvulcanized rubber, gloss/gloss finish; Specialty Manufacturing, Inc., Saginaw, MI) were mounted into the inserts and secured using silicon sealant (Superflex Clear RTV, 59530; Loctite, Rocky Hill, CT). The silastic membranes were sprayed twice with 70% ethanol and sterilized overnight under a germicidal UV lamp. The inserts were then coated with collagen by incubating the membranes with 10 ml of a 50 µg/ml solution of collagen I in phosphate buffered saline (BD Biosciences, San Jose, CA) containing penicillin and streptomycin for 48 hrs at 37°C. The membranes were then washed twice with PBS and endothelial cells were passaged onto the plate at a 1:4 density from confluence. The cells were grown to confluence and kept in this state for 2 days prior to performing the experiment. Endothelial cells were grown on the collagen-coated silastic membranes and cyclic mechanical strain was applied with maximal strain of 3% or 5% and frequency of 1 Hz.

Metabolic labeling and Proteoglycan Isolation. At the time of mechanical loading, 100 μCi of $^{35}\text{SO}_4$ and 80 μCi of ^3H -glucosamine was added to each plate. After loading, the conditioned media was collected and combined with guanidine-HCl to a final concentration of 4 M. The cell layers were then washed three times with cold PBS then PBS with 1.0 mM EDTA was added and the cells were allowed to detach. The cells were spun down and washed with PBS twice and then resuspended in 1 ml of 0.05% trypsin-EDTA solution (Invitrogen, Carlsbad, CA) and placed on ice for 10 min. Mild trypsin digestion has been shown to isolate almost exclusively cell surface proteoglycans due to the high sensitivity of the syndecans to proteolysis [128]. After the trypsin digestion, the samples were centrifuged and 1 ml of DMEM with 5% CS was added to neutralize the trypsin. This solution was then brought to a final concentration of 4 M guanidine-HCl.

Analysis of Proteoglycans. A diagram of the experimental procedures for the analysis of the proteoglycans is shown in Figure 13. Briefly, the isolated conditioned media and cell surface digests were desalted into Buffer A (20 mM Tris, 8 M Urea, pH = 8.0) using a HiTrap desalting column (Amersham Biosciences, Piscataway, NJ). The proteoglycans were separated from other proteins by fractionation on a 1 ml HiTrap Q ion exchange column (Amersham) with a linear salt gradient from 0 to 2 M NaCl. One ml fractions were collected and aliquots of these samples were counted using liquid scintillation. Aliquots were subjected to digestion with 0.6 U/ml of protease free chondroitinase ABC (Seikagaku, Japan) for 4 hrs. Control samples were subjected to digestion conditions

without the addition of enzyme. The GAG fractions were pooled, desalted, and subjected to β -elimination in 0.1 M NaOH and 1 M NaBH₄ at 40 °C for 24 hrs. The solution was then neutralized with 50% acetic acid and the GAGs separated from protein by Q column chromatography. The free GAG chains were separated by gel filtration chromatography on a Superose 12 column (Amersham) using Buffer A with a flow rate of 0.4 ml/ml. Fractions were taken throughout the run using 0.5 ml fractions and were counted using liquid scintillation.

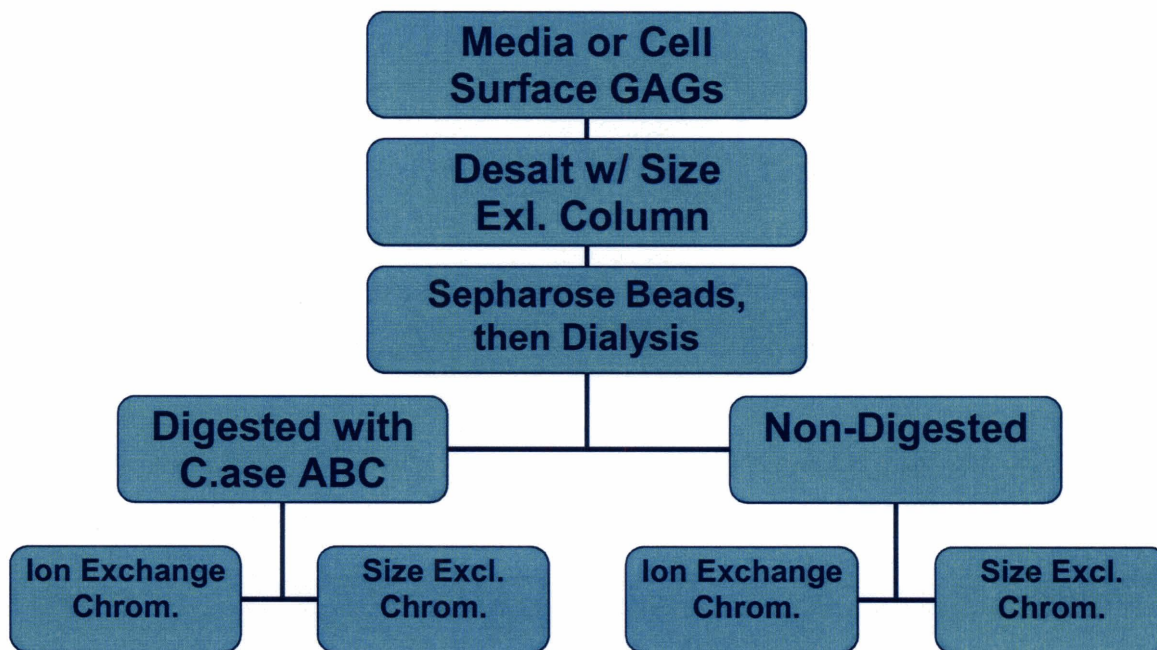


Figure 13. Flow diagram for analysis of glycosaminoglycans. C.ase = Chondroitinase. Size Excl. Chrom. = Size Exclusion Chromatography. Ion Exchange Chrom. = Ion Exchange Chromatography.

Cell Lysis and Western Blotting. Cells exposed to various treatments were placed on ice and washed twice with cold PBS. One ml of lysis buffer containing 20 mM Tris, 150 mM NaCl, 1% Triton X-100, 1% deoxycholate, 0.1% SDS, 1 mM sodium orthovanadate, 50mM NaF, 2 mM PMSF, and the standard concentration of mini-complete protease inhibitor cocktail (Roche, Nutley, NJ) was added to each plate. After 10 minutes of incubation in lysis buffer, the plates were scraped and the lysates pipetted into a centrifuge tube. The samples were cleared by centrifugation at 14,000 g for 15 minutes prior to western blotting. The samples were run on 4-15% polyacrylamide gradient gels and transferred to PVDF membranes (Millipore, Billerica, MA). The membranes were blocked for 1 hr in 5% non-fat milk in PBS with 0.01% tween-20 (PBST) and exposed to the following antibody dilutions at 4°C overnight in 1% non-fat milk: mouse anti-heparanase (1:200; Cell Sciences, Canton, MA), mouse anti-perlecan (1:100; Invitrogen), mouse anti-Sp1 (1:100; Santa Cruz Biotechnology, Santa Cruz, CA), rabbit anti-TGF- β 1 antibody (product #G122A; Promega, Madison WI), an anti-phospho-Smad-2 (Ser465/467; 138D4; Cell Signaling), rabbit anti-phospho-p38 MAPK (Thr180/Tyr182; 12F8; Cell Signaling), and rabbit anti-phospho-p44/42MAPK (Thr202/Tyr204; 20G11; Cell Signaling). The membranes were washed with PBST, incubated at room temperature for 2 hrs with a 1:3000 dilution of a horseradish peroxidase linked secondary antibody (Promega), and detected using a chemiluminescent reagent (Western Lightning Plus; Perkin Elmer, Boston, MA).

ELISA Measurement of TGF- β 1 and FGF-2. TGF- β 1 was measured using an ELISA assay (R&D Systems, Minneapolis, MN) according to the manufacturer's instructions.

Latent TGF- β 1 was activated by adding 20 μ l of 1 N HCl to 100 μ l of sample. The samples were incubated for 10 minutes at room temperature and then neutralized with 20 μ l of 1.2 N NaOH/0.5 M HEPES and assayed immediately. To extract FGF-2 from the extracellular matrix the cells were lysed and the culture plates washed three times with cold PBS. The PBS was removed and 10 ml of extraction buffer containing 2 M urea and 2.5 mg/ml heparin in PBS was added. The plates were incubated 48 hours with rocking to extract the FGF-2 and then dialyzed against three changes of distilled water for 48 hrs. The dialysis was performed using a 3500 molecular weight cutoff membrane in a slidealzer cassette (Pierce Biotechnology, Rockport IL). The samples were then snap frozen using liquid nitrogen, lyophilized, and reconstituted in 1 ml of PBS. Media samples were assayed without further preparation. An ELISA assay (R&D Systems, Minneapolis, MN) was used to measure FGF-2 in the media and matrix extracts.

Gene Expression Analysis by Real Time RT-PCR. Cell were grown to confluence and exposed to mechanical loading as described above. The cells were washed twice with PBS and mRNA was isolated using a RNAeasy Mini Protect Kit (Qiagen, Valencia, CA) following the manufacturer's instructions. Homogenation of the samples was performed using QIAshredder columns (Qiagen). A DNase digestion was performed while the RNA was bound to the column using RNase free DNase (Qiagen). Reverse transcription was performed using polyA primers (Applied Biosystems). Real time PCR was performed using an MJ Research Real Time PCR Machine at MIT BioMicro Center (Cambridge MA) using a SYBR Green Master Mix (Applied Biosystems). Cycle conditions were as follows: 2 min at 50°C, 10 min at 95°C, and 40 cycles of of 15 s at 94°C and 1 min at

60°C. Primers used for the real time PCR were as follows: GAPDH, GGCCTCCAAGGAGTAAGACC (sense, S), AGGGGTCTA CATGGCAACTG (anti-sense, AS); syndecan-1, AGGGGACAGGAGTC CACTTT (S), GGGGGATACCGAAT CAACTT (AS); syndecan-2, CTCAAGGATGAC GTGGGTTT (S), GATTCCTCTGG CCAATTCA (AS); syndecan-4, TCGATCCGAGAGACTGAGG T (S), CCAGATCTCC AGAGCCAGAC (AS); heparanase, ATCAATGGG TCGCAGTT AGG (S), AGGCTGA CCAACATCAGGAC (AS); perlecan, TCCACCTG AGTACCCG AAAC (S), CTGAAG TGACCAGGCTCCTC (AS).

Smooth Muscle Cell Proliferation Assay. Rat smooth muscle cells were passaged into six-well plates at low density. Endothelial cell conditioned media was isolated and used in an assay of vascular smooth muscle cell proliferation. Smooth muscle cells were serum starved in 0.5% calf serum for 24 hours, washed with PBS, and incubated in conditioned media with 1 $\mu\text{Ci/ml}$ ^3H -thymidine for 24 hours. The cells were then washed three times with PBS at 4°C. The cells were then incubated with 10% TCA for 30 min at 4°C, washed twice in 95% ethanol, and solubilized in 1 ml of 0.25 M NaOH with 0.1% SDS for 1 hour. The samples were then added to scintillation cocktail and radioactivity was measured using a liquid scintillation counter.

Statistics. All results are shown as mean \pm one standard deviation. An ANOVA was used to make comparisons between groups of continuous variables. A two-tailed Student's *t* test was used to make comparisons between groups; $p < 0.05$ was defined as being statistically significant.

Results

Mechanical strains of 5% Maximal Strain are Not Cytotoxic to Endothelial Cells in Culture

As these experiments were aimed at understanding the affects of chronic load and not acute injury and cell death, an experiment was performed to assess cell viability as a function of maximal strain. Lactate dehydrogenase (LDH) is an intracellular enzyme that is constitutively expressed by virtually all cell types. The release of this enzyme from the cell indicates that the cell membrane integrity has been compromised and that cell damage has occurred. The release of this enzyme in response to mechanical load was measured under experimental conditions at various maximal strains. In HUVEC there is little release of LDH into the conditioned media at 1%, 3%, or 5% maximal strain (1 hz for 24 hrs) and a significant increase at 8% strain (see Figure 14). These results support that the effects of mechanical load were not from cell death or injury as there was no substantial increase in LDH release after 24 hours of load of 5% stain or less ($2.6\% \pm 2.6\%$ increase in LDH release, $n = 4$).

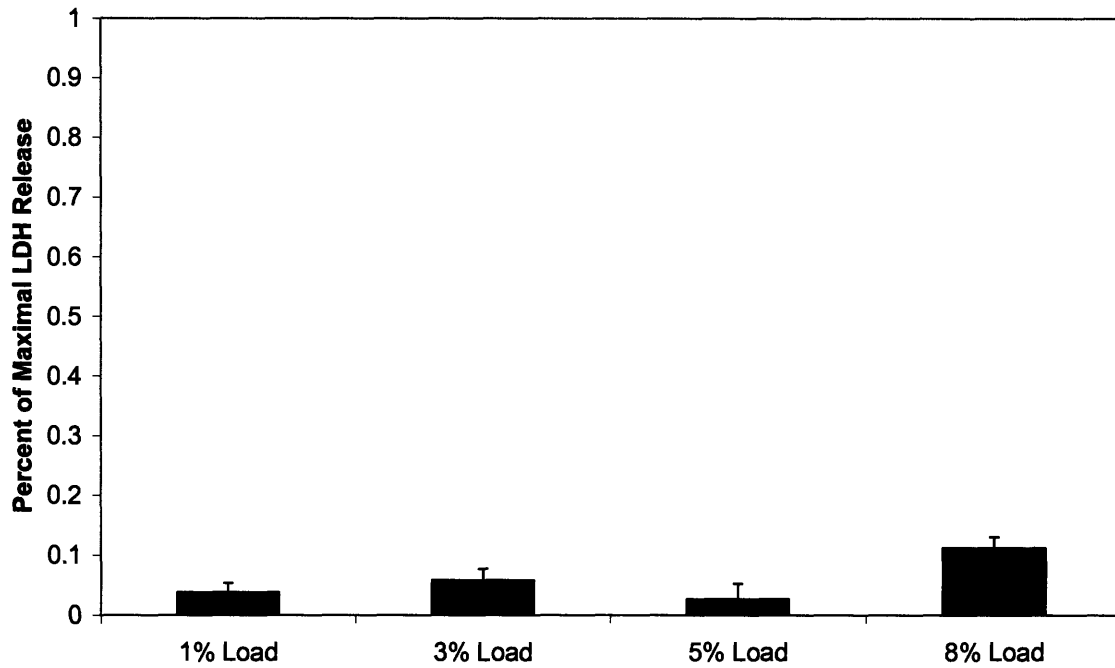


Figure 14. Lactate dehydrogenase (LDH) release relative to static cultures in response to mechanical strain.

Mechanical Strain Increases Endothelial Inhibition of Vascular Smooth Muscle Cell Proliferation

A fundamental question that we would like to address is whether mechanical strain causes endothelial cells to produce more or less inhibitory factors in response to mechanical stimuli. To explore the role of mechanical strain in modulating endothelial cell control of vascular smooth muscle cells, endothelial cells were grown on silastic membranes until 2 days postconfluent and then exposed to uniform, cyclic mechanical strain (5% maximal strain, 1 Hz) for 24 hrs. Conditioned media was harvested from endothelial cells under strain and non-strain conditions, and applied to vascular smooth muscle cells in culture. Proliferation of the vSMCs was measured using incorporation of radiolabeled thymidine. Cyclic mechanical strain increased the inhibitory properties of HUVEC conditioned media by two fold over the inhibition from non-strained HUVEC cultures (80% total inhibition compared to growth media; Figure 15). This effect was present in multiple endothelial cell types and increased with the magnitude of the load (Figure 16).

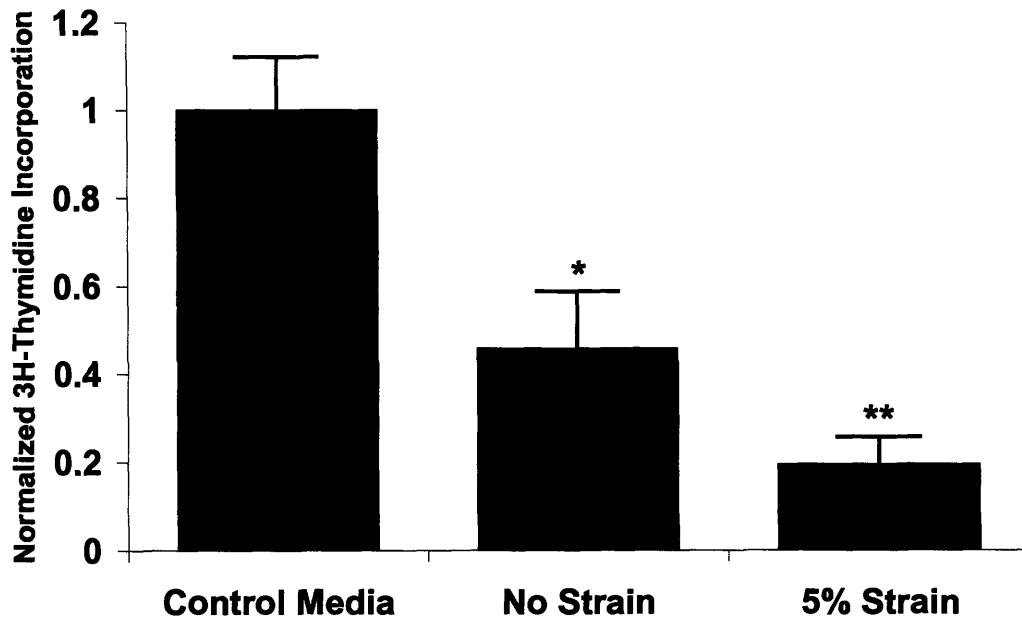


Figure 15. Inhibition of vascular smooth muscle cell proliferation by human umbilical endothelial cell conditioned media. “Control media” has not been exposed to endothelial cell. “No strain” is conditioned medium from endothelial cells that are under static conditions. “Five percent strain” is conditioned medium from endothelial cells exposed to mechanical load for 24 hrs. Results are mean \pm standard deviation, * $p < 0.05$ versus 5% control media; ** $p < 0.05$ versus no strain and control media; $n = 5-12$.

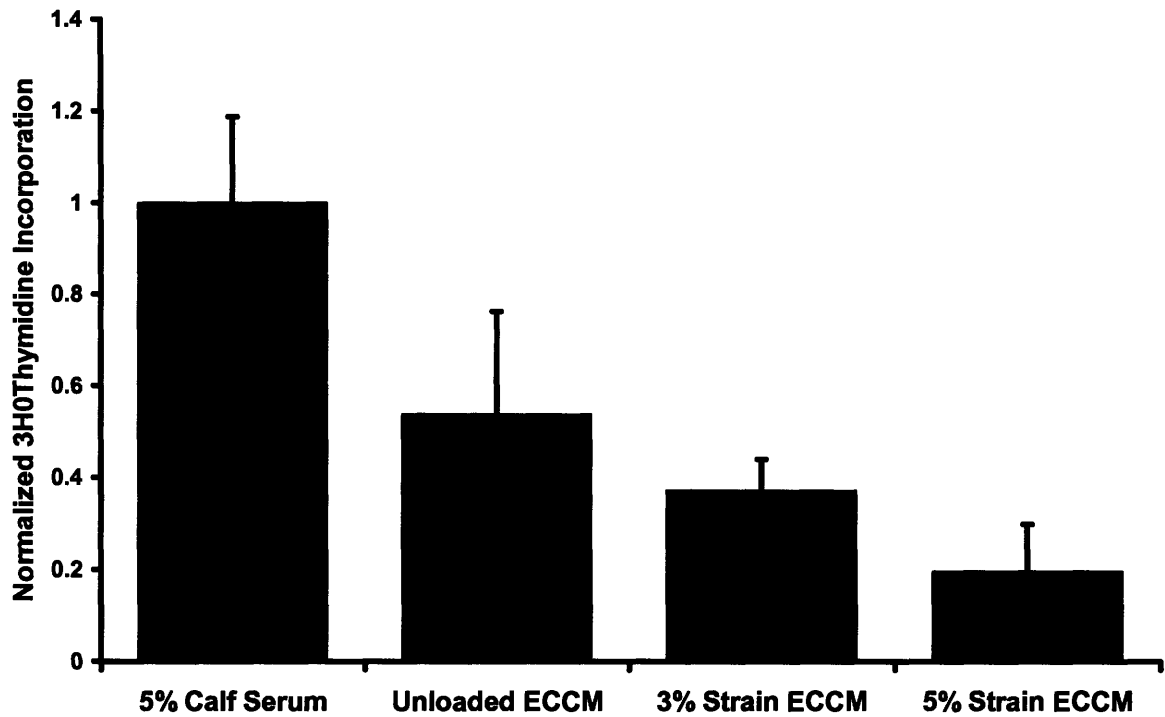


Figure 16. Inhibition of vascular smooth muscle cell proliferation by bovine aortic endothelial cell conditioned media. Five percent calf serum is control media that has not been exposed to endothelial cells. No strain is endothelial cell conditioned medium (ECCM) from endothelial cells that are under static conditions. Three or five percent strain is conditioned medium from endothelial cells exposed to mechanical load for 24 hrs at either 3% or 5% maximal strain. All comparisons have $p < 0.05$.

Mechanical Strain Increases Production of Heparan Sulfate Proteoglycans

To examine the mechanism behind the observed increase in inhibitory molecules we quantified the production of heparan sulfate proteoglycan core proteins in static and mechanically loaded cultures (5% cyclic load for 24 hrs). Western blotting for heparan sulfate proteoglycan (HSPG) core proteins revealed an increase in cell-associated syndecan-1 and -4 as well as an increase in perlecan in the conditioned medium (Figure 17). A control for equal loading of protein was done using an antibody for β -actin.

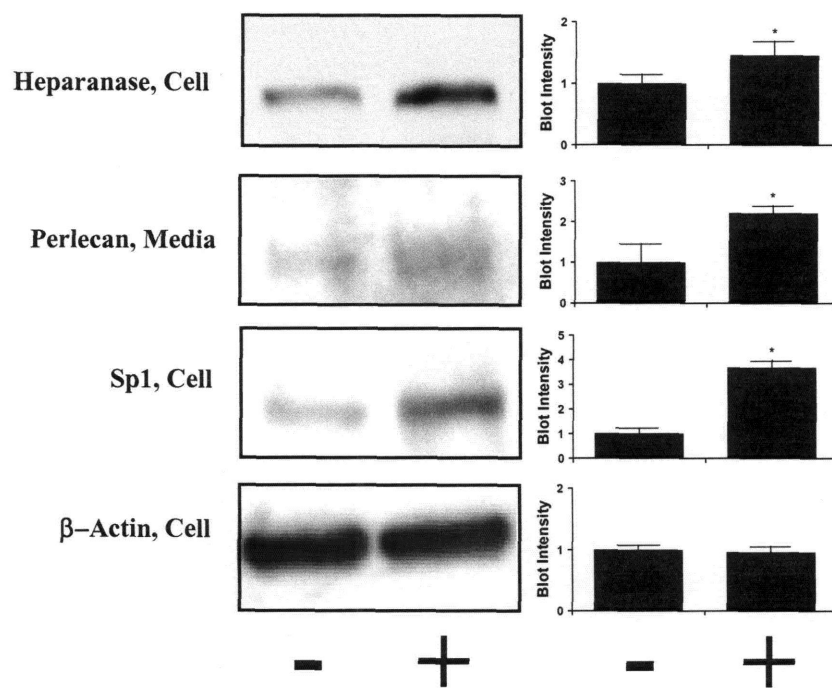


Figure 17. Western blot for HSPG core proteins, heparanase and the transcription factor Sp1 from endothelial cells exposed to 5% cyclic strain for 24 hrs. β -actin are from cell lysate samples. Perlecan is from conditioned medium. Results are mean \pm standard deviation, * $p < 0.05$ versus 5% control media; $n = 3-4$.

Real time PCR was also used to examine the level of mRNA of the genes for the heparan sulfate proteoglycan core proteins (Figure 18). Mechanical strain of 5% at 1 Hz for 24 hours also led to an increase in mRNA expression of syndecan-1 and -4, as well as a decrease in the expression of syndecan-2 mRNA. An increase in perlecan mRNA was seen but was not statistically significant. No changes in the level of heparanase mRNA was found. All samples were normalized to a GAPDH gene control before normalization to the non-loaded control.

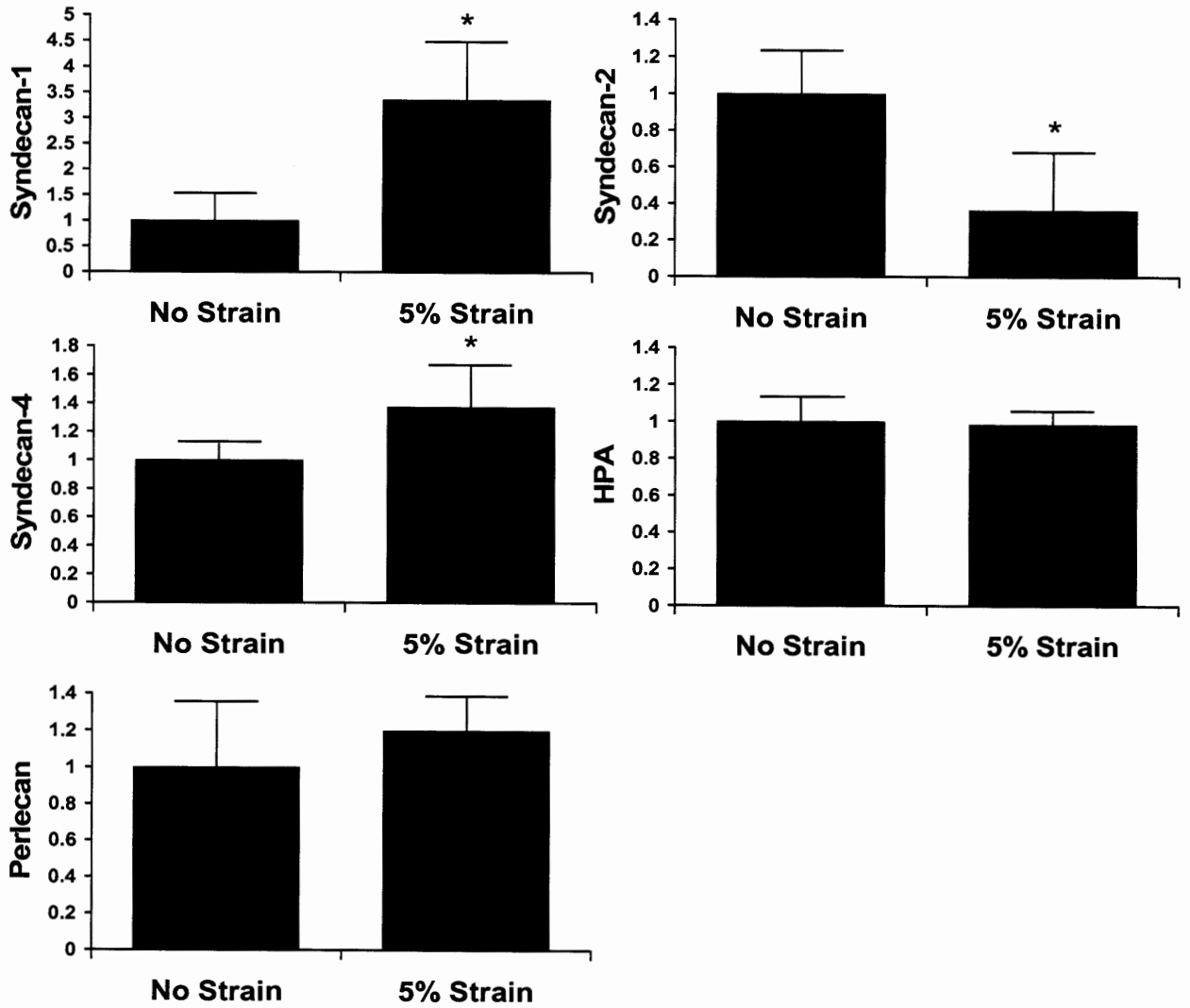


Figure 18. Real time PCR analysis of alterations in syndecan gene expression. Values are normalized to No Strain controls. HPA = Heparanase.

Proteoglycans production can be regulated on multiple levels. Consequently, it is possible to regulate the production of the glycosaminoglycan sugar chains without altering the core protein production or *visa versa*. To investigate the effect of mechanical strain on endothelial heparan sulfate glycosaminoglycan (GAG) chain production, cells were exposed to mechanical strain and metabolically labeled using ^3H -glucosamine and $^{35}\text{SO}_4$. Mechanical strain induced an increase of 24% in total soluble GAG production in HUVECs (Figure 19 and Figure 23). A 38% increase in soluble heparan sulfate was also observed (Figure 20 and Figure 23). No change in cell surface total GAG was observed (Figure 21 and Figure 23), but a decrease in cell heparan sulfate was observed (Figure 22 and Figure 23). The GAGs extracted from the matrix were also measured and found to be increased in the extracellular matrix after mechanical load. Total normalized GAGs and heparan sulfate GAGs increased from 1.00 ± 0.09 to 1.85 ± 0.05 and from 1.00 ± 0.03 to 1.19 ± 0.04 , respectively for mechanically loaded versus non-loaded.

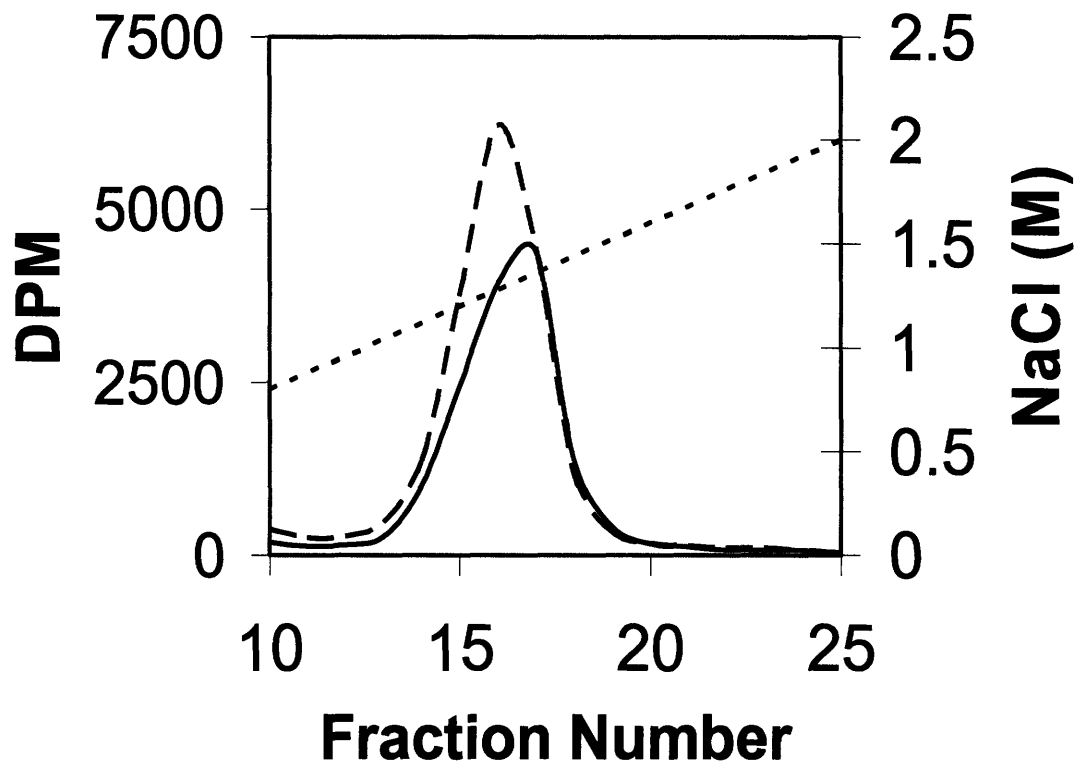


Figure 19. Total proteoglycans in endothelial cell conditioned media labeled with ^3H -glucosamine and separated by ion exchange chromatography. Samples treated with 5% strain (dashed line) and no strain (solid line) are shown with the applied salt gradient (dotted line) on the second axis.

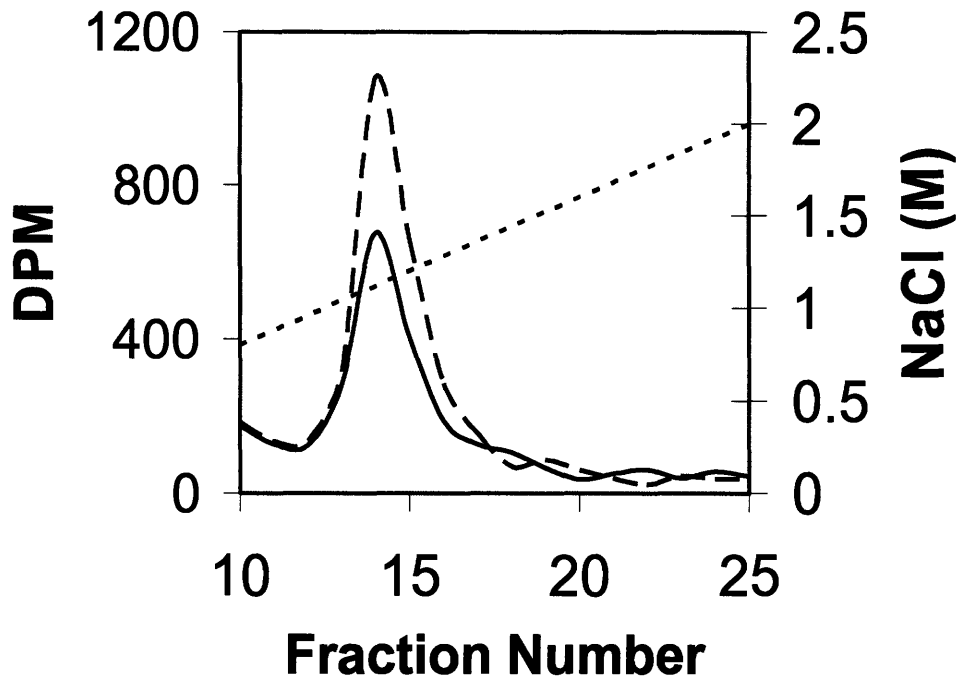


Figure 20. Heparan sulfate proteoglycans in the endothelial conditioned media labeled with ^3H -glucosamine and separated by ion exchange chromatography. Samples treated with 5% strain (solid line) and no strain (dashed line) are shown with the applied salt gradient (dotted line) on the second axis.

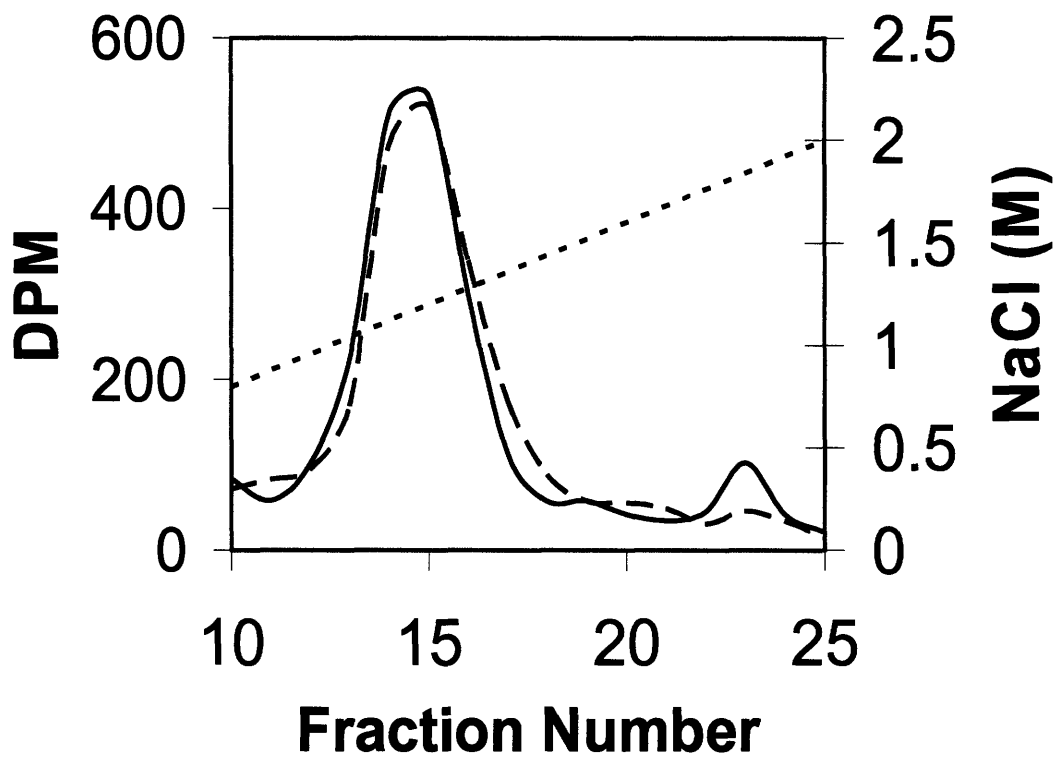


Figure 21. Total proteoglycans on the endothelial cell surface labeled with ^3H -glucosamine and separated by ion exchange chromatography. Samples treated with 5% strain (dashed line) and no strain (solid line) are shown with the applied salt gradient (dotted line) on the second axis.

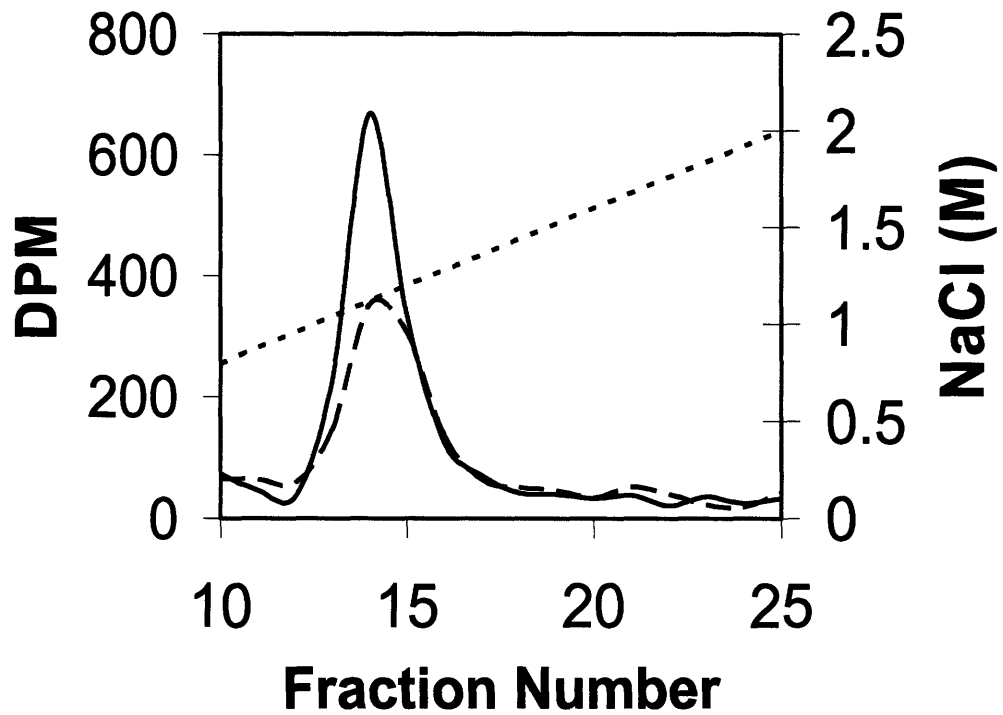


Figure 22. Heparan sulfate proteoglycans on the endothelial cell surface labeled with ^3H -glucosamine and separated by ion exchange chromatography. Samples treated with 5% strain (dashed line) and no strain (solid line) are shown with the applied salt gradient (dotted line) on the second axis.

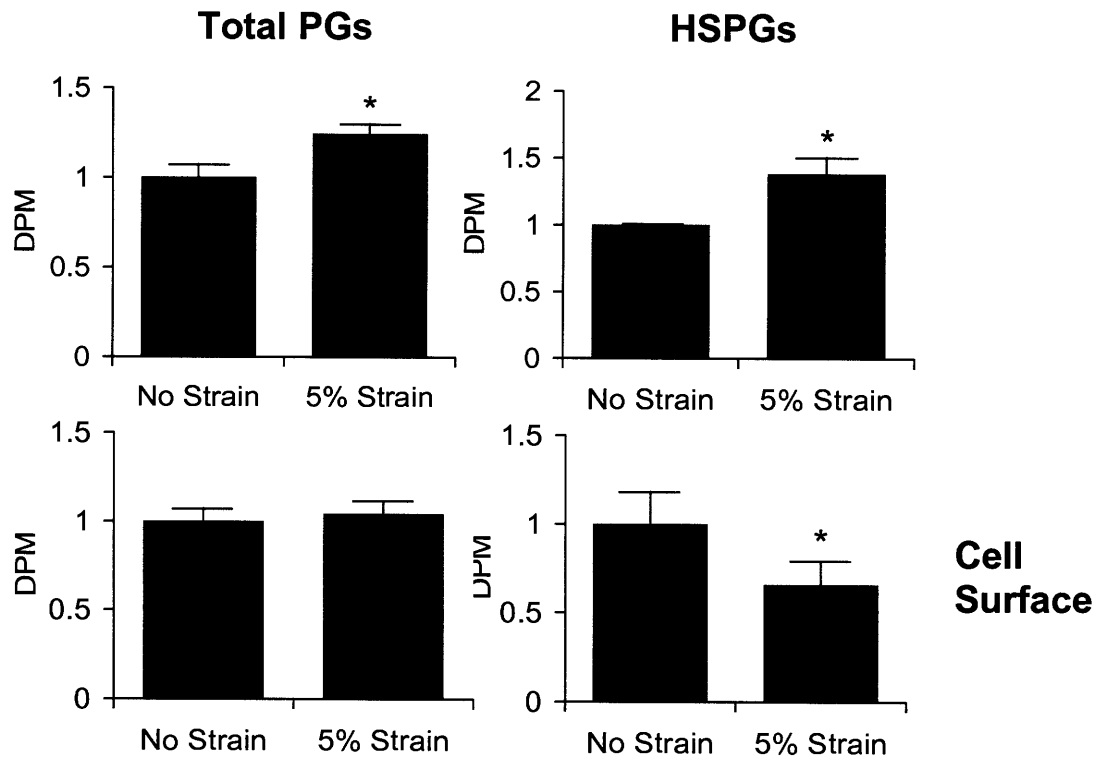


Figure 23. Total and isolated heparan sulfate proteoglycans in the endothelial conditioned media labeled with ^3H -glucosamine and separated by ion exchange chromatography (normalized to no strain, * comparison of $p < 0.05$).

Another potential pathway of regulation of proteoglycans is to alter the size of the glycosaminoglycan chains attached to the core protein. We examined the affect of mechanical strain on altering the hydrodynamic size of the glycosaminoglycan chains. The size distribution of total proteoglycans in the conditioned media was not altered by mechanical strain (Figure 24). There were increases in both low and high molecular weight heparan sulfate produced in the media (Figure 25). On the cell surface the size distribution was unaltered for both total and heparan sulfate proteoglycans, with decreases in both low and high molecular weight heparan sulfate (Figure 26 and Figure 27)

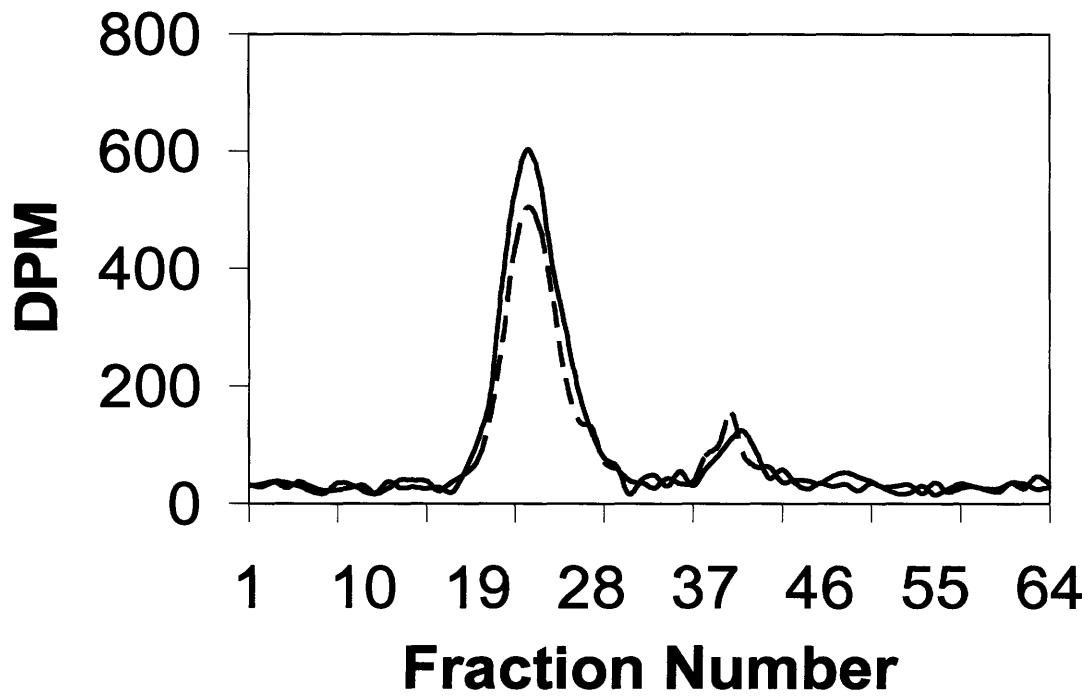


Figure 24. Total proteoglycans in the endothelial conditioned media labeled with ^3H -glucosamine separated by size exclusion chromatography. Representative samples treated with 5% strain (dashed line) and no strain (solid line) are shown.

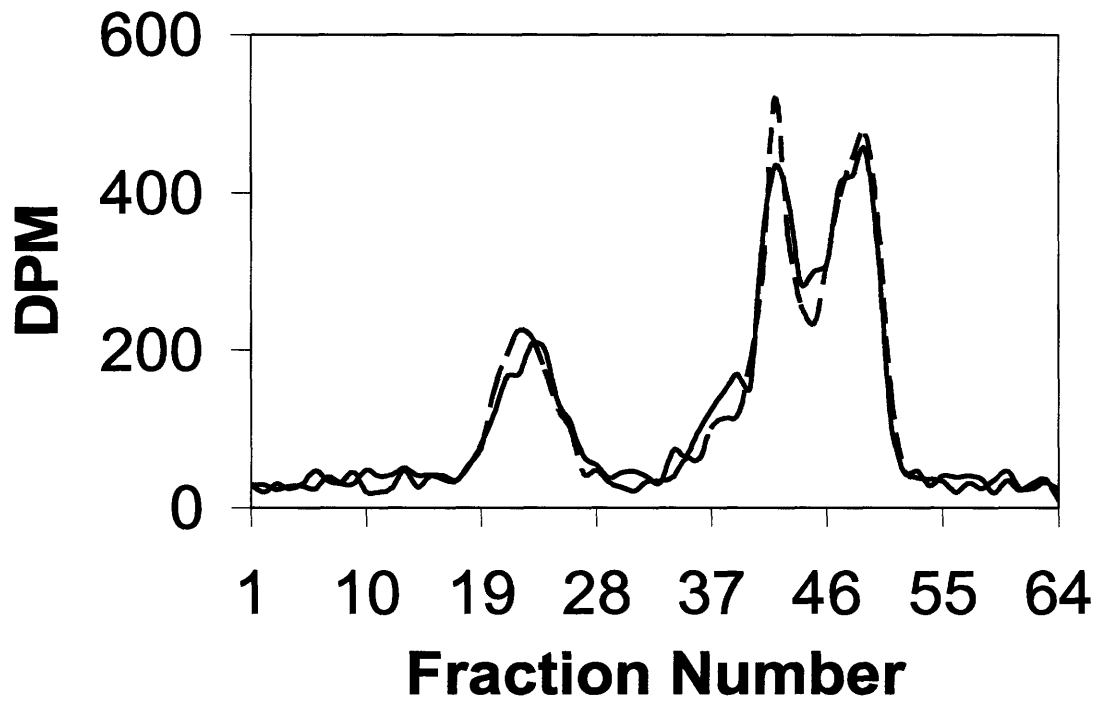


Figure 25. Heparan sulfate proteoglycans in the endothelial conditioned media labeled with ^3H -glucosamine separated by size exclusion chromatography. Representative samples treated with 5% strain (dashed line) and no strain (solid line) are shown.

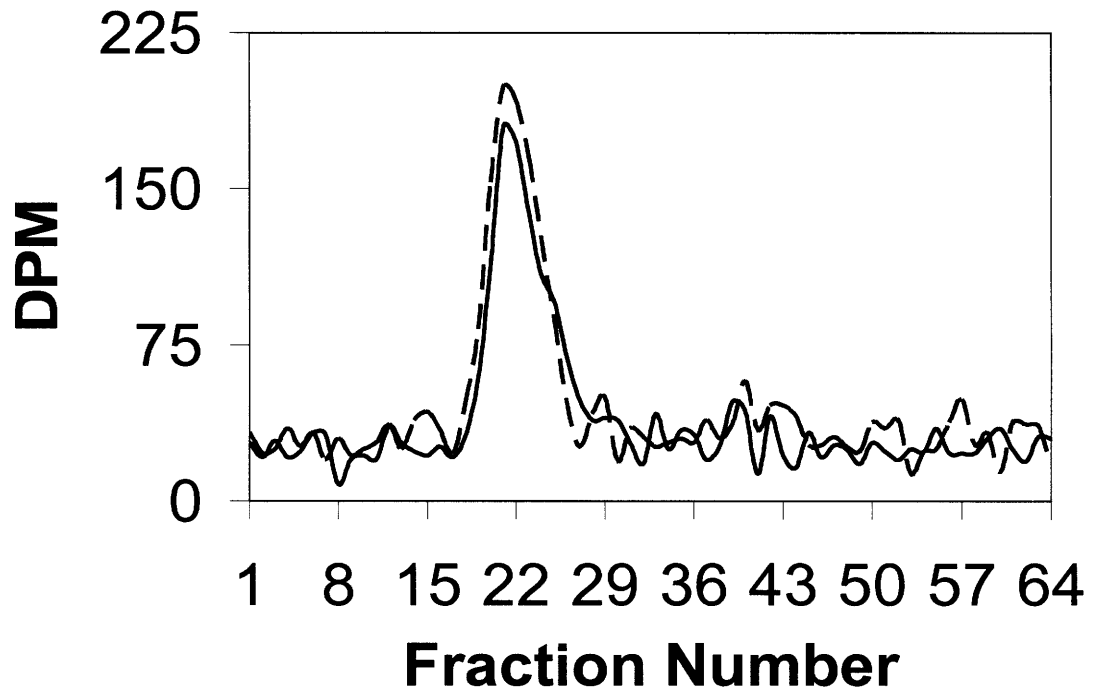


Figure 26. Cell surface total proteoglycans on the endothelial cell surface labeled with ^3H -glucosamine separated by size exclusion chromatography. Representative samples treated with 5% strain (dashed line) and no strain (solid line) are shown.

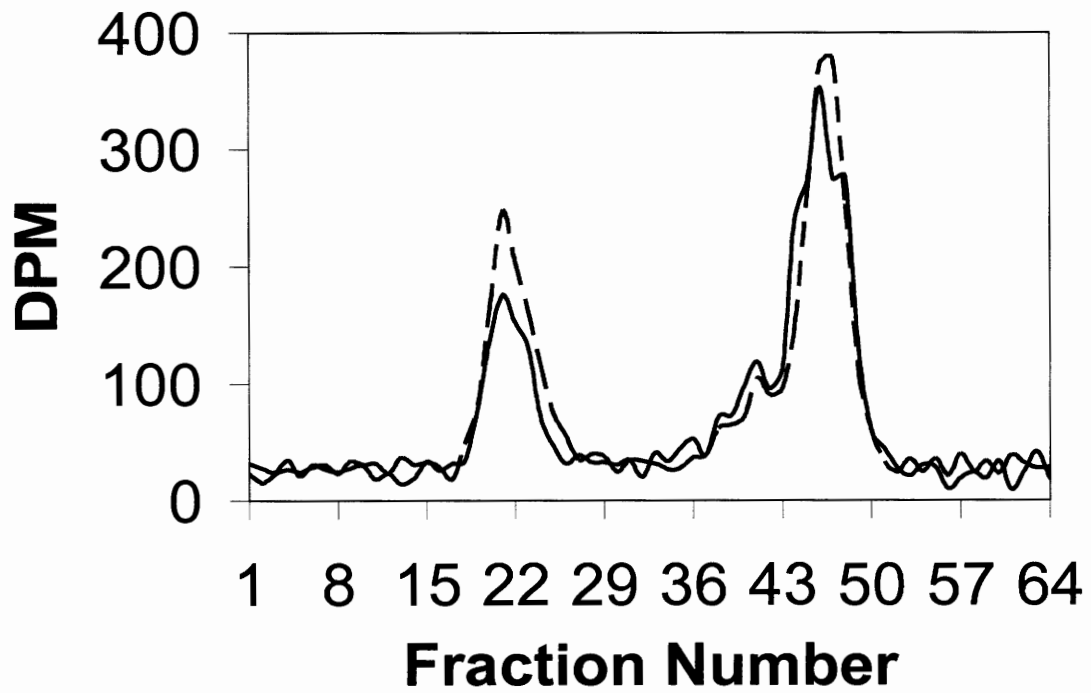


Figure 27. Cell surface heparan sulfate proteoglycans on the endothelial cell surface labeled with ^3H -glucosamine and separated by size exclusion chromatography. Representative samples treated with 5% strain (dashed line) and no strain (solid line) are shown.

Mechanical Strain Activates TGF- β 1 through p38 and ERK1/2 Dependant Pathway

Transforming growth factor- β (TGF- β) is another molecule intimately involved in the control of vascular smooth muscle cell growth as well as a regulator of extracellular matrix production in various cell types. This molecule is predominantly present in latent form that can be activated by various factors. We examined the amount of active TGF- β present with mechanical load in the presence of inhibitors to the MAPK and p38 MAPK signaling pathways. In non-loaded cultures active TGF- β was undetectable by ELISA (Figure 28). Following treatment with mechanical strain for 24 hrs, significant amounts of active TGF- β were found in the condition media. This effect was significantly blocked by both inhibitors to MAPK (U0126) and p38 MAPK (SB029063). Total TGF- β was assayed after acidification and neutralization of the conditioned media revealing similar amounts of total TGF- β under all conditions (Figure 29).

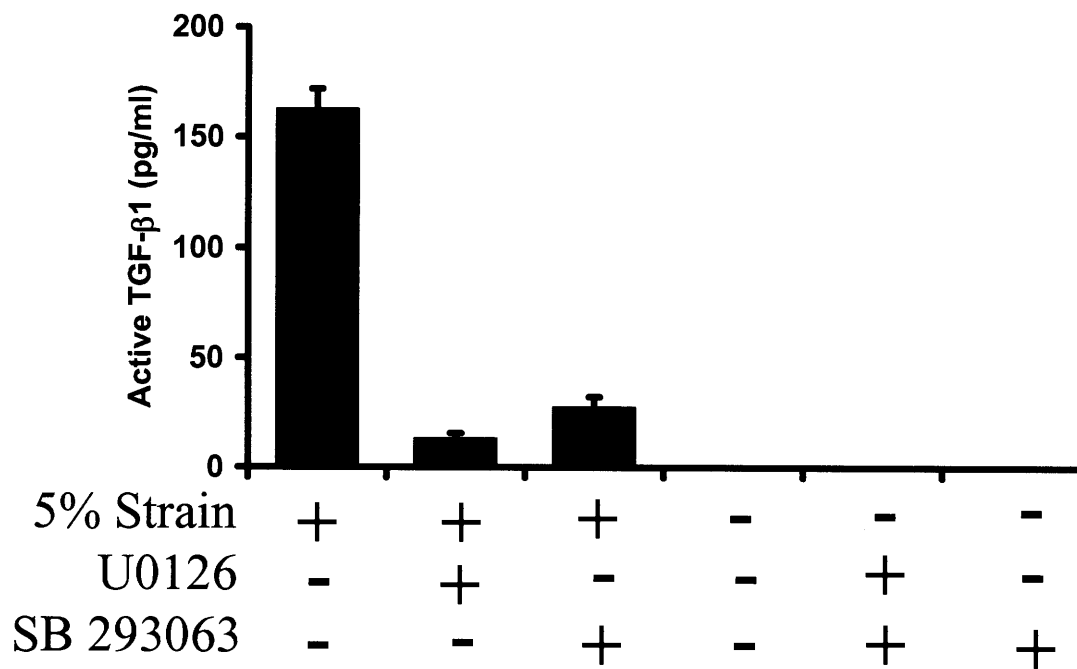


Figure 28. Active TGF-β in endothelial cell conditioned media after 24 hrs of mechanical strain or static conditions measured by ELISA assay.

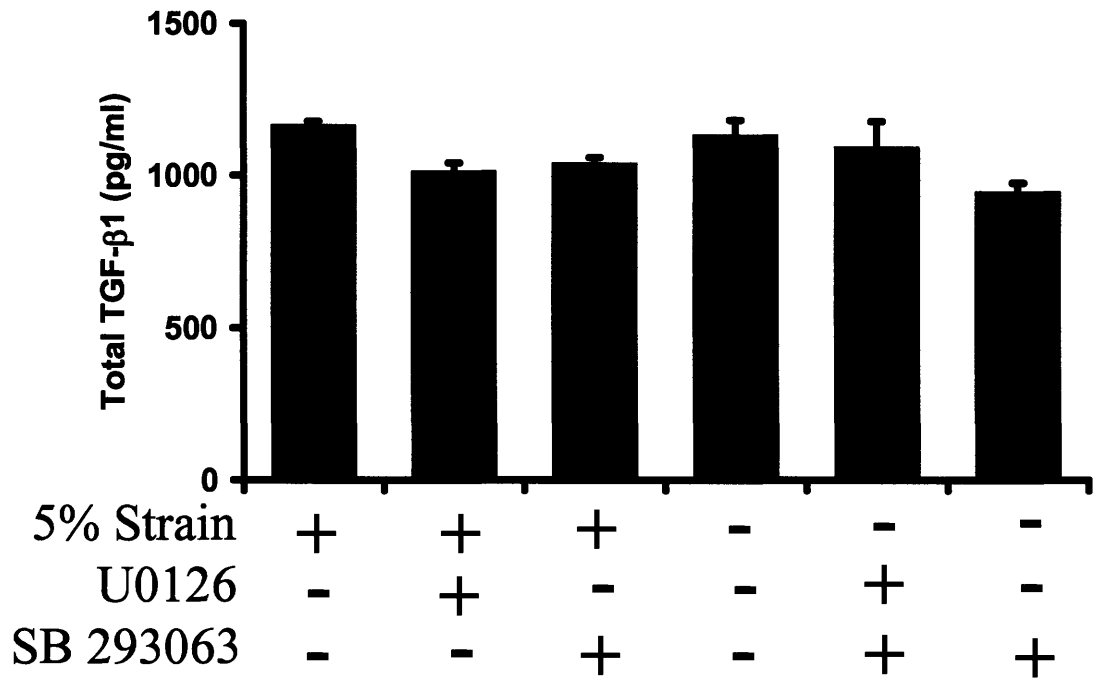


Figure 29. Total TGF- β in endothelial cell conditioned media after 24 hrs of mechanical strain or static conditions measured by ELISA assay. Total TGF-b was activated by treatment with acid pH prior to ELISA assay.

Mechanical Strain Alters Extracellular Matrix Bound FGF-2 through p38, ERK1/2, and TGF- β 1 Mediated Mechanism

Heparan sulfate proteoglycans are involved in many aspects of FGF-2 signaling, uptake and sequestration. To examine the role of mechanical strain in regulating FGF-2 we measured FGF-2 in the condition media and extracellular matrix fractions of cells exposed to static and mechanical strain conditions. In the extracellular matrix, mechanical strain decreased the amount of FGF-2 present (Figure 30). This effect was blocked completely by inhibitors to MAPK (U0126) and partially inhibited by an inhibitor to p38 MAPK (SB 293063). In the condition media the amount of FGF-2 was slightly lowered due to mechanical load (Figure 31). Similar experiments were performed examining the affects of a neutralizing antibody to TGF- β on the FGF-2 content of the extracellular matrix and conditioned media (Figure 32 and Figure 33). Pretreatment with a neutralizing antibody to TGF- β blocked the decrease in extracellular matrix associated FGF-2.

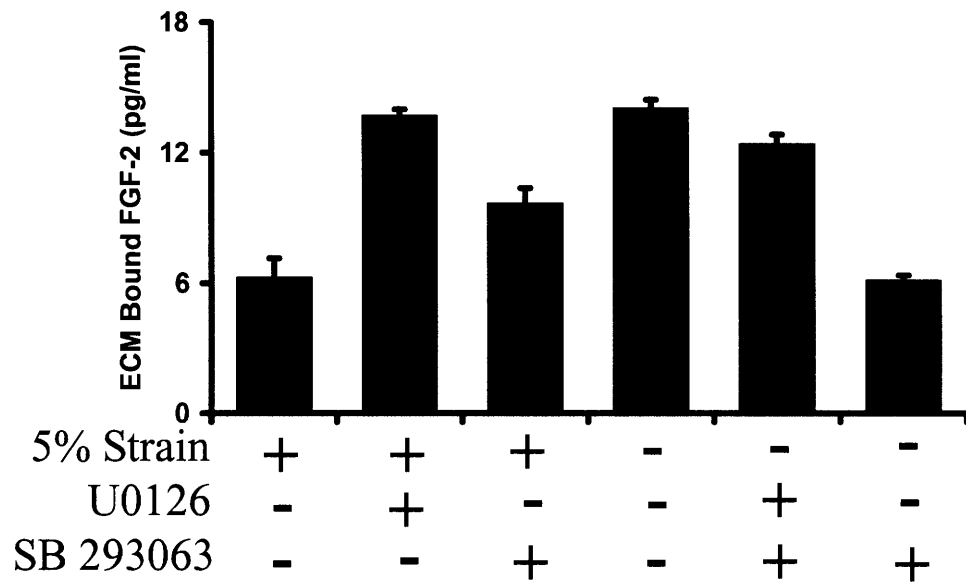


Figure 30. Fibroblast growth factor-2 (FGF-2) extracted from the extracellular matrix of endothelial cultures pretreated for 1 hr with U0126 or SB 293063 and exposed to 24 hrs of static or strain conditions.

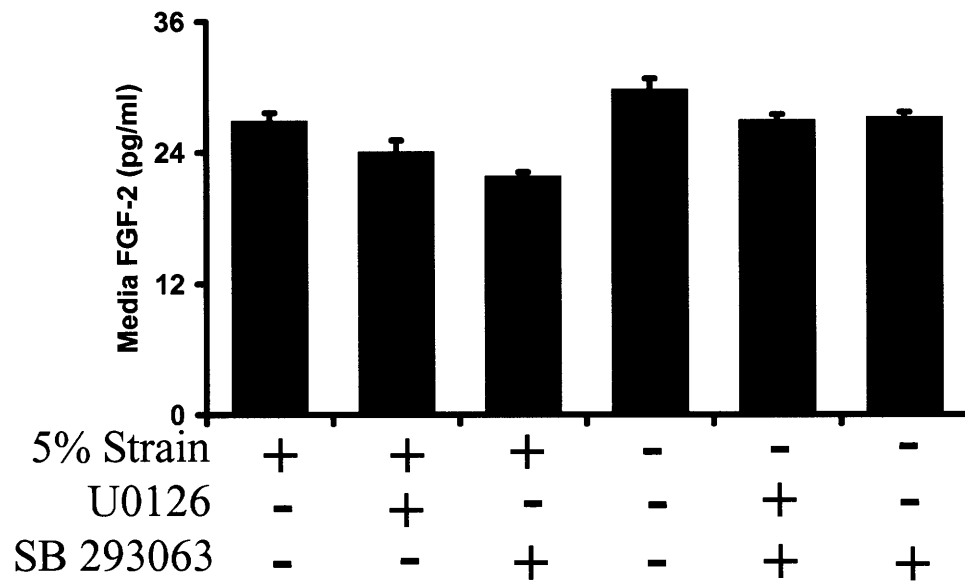


Figure 31. Fibroblast growth factor-2 (FGF-2) in the conditioned media of culture pretreated with U0126 or SB 293063 for 1 hr and exposed to static or strain conditions for 24 hrs.

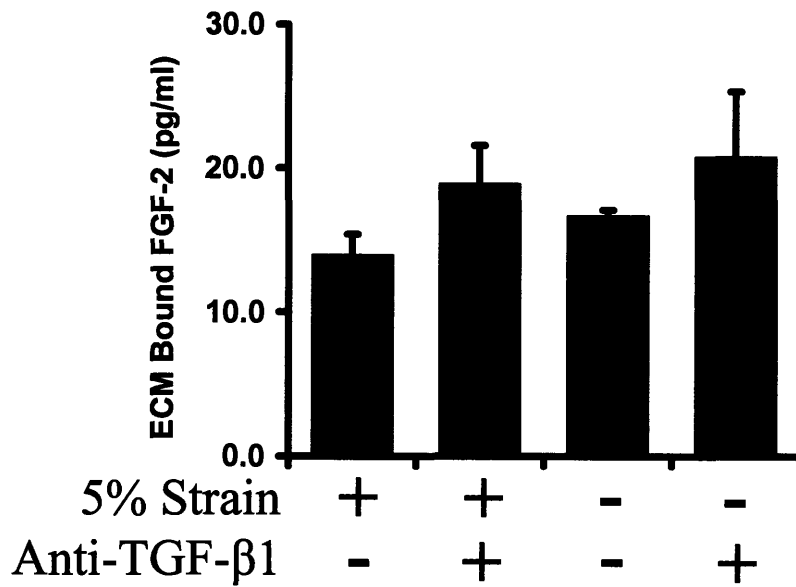


Figure 32. A neutralizing antibody to TGF-β reduces blocks the load induced decrease in extracellular matrix (ECM) bound FGF-2. Endothelial cells were treated with a neutralizing antibody for 1 hr prior to exposure to 24 hrs of 5% mechanical strain.

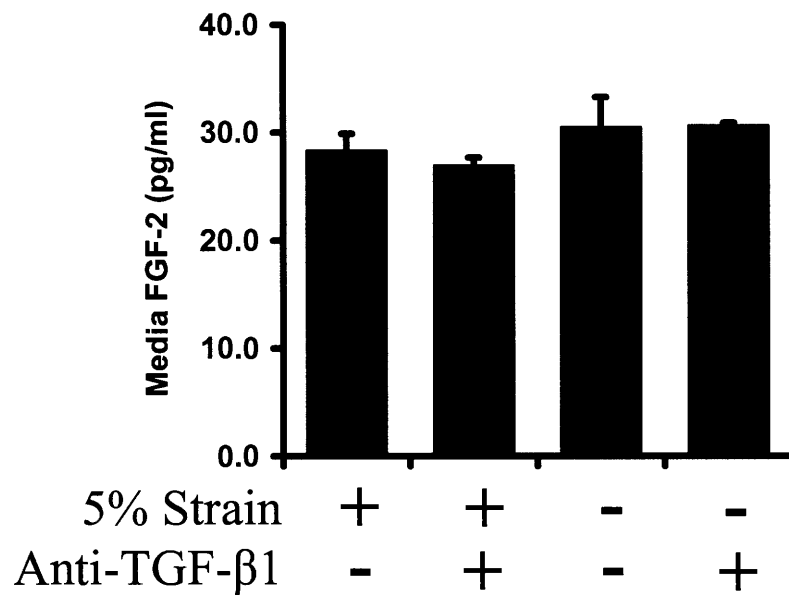


Figure 33. The content of the conditioned media is unaffected by mechanical strain or a TGF- β neutralizing antibody. Endothelial cells were treated with a neutralizing antibody for 1 hr prior to exposure to 24 hrs of 5% mechanical strain.

Mechanotransduction Pathway Controlling Load-Induced Heparan Sulfate Proteoglycans Involves p38/ERK activation and Autocrine TGF- β 1 signaling

To examine the intracellular signaling pathways responsible for mechanical strain-mediated modulation of heparan sulfate proteoglycans we pretreated cells with inhibitors to the MAPK (MEK1/2 inhibitor U0126) and p38 (SB 293063) signaling pathways. We hypothesized that since mechanical strain induced TGF- β activation, an autocrine signaling from this growth factor may be an important mechanism. Following inhibitor or neutralization antibody treatment we used western blotting to examine the levels of phosphorylated signaling intermediates including phospho-Smad-2 (a downstream effector of TGF- β), phospho-p38 MAPK, and phospho-ERK1/2 (shown in Figure 34). Mechanical strain activated all of these intermediates after 24 hrs of cyclic strain. Interestingly, there was crosstalk between each of the signaling pathways. Maximal Smad-2 only occurred in the absence of both inhibitors to MAPK and p38 MAPK. Further, phosphorylation of ERK1/2 and p38 MAPK was partially blocked by inhibitors to each of the other pathways. This suggests that these pathways are communicating through some type of common pathway or that the drugs have non-specific effects on other signaling pathways. We performed a similar western blotting analysis in mechanically stimulated cultures that were pretreated with a neutralizing antibody to TGF- β (shown in Figure 35). We also examined the role of these pathways in the production of the heparan sulfate proteoglycan core proteins in response to mechanical strain (Figure 36). The inhibitors to MAPK and p38 pathways and the

neutralizing antibody to TGF- β blocked the load induced increase in perlecan production.

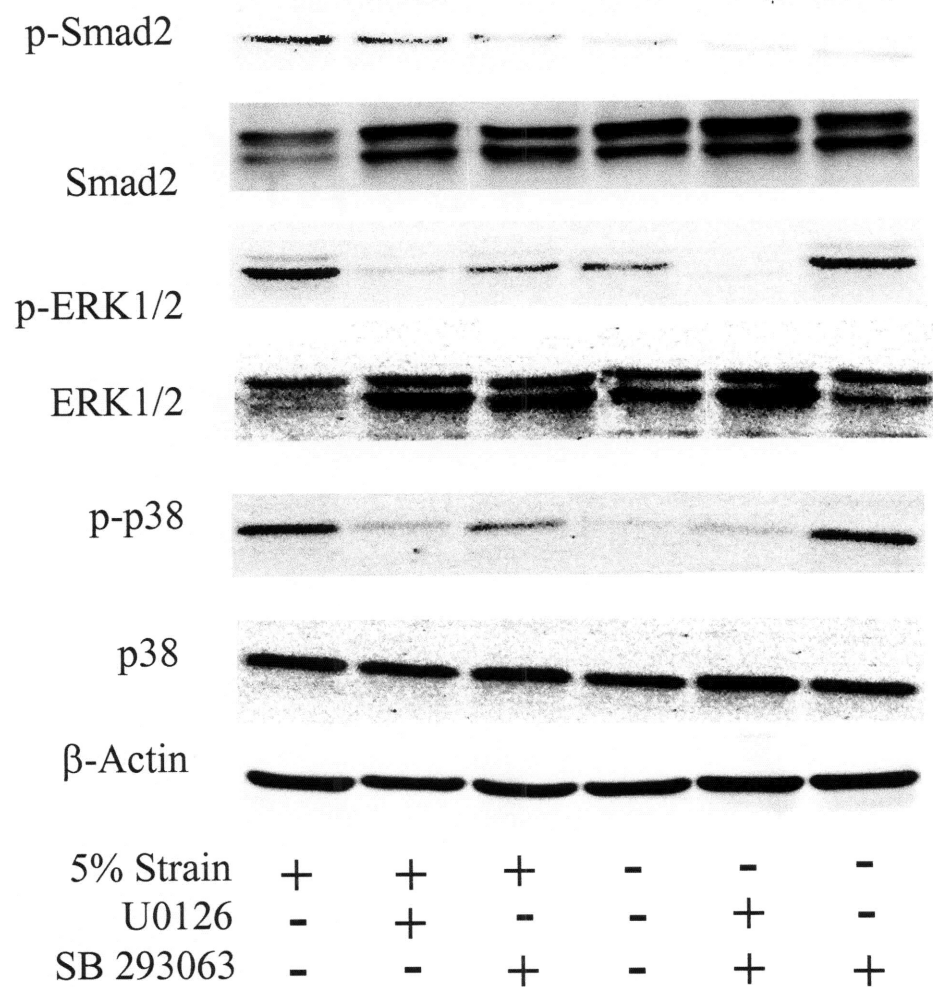


Figure 34. Western blot analysis of intracellular signaling intermediates of the TGF- β , MAPK, and p38 MAPK pathways. Cells were pretreated with the indicated inhibitors for 1 hr prior and during exposure to static or mechanical strain conditions for 24 hrs.

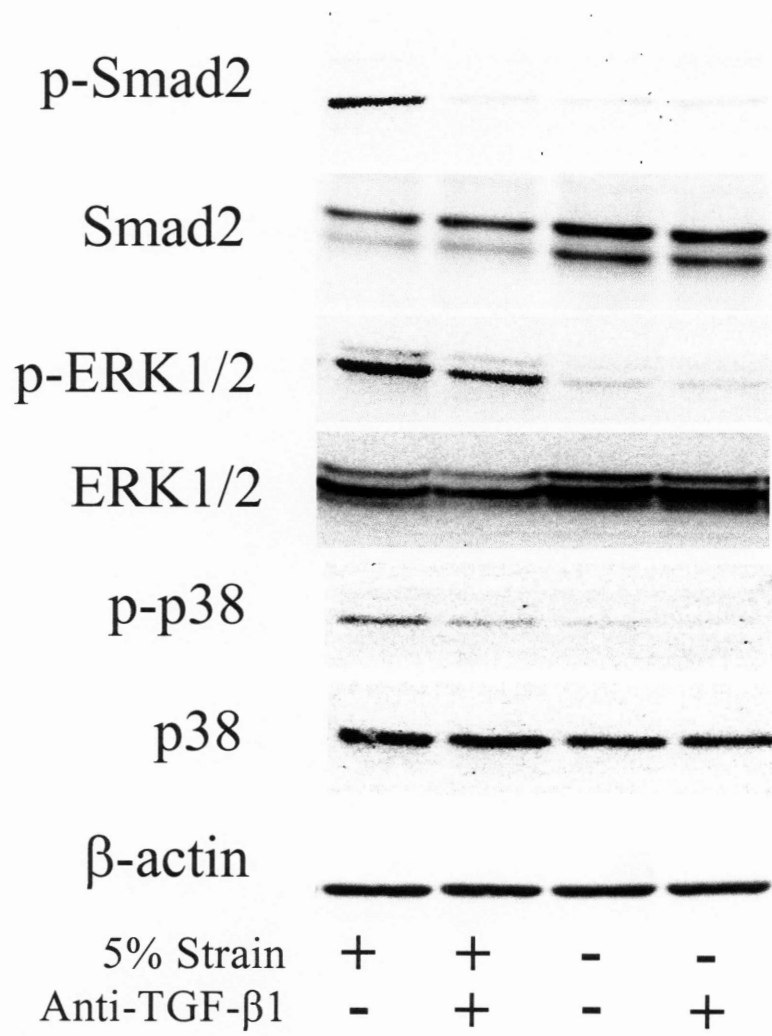


Figure 35. Western blot analysis of intracellular signaling intermediates of the TGF- β , MAPK, and p38 MAPK pathways. Cells were pretreated with the neutralizing antibody for 1 hr prior and during exposure to static or mechanical strain conditions for 24 hrs.

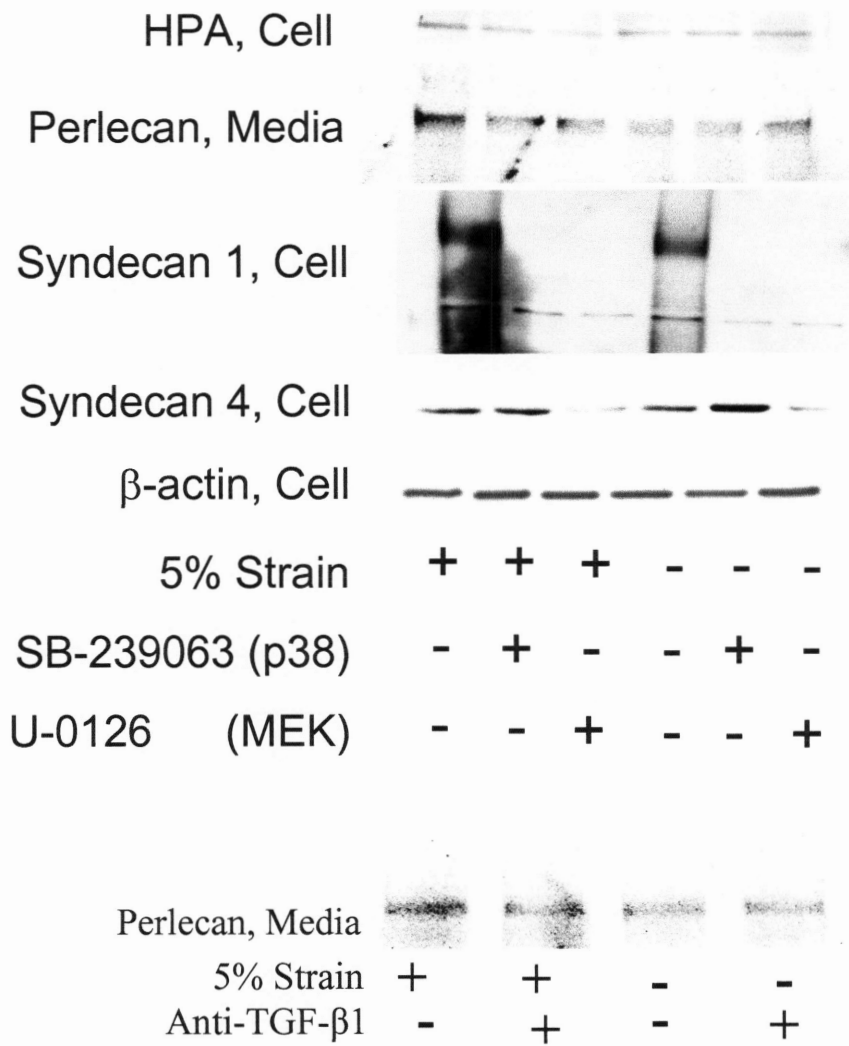


Figure 36. Western blot analysis of heparan sulfate core proteins and heparanase. Cells were pretreated with the indicated inhibitors or neutralizing antibody for 1 hr prior and during exposure to static or mechanical strain conditions for 24 hrs.

Promoter Analysis of Heparan Sulfate Proteoglycan Core Proteins and Heparanase

A promoter analysis was performed on the various genes using PROSCAN (v. 1.7). This analysis revealed several common transcription factor binding sites found in the syndecan-1, 4, perlecan, and the heparanase promoter region. Notably, a Sp1 binding site was found in the promoter region of all the genes. To test whether Sp1 was regulated by mechanical strain, Sp1 expression was found to be increased in measurements by Western blotting (Figure 17).

Inhibition of Transcription Factor Sp1 Leads to Maladaptation of Endothelial Cells to Mechanical Strain

To examine the role of Sp1 in the response to mechanical strain cells were incubated with mithramycin for 1 hr prior to mechanical loading for 24 hrs. Mithramycin is an antibiotic that has been used to treat certain cancers [129]. The drug binds to CG-rich regions of the DNA and prevents the binding of Sp1 [130]. Pretreatment of cells with mithramycin led to an increase in cell damage due to mechanical loading. Both cell attachment (Figure 37a) and LDH release in the media (Figure 37b) were observed as a result of mechanical strain on mithramycin treated cultures. The conditioned media and cell lysates were analyzed for perlecan and heparanase expression revealing a decrease in both perlecan and heparanase in the mithramycin treated, non-loaded cells (Figure 38). An increase in both perlecan and heparanase was found in the treated, loaded cell (Figure 38).

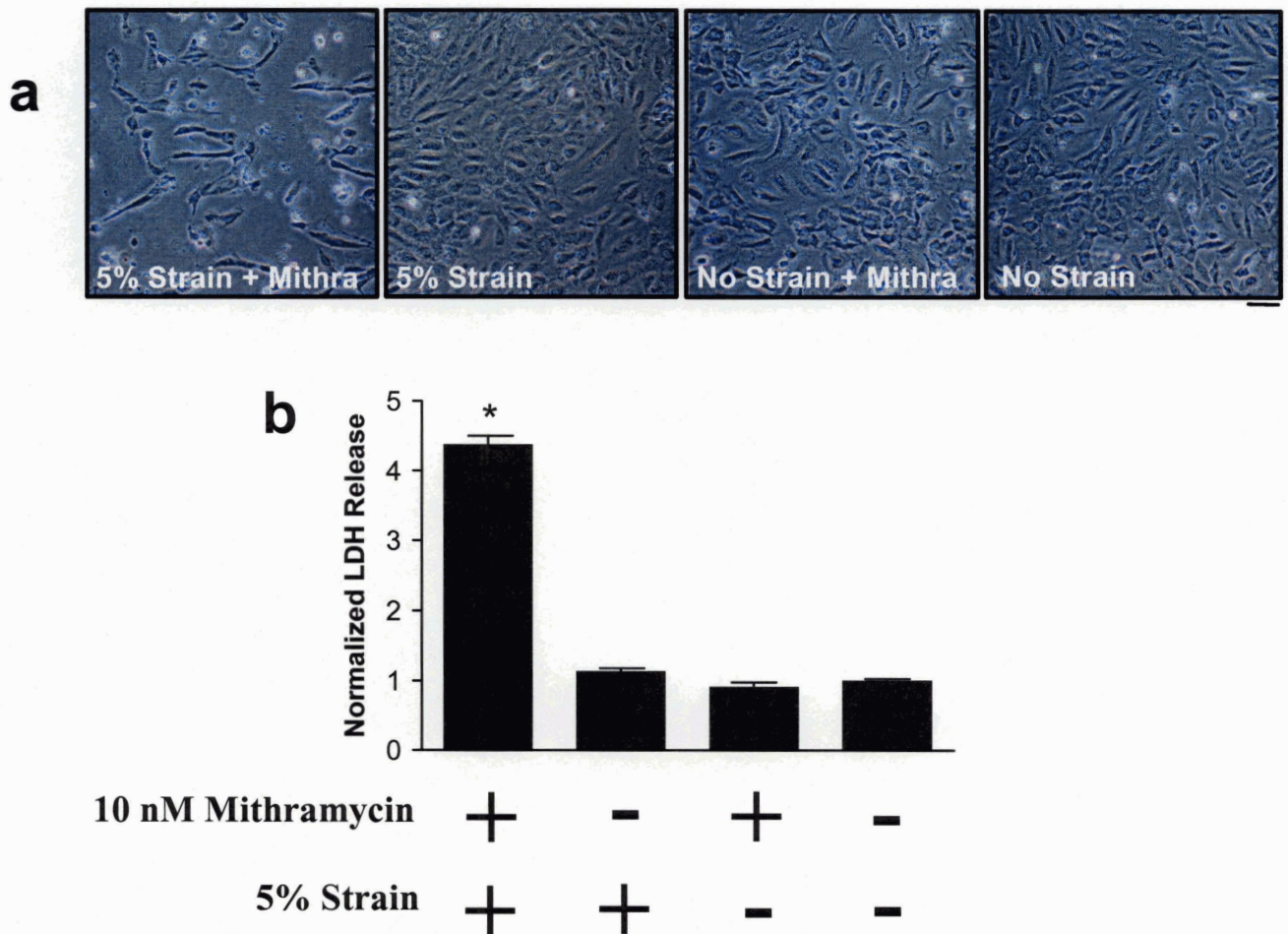


Figure 37. Mithramycin and mechanical load together cause cell detachment and lactate dehydrogenase (LDH) release. (a) Phase contrast microscopy of cells treated with combinations of load and mithramycin. (b) Total LDH release into culture media of treated cell cultures (normalized to no strain controls).

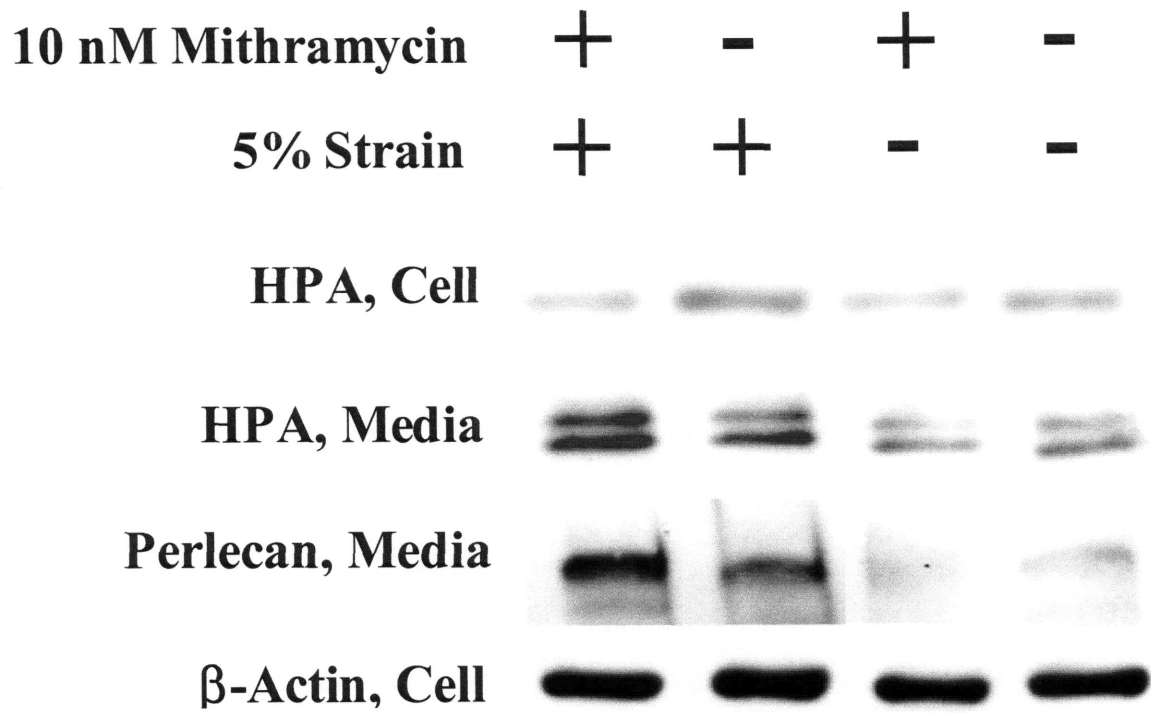


Figure 38. Control of perlecan and heparanase (HPA) expression by mechanical strain in mithramycin treated cells.

Discussion

An initial control experiment revealed that mechanical strains of 5% or less for 24 hrs did not cause cytotoxicity. This is an important control not only for the interpretation of our experiments but also those present in the literature. Papers in the literature routinely report strain levels of 20% or more using the Flexcell system without measuring cytotoxicity. As a consequence these studies may be looking at an injury response of the endothelial cells rather than a physiologic response to increased hemodynamic stimuli.

We began our studies with an experiment examining the role of physiologic loading on endothelial inhibition of vascular smooth muscle cell proliferation. In humans the maximal strain, in the aorta varies along the aorta from around 18% in the ascending aorta to 4-15% in the abdominal aorta [131, 132]. With chronic hypertension or diabetes this strain can decrease by 40-60% due to arterial stiffening [131]. Our studies revealed that mechanical strain increased endothelial production of inhibitory factors towards vascular smooth muscle cells. Heparan sulfate proteoglycans have been shown to be an essential component of endothelial inhibition of vascular smooth muscle cells [6]. A major question is the source of the additional heparan sulfate proteoglycan found in the media. The studies quantifying the mRNA levels in mechanically strained cells would indicate that the syndecans are transcriptionally regulated but heparanase and perlecan are not. Notably, multiple studies have shown heparan sulfate proteoglycan core proteins are known to show alterations in protein level without alterations in mRNA [77]. In one study a 10-fold change in protein was observed without a change in mRNA levels [133]. Various forms of post-transcriptional regulation may act on these genes as well as potential alterations in protein stability or degradation.

The presence of additional perlecan is likely due to increased production rather than purely release from the extracellular matrix. Our studies on FGF-2 binding to the matrix indicate a reduction in bound FGF-2 to the extracellular matrix but our measurements of heparan sulfate in the matrix show increased heparan sulfate. The growth medium used in these experiments was complete growth medium containing serum and FGF-2 supplements. As a consequence there is likely an excess amount of FGF-2 in the growth media and this could saturate any potential binding sites for FGF. Perlecan is the major heparan sulfate proteoglycan in the endothelial extracellular matrix [3]. Heparan sulfate proteoglycans are the primary binding site for FGF-2 in this type of extracellular matrix [134]. These results are somewhat paradoxical unless we consider that the endothelium is acting as a barrier layer (after reaching confluency) preventing media FGF-2 binding to matrix. This would imply that the endothelium is increasing FGF-2 uptake from the matrix in response to load and would also be consistent with our observation that the FGF in the conditioned media remains constant. Syndecan-4 has been shown to be important in the endocytosis of FGF-2 and the increased FGF-2 uptake by the cell may be result of increased cell surface syndecan-4 [135].

Another potential source of increased vascular smooth muscle cell inhibition is the increased shed syndecan-1 observed as a consequence of mechanical strain. Shed syndecan-1 has been shown to be an effective inhibitor of FGF-2 signaling [84]. Syndecan-1 was found to be upregulated transcriptionally and on the cell surface by western blotting. Cell surface syndecan-1 has been shown to be important for the adhesion to collagen type-I [86]. The silastic membrane used in these experiments were coated with type-I collagen and these results would be consistent with the idea that the

cells were increasing the strength of attachment to this substrate in response to mechanical load. A similar argument could be made for the upregulation of syndecan-4 that was observed as well. Mechanical strain has been shown to increase formation of focal adhesions and stress fibers [15]. Syndecan-4 is intimately involved in these processes and has been shown to respond to stretch and injury in vascular smooth muscle cells [94]. Heparanase has also been shown to act as an adhesion molecule by binding to cell surface heparan sulfate proteoglycans independent of its enzymatic activity [136]. The syndecans can bind heparanase and may act synergistically to allow the cells to properly alter their adherence to the substratum to allow cell survival under loading conditions.

The activation of TGF- β observed in response to mechanical load could also serve to inhibit vascular smooth muscle cell proliferation. Active TGF- β has been shown to regulate vascular smooth muscle growth and may act as either an inhibitor or an stimulator depending on the growth state of the cells [137, 138]. Heparan sulfate has been shown to facilitate the activation of TGF- β [57] and the increased cell surface proteoglycans and extracellular heparan sulfate may play a role in this process. It is also interesting to note that MMP-2 activation is enhanced by syndecan-1, giving another potential role to the regulation pattern observed for the syndecans [139]. The syndecans can also function as regulators of growth factor response and transmembrane signaling [11]. Syndecan-2 interacts with TGF- β via a protein-protein interaction but the exact nature and purpose of this interaction is unclear [85]. Studies have shown that the type III receptor for TGF- β (betaglycan) is stabilized in the membrane by syndectin. Syndecan-2 competes for binding to syndectin and may disregulate TGF- β signaling [11, 85]. Our

results show a reduction in mRNA for syndecan-2, implying that the cell may have an increases sensitivity and response to TGF- β stimulation.

Our in-vitro studies also indicate a role for the transcription factor Sp1 in the response to mechanical strain. Inhibition of Sp1 binding led to sensitization of the cells to load. Sp1 binding sites (GC boxes) are located in the promoter regions of heparanase[140], perlecan[141], syndecan-1[142], and syndecan-4[143]. Endothelial Sp1 phosphorylation and DNA binding has been shown to be increased in response to fluid shear stress[144], and, in our work, the total Sp1 increased with mechanical strain. We show here that inhibition of Sp1 leads to maladaptation of endothelial cells to mechanical strain leading to cell damage and detachment. This result highlights the critical nature of Sp1 activation in controlling the cell response to mechanical strain. While many genes have Sp1 transcription factor binding domains in their promoter regions, our work shows that the syndecan core proteins are highly responsive to mechanical stimuli. The transcription factor Sp1 and TGF- β induced Smads have been shown to interact and facilitate gene transcription [62] and may present a model of regulation for the heparan sulfate proteoglycan protein increase observed in these studies. Another potential mechanism is the regulation of the Kruppel-like factor (KLF) family of transcription factors that has been shown bind sequences similar to Sp1 and has been shown to be important for response to mechanical stimuli [145].

A major contribution of this work is the elucidation of the mechanotransduction pathway governing the response of heparan sulfate proteoglycan to mechanical strain. Our results indicate that optimal stimulation of MAPK requires p38 signaling and autocrine TGF- β . Similarly, optimal p38 MAPK signaling requires MAPK and autocrine

TGF- β . Finally, TGF activation and stimulation of phospho-Smad-2 is partially blocked by inhibitors to both of these pathways. These results taken together suggest a signaling model in which MAPK and p38 are important for activation of TGF- β and that TGF- β is important for the continued stimulation of MAPK and p38 pathways. Our experiments also suggest that this autocrine TGF- β signaling loop controls the increase in perlecan observed in response mechanical strain.

An overall model suggested by this work is shown in Figure 39. In this model a TGF autocrine signaling loop controls the response of cells through controlling heparan sulfate proteoglycan production. There is also some synergistic feedback in the system from the heparan sulfate proteoglycans acting to facilitate TGF activation and signaling potentially through MMP-2, heparan sulfate binding and downregulation of syndecan-2. Prior work has shown that mechanical stimuli may increase vascular smooth muscle cell proliferation through multiple mechanisms [127, 146-148]. Taken along with previous studies, our work fills in the endothelial side of a dynamic equilibrium which controls vascular remodeling to load. Explicitly, mechanical strain stimulates vascular smooth muscle cells to proliferate while in causing endothelial cells to increase their inhibition. These two processes lead to a balance between growth and inhibitory processes that can control vascular homeostasis. In hypertension, this increased activity would make the artery more vulnerable to disease processes that causing endothelial dysfunction. In this case the endothelial side of the balance would be compromised leaving the vascular smooth muscle cell growth uncompensated by endothelial inhibition.

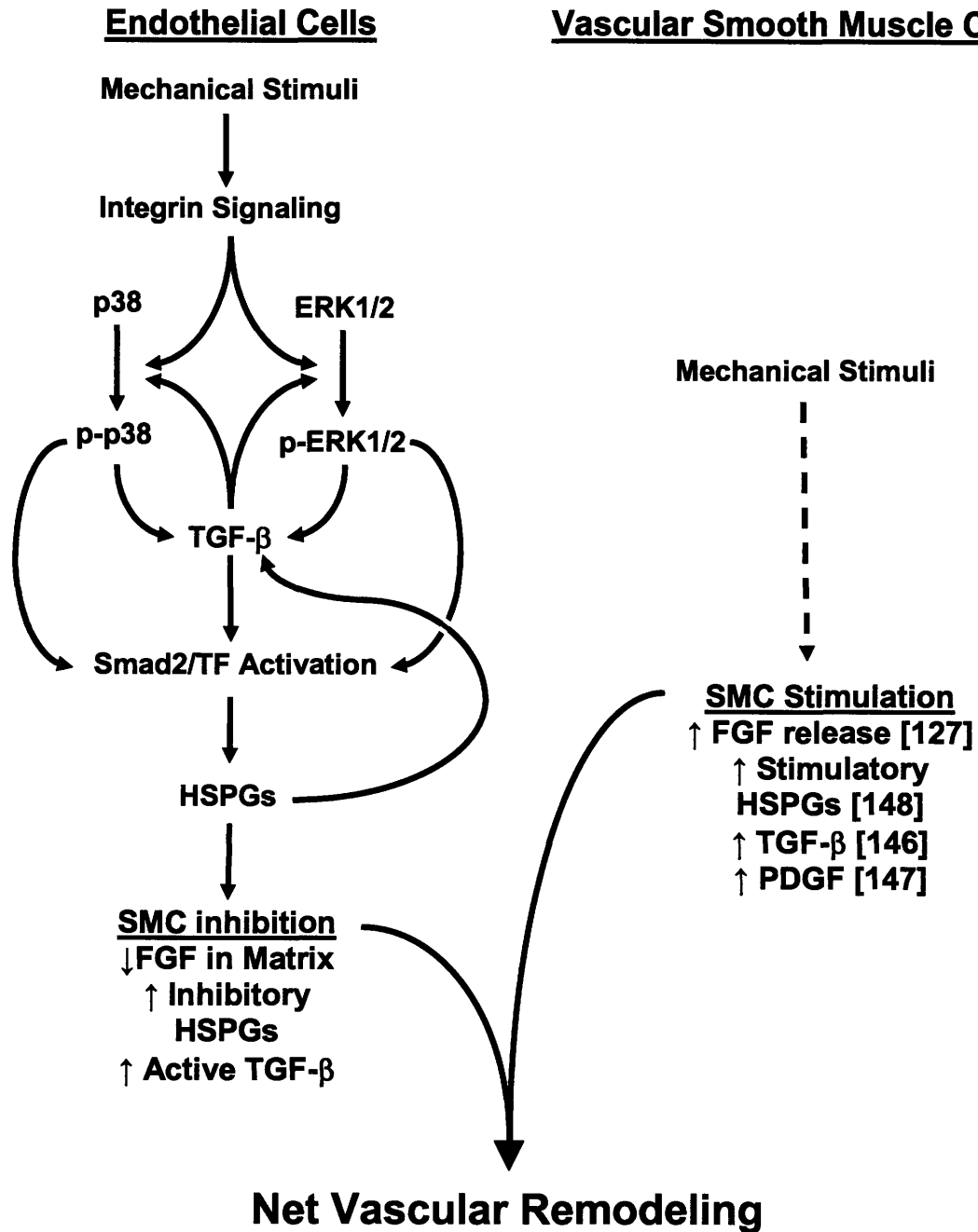


Figure 39. Overall mechanistic scheme of endothelial control of vascular remodeling to mechanical stimuli. This study supports the signaling network outlined underneath the endothelial cell portion of this scheme.

Conclusion

In this chapter, we gave evidence for a unified model of vascular response to mechanical forces in which mechanical stimuli enhanced both endothelial inhibition and vascular smooth muscle cell proliferation. We given evidence that supports that underlying the endothelial side of this balance is the regulation of heparan sulfate proteoglycans by an autocrine signaling loop consisting of TGF- β as well as the MAPK and p38 signaling pathways. In the next chapter we explore this model further in-vivo in an animal model of hypertension.

Chapter 4: Role of Heparan Sulfate Proteoglycans and Heparanase in Spontaneously Hypertensive Rats

Introduction

Hypertension, or elevated blood pressure, is the most common primary diagnosis in the United States affecting about 50 million people in the country and

Table 1. Classification of Blood Pressure in Adults

BP Classification	SBP (mmHg)	DBP (mmHg)
Normal	<120	and <80
Prehypertension	<120-139	or 80-89
Stage 1	140-159	or 90-99
Hypertension		
Stage 2	≥ 160	Or ≥ 100
Hypertension		

BP, blood pressure; SBP, systolic blood pressure; DBP, diastolic blood pressure.

1 billion people worldwide [149, 150]. Hypertension is classified into stages based on systolic (SBP) and diastolic blood pressure (DBP) as shown in Table 1 (adapted from [150]). A strong relationship exists between blood pressure and heart attack, heart failure, stroke and kidney disease. Each increment of 20 mmHg in systolic blood pressure or 10 mmHg in diastolic blood pressure doubles the risk of cardiovascular events [151].

In the previous chapter, a set of experiments were performed that gave rise to a model of vascular response to mechanical strain. The aim of this section is to take this model developed in in-vitro and examine its relevance in the spontaneously hypertensive rat model of hypertension. To this end, we examined the expression of heparan sulfate proteoglycans, heparanase, TGF- β and the phosphorylated intracellular signaling intermediates Smad-2, ERK1/2 and p38 MAPK in hypertensive and normal rats.

Materials and Methods

Animal Model of Hypertension. All experimental procedures and protocols used in this investigation were reviewed and approved by the Animal Care and Use Committee of the Massachusetts Institute of Technology and conformed to the “Guiding Principles in the Care and Use of Animals” of the American Physiological Society and the NIH *Guide for the Care and Use of Laboratory Animals*. Age matched Wild-Type Wistar-Kyoto Rats and Spontaneously Hypertensive (SHR; NTac:SHR) rats were obtained from (Taconic, Germantown, NY). At 20 weeks of age the animals were sacrificed and the aortae were harvested. A total of 16 rats from each group were used in these experiments.

Immunohistochemistry. The abdominal aortae from hypertensive rats were formalin fixed and sectioned using standard methods. The sections were heated for 10 min in a 60°C oven, deparaffinized in xylene, and rehydrated. Antigen retrieval was performed by placing the slides in 10mM citrate buffer (pH = 6.0) and heating in the microwave for 10 min. The samples were allowed to cool for 20 min and were then incubated in 3% hydrogen peroxide for 10 min. The samples were rinsed 3 times with PBS with 0.01% tween-20 (PBST) between each of the following steps. The sections were blocked with 20% normal goat serum for 45 minutes at room temperature. For staining of heparan sulfate proteoglycans the slides were treated for 2 hrs with a 0.4 U/ml solution of heparitinase III (Ibex, Canada). Primary antibodies were diluted in PBS containing 1% BSA, applied to slides, and incubated in a humid chamber for overnight at 4°C. The following antibodies were used for staining: an anti-heparanase (Cell Sciences, Canton, MA); a monoclonal antibody recognizing “stubs” of digested heparan sulfate (3G10;

Seikagaku); an anti-TGF- β 1 antibody (product #G122A; Promega, Madison WI); an anti-phospho-Smad-2 (Ser465/467; 138D4; Cell Signaling); an anti-phospho-p38 MAPK (Thr180/Tyr182; 12F8; Cell Signaling); anti-phospho-p44/42MAPK (Thr202/Tyr204; 20G11; Cell Signaling); and anti-sp1 (1C6; Santa Cruz Biotechnology). Secondary antibody staining at detection was performed using the LSAB 2 kit (DakoCytomation, Carpinteria, CA) according to the manufacturer's instructions. An AEC substrate (DakoCytomation) was used for detection of the horseradish peroxidase conjugate. The samples were counterstained in Mayer's hematoxylin for 3 min, washed with tap water, and mounted in aqueous mounting medium (DakoCytomation). After 24 hrs the sections were mounted and coverslipped with Cytoseal XYL (8312-4; Richard Allen Scientific, Kalamazoo, MI).

Quantitative Morphology. To quantify the immunohistochemical staining the sections were first imaged using an Olympus BX41 (Olympus, Melville, NY) with a DP70 CCD (Olympus). The images were captured using Microsuite Biological Suite 2.4 (Olympus). The images were quantified using Photoshop (Adobe Systems, Inc., San Jose, CA). To perform the quantitation of DAB or AEC substrate staining, the region of interest was selected using the magic wand tool in Photoshop (Adobe). The average intensity of each color channel was recorded (red, green, or blue) and number of pixels (area) were taken using the histogram function. A similar reading was taken for the background (white field) of each captured picture. The optical density (OD) was calculated using the following equation:

$$OD = -\log_{10}\left(\frac{I}{I_0}\right)$$

Where I is the color channel intensity and I_o is the color channel intensity of the background. A deconvolution matrix to separate DAB or AEC and hematoxylin staining was calculated using the method of Ruifrok and Johnston [152]. These matrices were used to separate the hematoxylin staining from immunostaining and give an overall density of staining within the region of interest.

Statistics. All results are shown as mean \pm standard deviation. An ANOVA was used to make comparisons between groups of continuous variables. A two-tailed Student's t test was used to make comparisons between groups; $p < 0.05$ was defined as being statistically significant. The Pearson product moment correlation statistic was used as a measure of correlation between variables.

Results

Hypertension Increases Heparan Sulfate Proteoglycan and Heparanase Expression in the Endothelium of Spontaneously Hypertensive Rats

To evaluate the role of heparan sulfate proteoglycans and heparanase in modulating arterial remodeling in hypertension, we examined the expression of heparan sulfate proteoglycans and heparanase in the spontaneously hypertensive (SHR) rats compared with age-matched Wistar-Kyoto (WKY) wild-type rats. Formalin fixed, paraffin embedded sections were made from rat aortae from each group. The sections were stained with hematoxylin and eosin and analyzed morphologically. This analysis revealed increased medial thickening in the medial region of the SHR rat aortae (Figure

40). The expression of total heparan sulfate proteoglycans was quantified immunohistochemically with an antibody that recognized the “stub” left over after digestion with heparitinase III. In the SHR and WKY animals the media, basement membrane, and endothelial layer stained heavily for heparan sulfate proteoglycan (Figure 41). The intensity of staining in the endothelial and basement membrane layers was quantified and compared between animals, indicating an increase in endothelial heparan sulfate proteoglycan staining of 58% in comparing the SHR rats to WKY controls. A similar analysis was performed following immunohistochemical staining for heparanase and an increase in heparanase expression of hypertensive rats was found to be two fold increased versus control rats (Figure 42). Local medial thickness correlated strongly with local endothelial heparanase staining (Figure 43; $R = 0.879$, $p < 0.0005$).

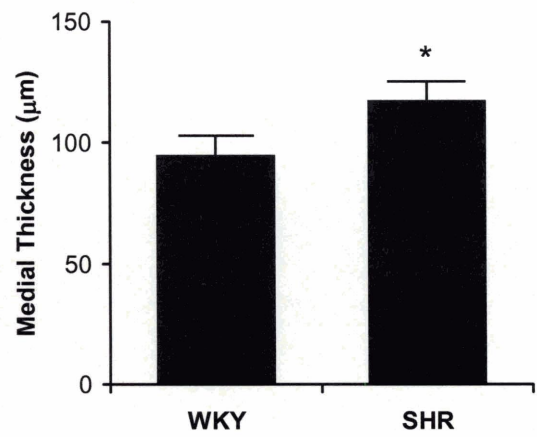
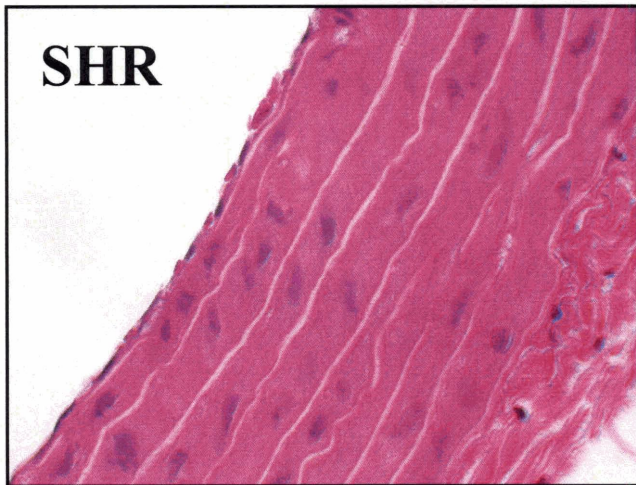
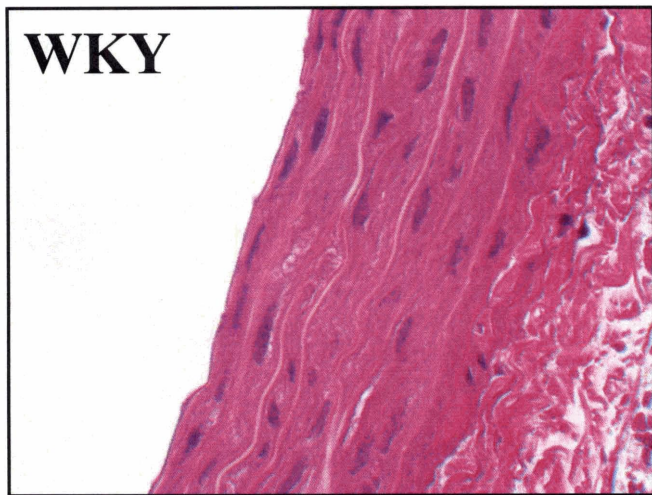


Figure 40. Hematoxylin and eosin staining of Wistar-Kyoto (WKY) and spontaneously hypertensive (SHR) rat aortae.

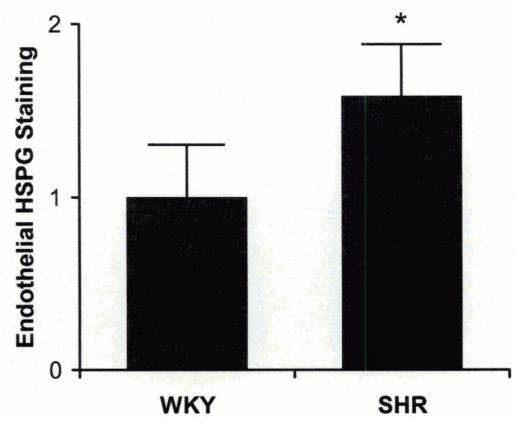
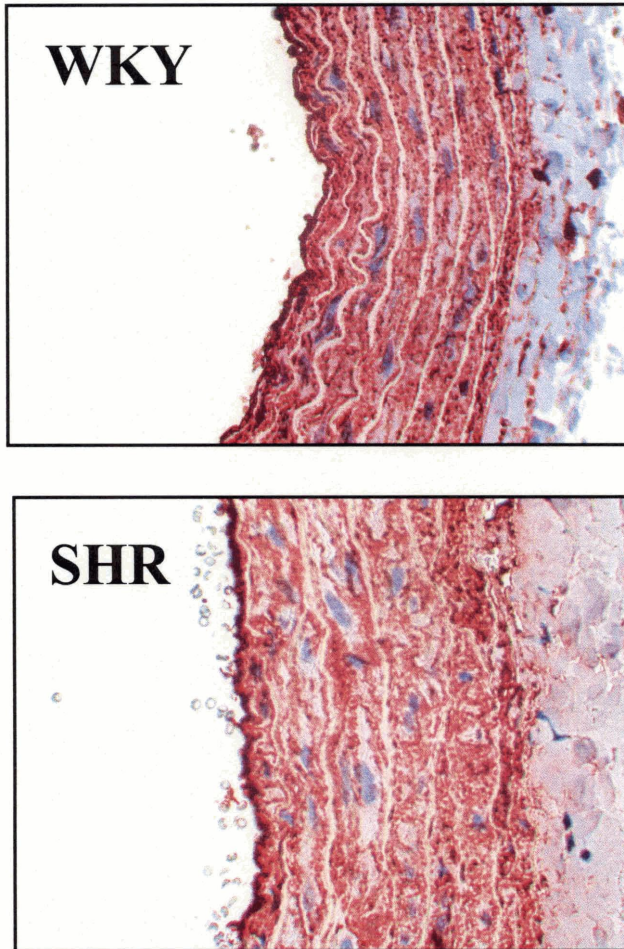


Figure 41. Immunohistochemical staining for heparan sulfate epitopes in Wistar-Kyoto (WKY) and spontaneously hypertensive (SHR) rat aortae. *Statistically significant comparison ($p < 0.05$).

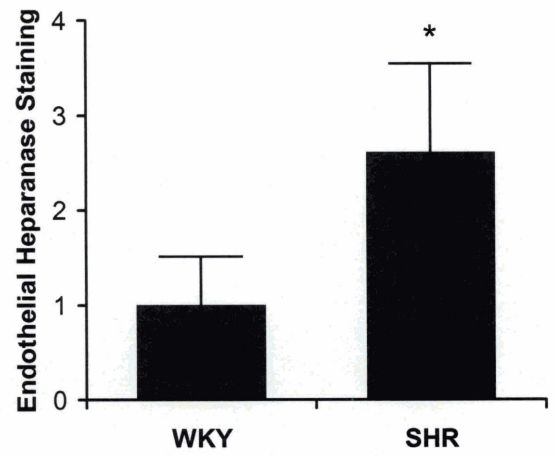
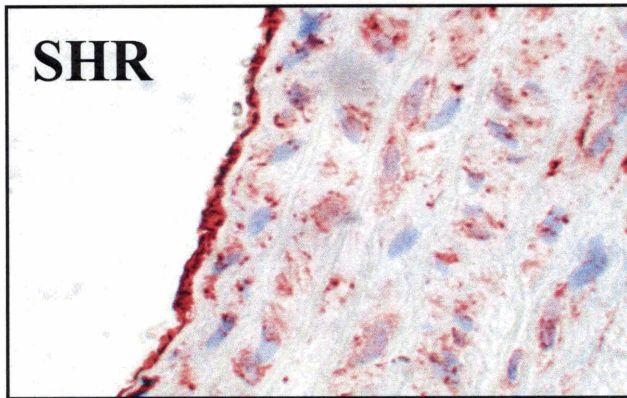
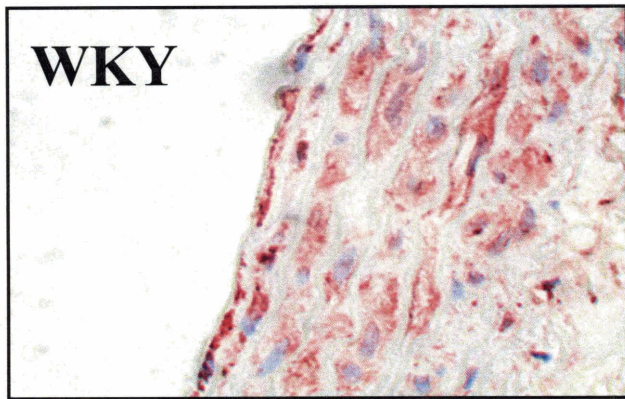


Figure 42. Immunohistochemical staining for heparanase in Wistar-Kyoto (WKY) and spontaneously hypertensive (SHR) rat aortae. *Statistically significant comparison ($p < 0.05$).

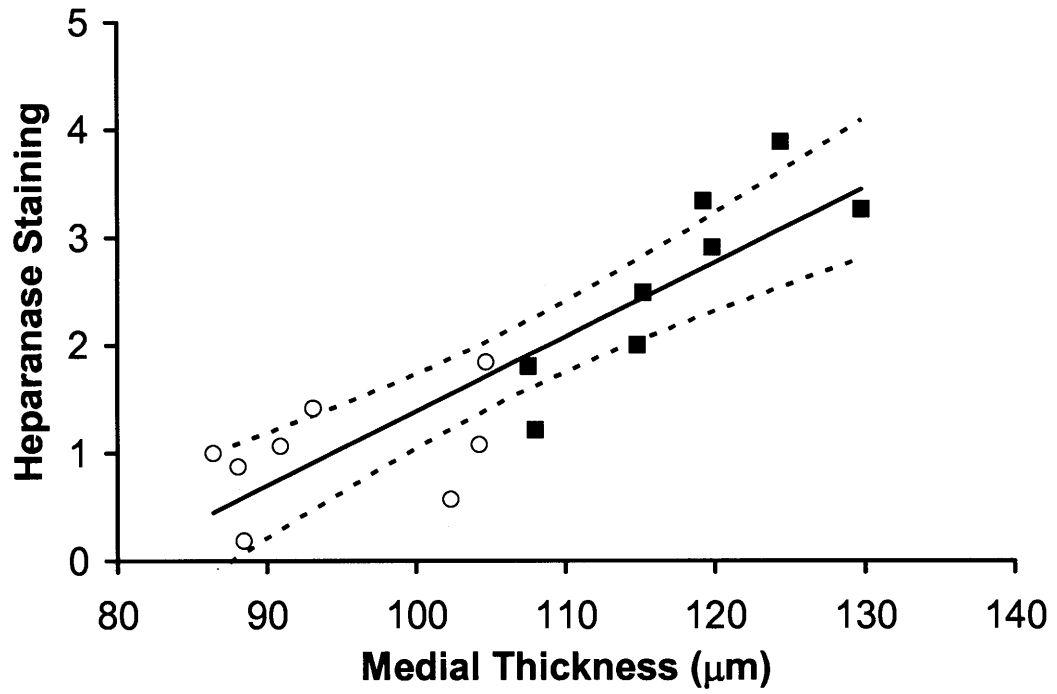


Figure 43. Quantitative morphometry of vessel remodeling in SHR and WKY rats. Correlation between medial thickening and endothelial heparanase expression in SHR (■) and WKY (□) rats.

Hypertension Alters Transforming Growth Factor-Beta Expression and Phosphorylation State of Intracellular Signaling Intermediates

In our studies hypertension causes a redistribution of TGF- β within the aorta. In the hypertensive animals the endothelial staining for TGF- β was increased and the medial staining reduced (Figure 44). A similar distribution of staining was found for phosphorylated Smad-2, a downstream element of TGF- β receptor signaling (Figure 45). Immunohistochemical staining also revealed an increase in endothelial staining for phosphorylated p38 MAPK and ERK (Figure 46 and Figure 47). The amount of total Sp1 was found to increase in the hypertensive animals as well (Figure 48).

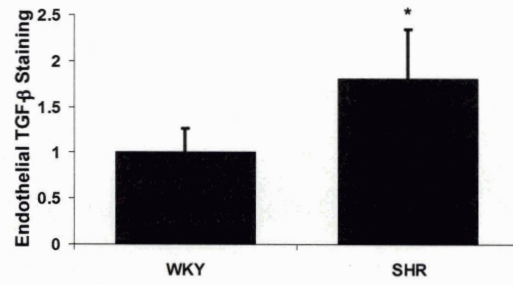
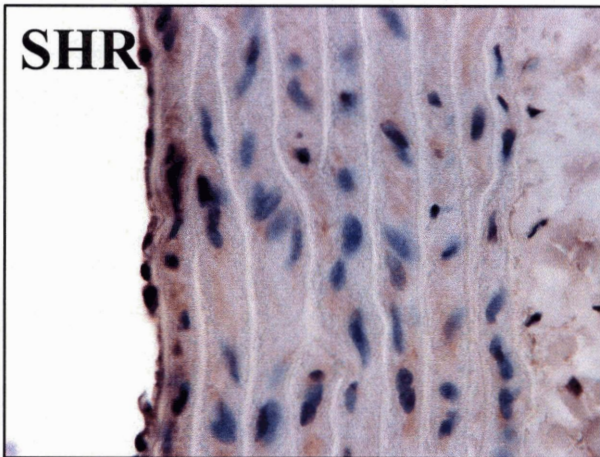
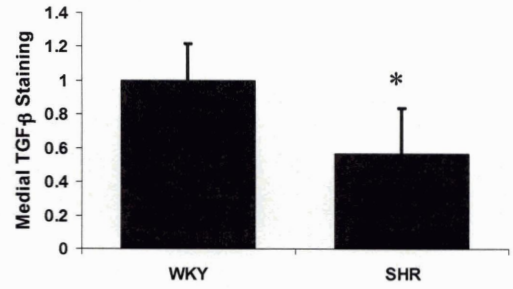


Figure 44. Immunohistochemical staining for TGF- β in Wistar-Kyoto (WKY) and spontaneously hypertensive (SHR) rat aortae (* $p < 0.05$, $n = 4$).

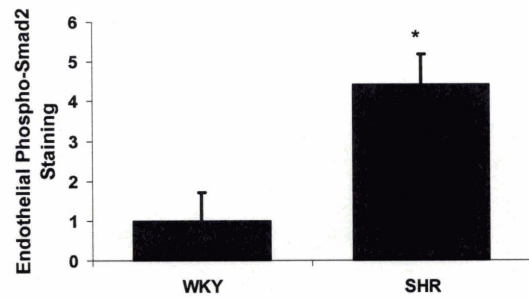
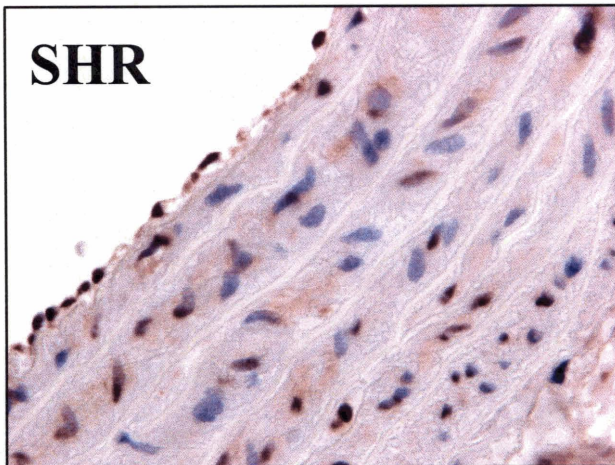
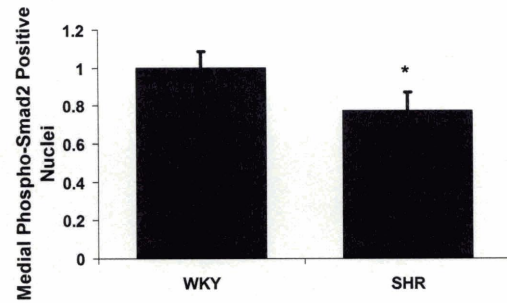


Figure 45. Immunohistochemical staining for phosphorylated Smad-2 in Wistar-Kyoto (WKY) and spontaneously hypertensive (SHR) rat aortae (* $p < 0.05$, $n = 4$).

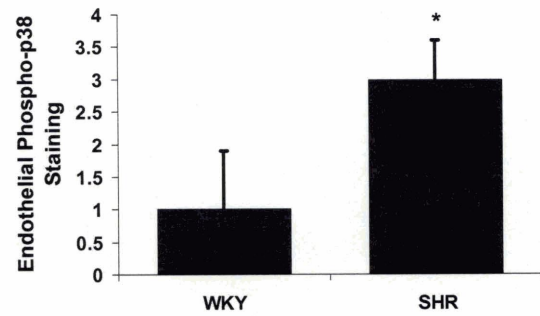
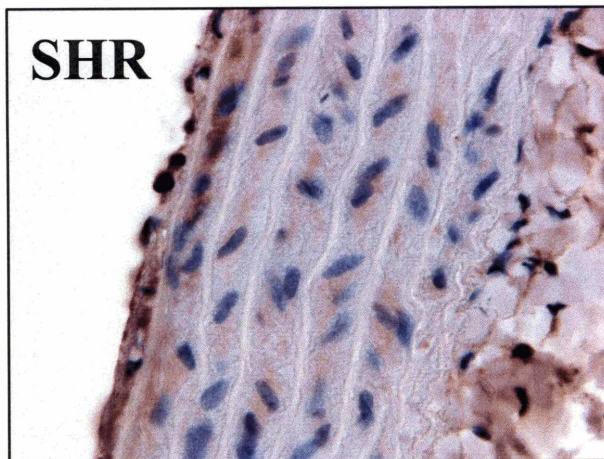
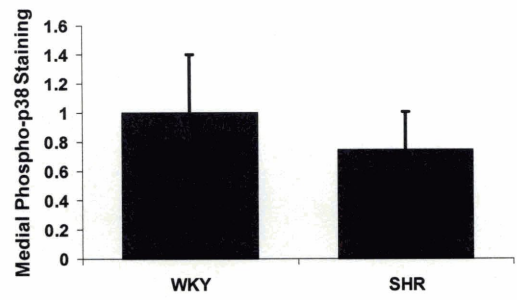
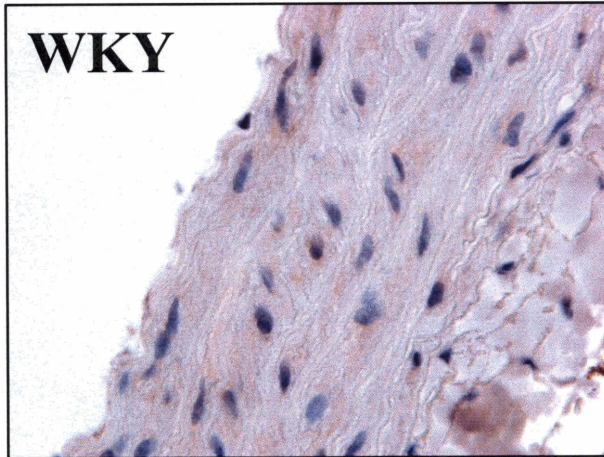


Figure 46. Immunohistochemical staining for phosphorylated p38 in Wistar-Kyoto (WKY) and spontaneously hypertensive (SHR) rat aortae (* $p < 0.05$, $n = 4$).

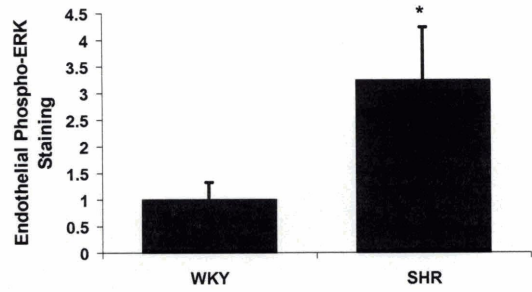
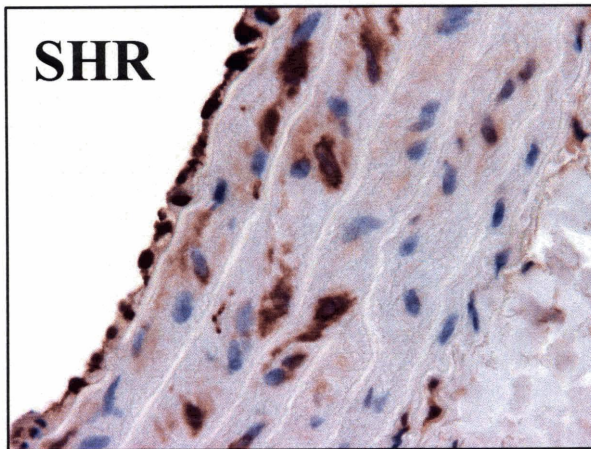
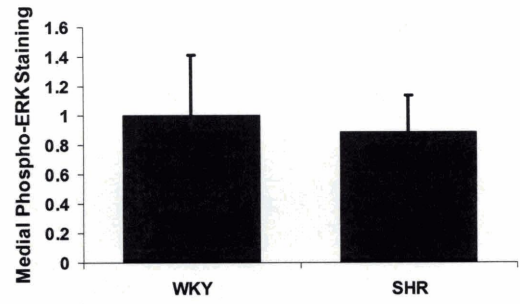
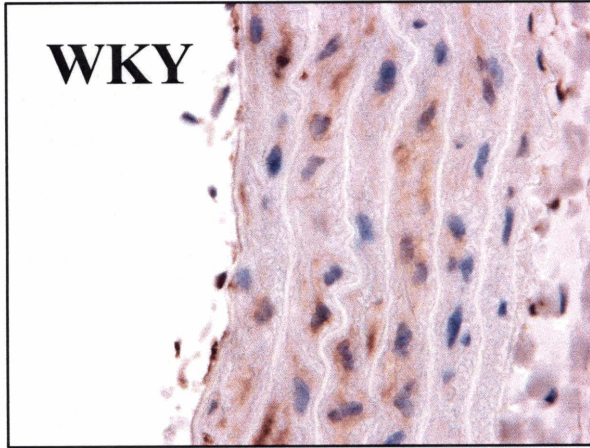


Figure 47. Immunohistochemical staining for phosphorylated ERK in Wistar-Kyoto (WKY) and spontaneously hypertensive (SHR) rat aortae ($p < 0.05$, $n = 4$).

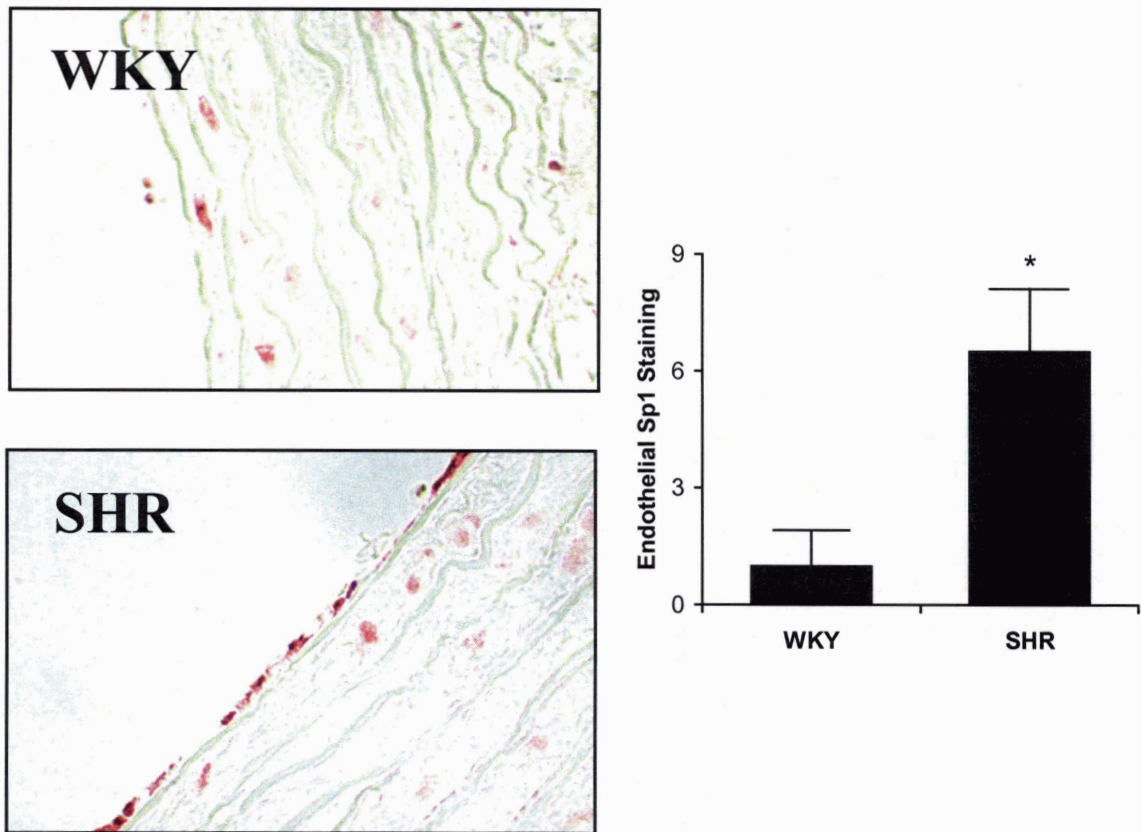


Figure 48. Immunohistochemical staining for transcription factor Sp1 in Wistar-Kyoto (WKY) and spontaneously hypertensive (SHR) rat aortae ($p < 0.05$, $n = 4$). No counterstain was used in this staining.

Correlation Analysis of Immunocytochemical Staining

To establish relationships between the various signaling factors examined in this work we performed a correlation analysis. This analysis revealed strong correlations between medial thickness, p38, ERK, and TGF- β in the endothelium (shown in Table 2, Figure 49, and Figure 50). Correlations values (R) range from 0.7 to 0.9 with a p-value less than 0.05. A similar analysis was performed examining the medial staining but no significant correlations were found (Table 3).

Table 2. Correlation Analysis of Immunohistochemical Staining of the Endothelium

Correlation Matrix (R)					
	<i>p-ERK</i>	<i>p-p38</i>	<i>TGF-β</i>	<i>p-Smad2</i>	<i>Medial Thickness</i>
Phospho-ERK	1.000	0.817	0.740	0.790	0.729
Phospho-p38	0.817	1.000	0.793	0.967	0.890
TGF-β	0.740	0.793	1.000	0.793	0.902
Phospho-Smad2	-0.511	-0.846	-0.631	1.000	-0.694
Medial Thickness	0.729	0.890	0.902	0.856	1.000
t Statistic					
	<i>p-ERK</i>	<i>p-p38</i>	<i>TGF-β</i>	<i>p-Smad2</i>	<i>Medial Thickness</i>
p-ERK	-	3.471	2.692	2.882	2.610
p	3.471	-	3.191	8.497	4.793
TGF-β	2.692	3.191	-	2.912	5.106
p-Smad2	1.329	3.549	1.819	-	2.153
Medial Thickness	2.610	4.793	5.106	3.707	-
Correlation Significance (P)					
	<i>p-ERK</i>	<i>p-p38</i>	<i>TGF-β</i>	<i>p-Smad2</i>	<i>Medial Thickness</i>
p-ERK	-	0.013	0.036	0.035	0.040
p-p38	0.013	-	0.019	0.000	0.003
TGF-β	0.036	0.019	-	0.033	0.002
p-Smad2	0.241	0.016	0.129	-	0.084
Medial Thickness	0.040	0.003	0.002	0.014	-

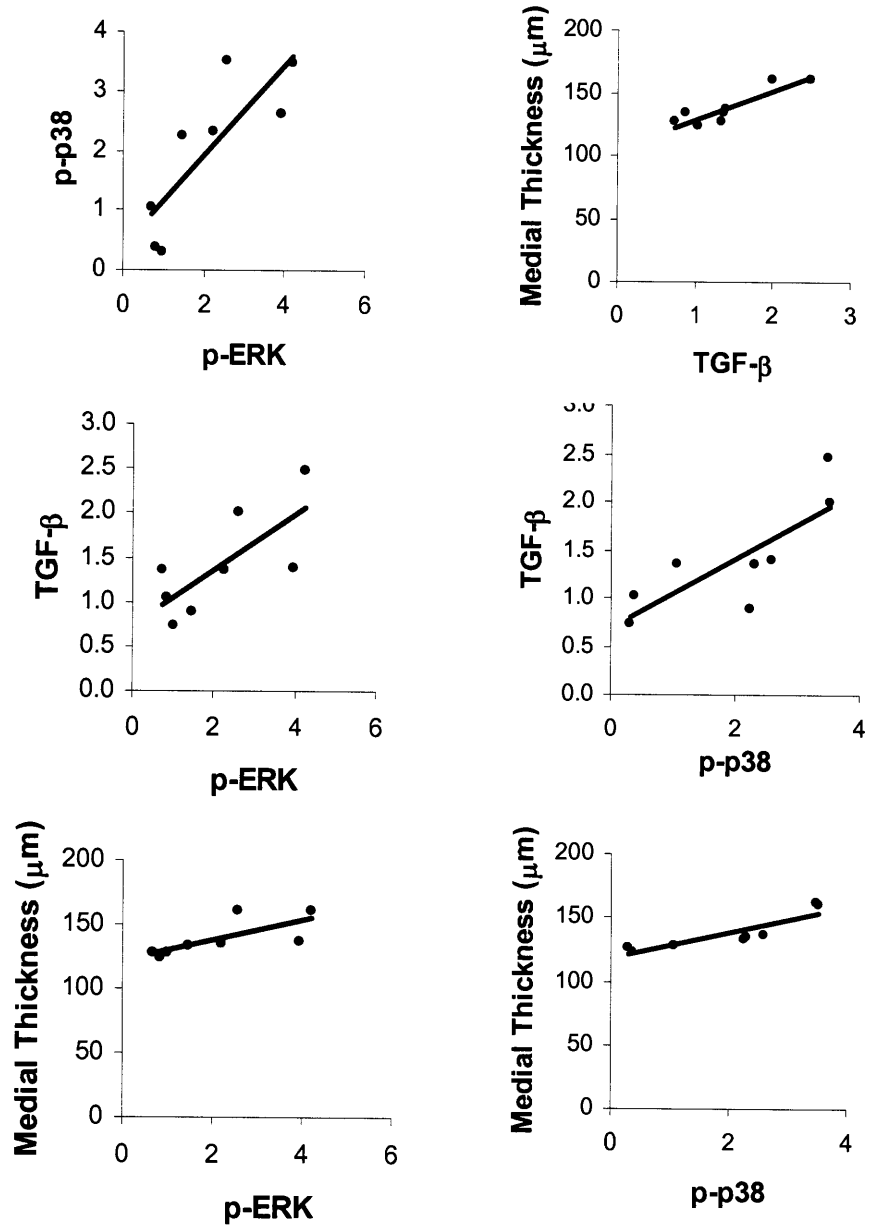


Figure 49. Correlation scatterplots for statistically significant correlations on the immunohistochemical staining of the endothelium on Wistar-Kyoto and spontaneously hypertensive rats.

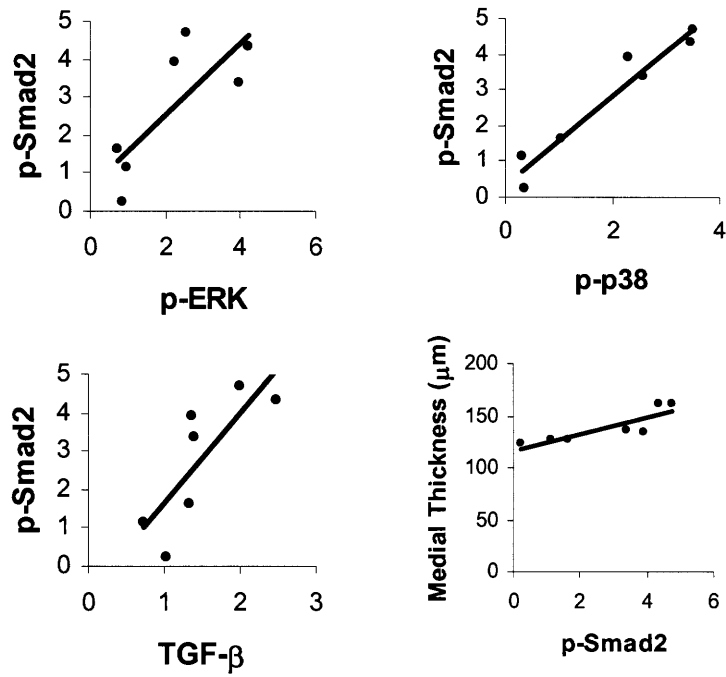


Figure 50. Correlation scatterplots for statistically significant correlations on the immunohistochemical staining of the endothelium on Wistar-Kyoto and spontaneously hypertensive rats.

Table 3. Correlation Analysis of Immunohistochemical Staining of the arterial media.

Correlation Matrix (R)					
	<i>p-ERK</i>	<i>p-p38</i>	<i>TGF-β</i>	<i>p-Smad2</i>	<i>Medial Thickness</i>
<i>p-ERK</i>	1.000	-0.016	-0.084	0.790	-0.480
<i>p-p38</i>	-0.016	1.000	0.214	0.967	-0.141
<i>TGF-β</i>	-0.084	0.214	1.000	0.793	-0.095
<i>p-Smad2</i>	0.482	0.677	0.519	1.000	-0.694
<i>Medial Thickness</i>	-0.480	-0.141	-0.095	0.856	1.000

t Statistic					
	<i>p-ERK</i>	<i>p-p38</i>	<i>TGF-β</i>	<i>p-Smad2</i>	<i>Medial Thickness</i>
<i>p-ERK</i>	-	0.040	0.207	1.229	1.342
<i>p-p38</i>	0.040	-	0.538	2.057	0.349
<i>TGF-β</i>	0.207	0.538	-	1.359	0.235
<i>p-Smad2</i>	1.229	2.057	1.359	-	2.153
<i>Medial Thickness</i>	1.342	0.349	0.235	2.153	-

Correlation Significance (P)					
	<i>p-ERK</i>	<i>p-p38</i>	<i>TGF-β</i>	<i>p-Smad2</i>	<i>Medial Thickness</i>
<i>p-ERK</i>	-	0.969	0.843	0.274	0.228
<i>p-p38</i>	0.969	-	0.610	0.095	0.739
<i>TGF-β</i>	0.843	0.610	-	0.232	0.822
<i>p-Smad2</i>	0.274	0.095	0.232	-	0.084
<i>Medial Thickness</i>	0.228	0.739	0.822	0.084	-

Discussion

The animal model of hypertension demonstrated an increase in heparanase and heparan sulfate proteoglycans in the endothelium of hypertensive rats. These results support that similar processes that control the in-vitro response to mechanical load may be governing the vascular response to hypertension. Both heparanase and heparan sulfate proteoglycans were increased in our in-vitro studies examining mechanical stretch on the endothelium.

TGF- β has been shown to be important in regulating the pathobiology of many vascular disorders [153]. Its role is made complex by its ability to act as both a stimulator and inhibitor of growth depending on other factors [137, 138]. Our results show increases in active TGF- β in the endothelium and a decrease in TGF- β in the media. Our previous in-vitro studies in Chapter 3 suggest that this may be due to the mechanically-induced activation of TGF- β by endothelial cells. These results support our paradigm of load increasing endothelial inhibition as well as increasing vascular smooth muscle cell proliferation. An interesting question not addressed in the current work is the reason for the loss of TGF- β in the media of the artery. Since the endothelial cell is producing a greater amount of TGF- β , it implies that the vascular smooth muscle cells are actively degrading or removing TGF- β .

The strong correlations between TGF- β and p38/ERK support the occurrence of an autocrine signaling loop in the endothelium of the SHR rats. Spontaneously hypertensive rats are known to have medial hypertrophy in the aorta due to their hypertension that correlates with the local severity of the blood pressure increase [154].

The fact that the members of the TGF- β autocrine signaling loop correlates with the thickness of the vascular wall implies a relationship between this signaling and the in-vivo mechanical environment.

One fundamental question that remains from this work is the role of heparanase in controlling the vascular remodeling in response to hypertension. The strong correlation between the thickness of the aorta and the heparanase expression in the overlying endothelium indicates that the balance between heparanase and heparan sulfate proteoglycan plays a role in growth factor induced hyperplasia as well as proliferation. However, it is unclear whether heparanase expression serves as a means to increase the inhibition of the endothelial cell or as a pathophysiologic mechanism underlying the endothelial dysfunction in hypertension.

Conclusion

These results are consistent with our model of vascular remodeling to mechanical strain. The endothelium in hypertension showed increases in HSPG, TGF- β and intracellular signaling factors that matched well with the in-vitro results presented in Chapter 3. It is interesting to note that alterations occurred in the media as well as in the endothelium. This supports the notion that the vascular smooth muscle cells may be counteracting the increased inhibition of the endothelium by inactivating or degrading TGF- β . In this chapter we identified a close correlation between endothelial heparanase expression and vascular wall thickness. These results imply that heparanase may play an essential role in controlling vascular remodeling. We will explore the fundamental question of heparanase's role in vascular remodeling in more detail in the following chapter.

Chapter 5: Role of Heparanase in Vascular Remodeling

Introduction

Heparanase is an enzyme that degrades heparan sulfate infrequently to yield glycosaminoglycan chains that are 10-20 disaccharides in length. The aim of this section is to examine the role of heparanase expression in endothelial cells in the macrovascular system and in injury. The fundamental question is whether heparanase serves as an enhancer or inhibitor of vascular smooth muscle cell proliferation. To study this question, heparanase expression in endothelial cells was enhanced or inhibited using overexpression and siRNA vectors. To examine the role of heparanase in vascular remodeling we used an in-vivo model diabetes and vascular injury.

Materials and Methods

Cell Culture. Rat vascular smooth muscle cells (RVSMCs) were isolated from fresh or rat aortae. These cells were cultured in Dulbecco's Modified Eagle's Medium (DMEM, Gibco BRL Life Technologies, Gaithersburg, MD) supplemented with 5% calf serum (Hyclone, Logan UT) and 100 units per ml of penicillin, 100 µg per ml streptomycin sulfate, and 2 mM L-glutamine. Human umbilical vascular endothelial cells (HUVECs; Cambrex, Walkersville, MD) were grown in DMEM with 5% fetal bovine serum (Hyclone) and EGM-2 supplements (Cambrex). All smooth muscle cells were used at passages 4 to 5 and all endothelial cultures were used at passage 3 to 5. All cells were incubated at 37°C in a humidified atmosphere containing 5% CO₂.

Gene Silencing and Expression Vectors. Gene silencing for heparanase was performed using previously validated hairpin RNA sequence[116]. Briefly, oligonucleotides with the sequence 5'-

GATCCCCACTCCAGGTGGAATGGCCCTTCAAGAGAGGGGCCATTCC

ACCTGGAGTTTTTTGGAAA-3' and 5'-GATCCCCACTCCAGGTGGAATGGCCCTT

CAAGAGAGGGGCCATTCCACCTGGAGTTTTTTGGAAA-3' were hybridized and

cloned into a pSUPER expression vector (OligoEngine, Inc., Seattle, WA). Confirmation

of insertion of the siRNA sequence was performed using automated DNA sequencing by

the Biopolymers Laboratory at the MIT Center for Cancer Research, Cambridge, MA.

The full length cDNA for human heparanase in a pCMV6 vector was obtained from

Origene Technologies Inc. (Rockville, MD).

Transfection of HUVECs. Transfection of HUVECs was performed using Targefect F-2, according to the manufacturer's protocol (Targeting Systems, Santee, CA).

Transfection conditions were optimized using a pTRACER vector (Invitrogen) that constitutively expresses green fluorescent protein.

Animal Model of Vascular Injury. Zucker fatty (Crl:(ZUC)-faBR) and Zucker lean rats were used in an animal model of vascular injury and stenting in the presence of metabolic syndrome and insulin resistance[155]. At the time of stenting the rats were 12 and 14 weeks old for the fatty and lean rats, respectively. The rats were anesthetized using isoflurane, given a 100 U/kg dose of heparin, and a small incision was made to expose the right femoral artery. This artery was ligated and an arteriotomy was performed proximal to the ligature. A 0.014" angioplasty guidewire was passed into the aorta and an

9-mm long endovascular stent (Nirflex; Medinol Inc., Tel Aviv, Israel) mounted on a 15 x 2.5-mm angioplasty balloon (Crossail; Guidant Inc., Santa Clara, CA) was passed into the abdominal aorta (Figure 51). The stent was deployed with a 15 s inflation at 8 atm inflation pressure. Post-stenting the animals were given aspirin via drinking water at an approximate dose of 5 mg/kg/day. The animals were sacrificed at 14 days post-stenting using inhaled CO₂.

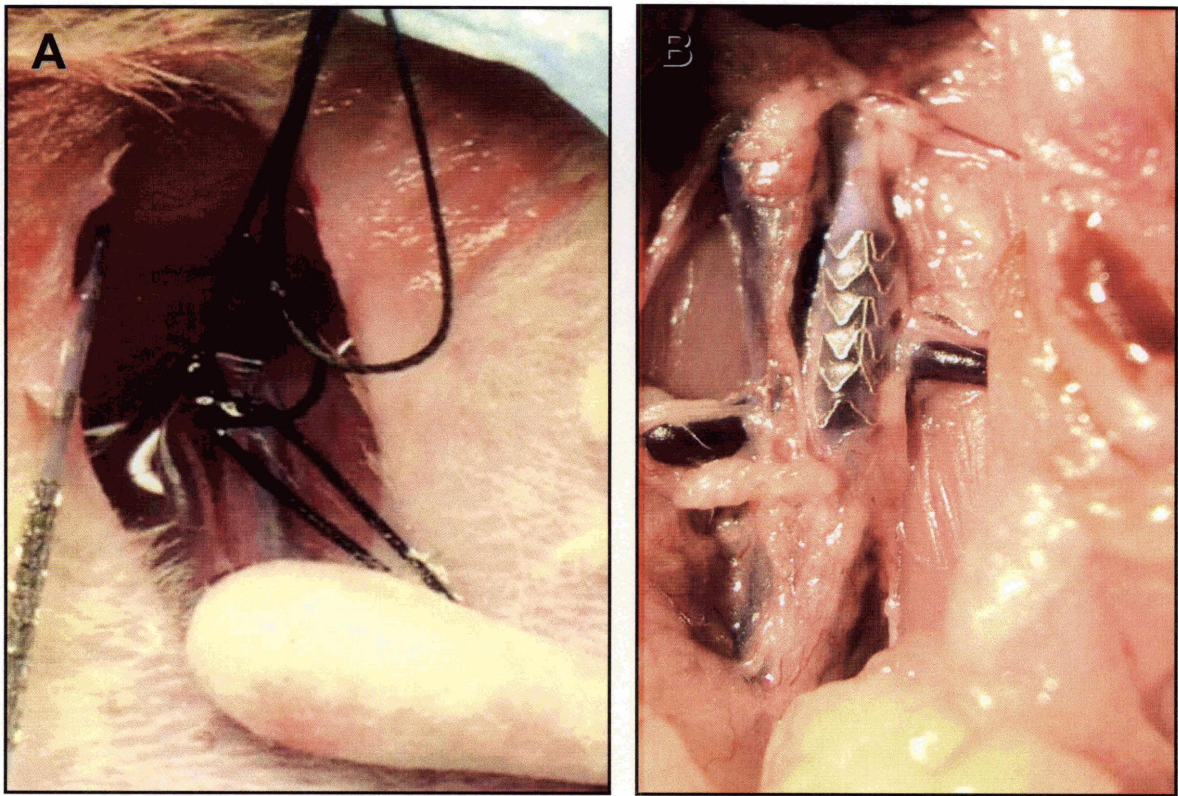


Figure 51. Photographs of the stenting procedure. A) The femoral arteriotomy prior to catheter insertion and stent placement. B) The stent in the abdominal aorta at time of harvest.

Smooth Muscle Cell Proliferation Assay. Rat smooth muscle cells were passaged into six-well plates at low density. Endothelial cell conditioned media was collected and used in an assay of vascular smooth muscle cell proliferation. Smooth muscle cells were serum starved in 0.5% calf serum for 24 hours, washed with PBS, and incubated in conditioned media with 1 $\mu\text{Ci/ml}$ ^3H -thymidine for 24 hours. The cells were then washed three times with PBS at 4°C. The cells were then incubated with 10% TCA for 30 min at 4°C, washed twice in 95% ethanol, and solubilized in 1 ml of 0.25 M NaOH with 0.1% SDS for 1 hour. The samples were then added to scintillation cocktail and radioactivity measured using a liquid scintillation counter.

Statistics. All results are shown as mean \pm standard deviation. An ANOVA was used to make comparisons between groups of continuous variables. A two-tailed Student's *t* test was used to make comparisons between groups; $p < 0.05$ was defined as being statistically significant. The Pearson product moment correlation statistic was used as a measure of correlation between variables.

Results

To investigate the role of heparanase expression by endothelial cells, we over- and underexpressed heparanase using a vector expressing heparanase and a vector

expressing a small interfering RNA (siRNA) hairpin sequence specific to heparanase. Human umbilical vein endothelial cells were transfected with the gene silencing vector (siHPA) containing an insert to express an siRNA sequence specific for inhibiting heparanase, a vector expressing the heparanase protein (pHPA), or a control vector for expressing siRNA but with no siRNA sequence (siCON). Following transfection, the cells were fixed, stained, and examined by immunofluorescent microscopy to confirm alterations in the expression of heparanase protein (Figure 52). Transfected cells were also lysed and assayed for heparanase by immunoblotting to confirm alterations in protein expression of heparanase (Figure 53). Transfection of cells with siRNA specific to heparanase led to almost complete silencing of heparanase protein expression.

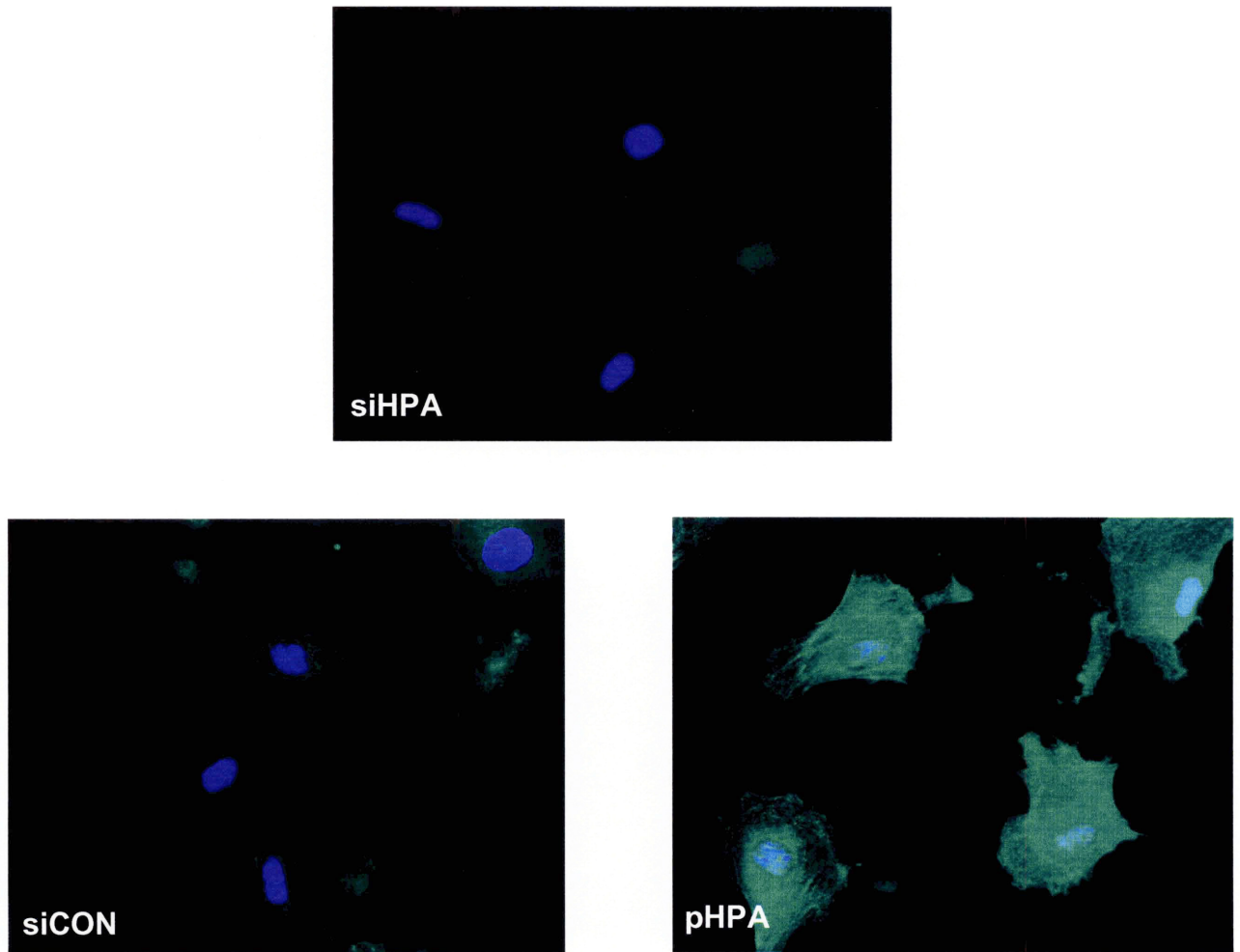


Figure 52. Immunocytochemical staining for heparanase in endothelial cells transfected with a control vector (siCON), a heparanase targeted siRNA vector (siHPA) or a heparanase expression vector (pHPA). Cells were transfected with the various vector, incubated for 48 hrs and then stained using antibody to heparanase and a fluorescently labeled secondary antibody.

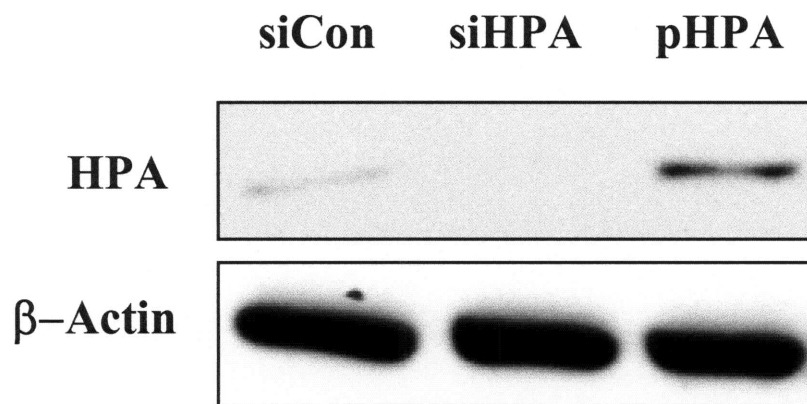


Figure 53. Western blot for heparanase in endothelial cells transfected with a control vector (siCON), a heparanase targeted siRNA vector (siHPA) or a heparanase expression vector (pHPA). Cells were transfected with the various vector, incubated for 48 hrs, lysed and subjected to Western blot analysis.

One of the primary functions of the macrovascular endothelial cell layer is to control vascular smooth muscle cell (vSMC) growth and proliferation. Secreted heparan sulfate proteoglycans (HSPGs) are the major inhibitory molecules involved in endothelial control of vSMC proliferation [6, 68]. To examine heparanase's role in modulating this control, conditioned media was prepared from each transfection group and applied in an assay of SMC proliferation (Figure 54). Overexpression of heparanase removed most of the inhibitory properties of endothelial cell conditioned medium ($90.8 \pm 8.8\%$ thymidine incorporation versus control, $p =$ not significant). Interestingly, the siRNA knock-down of heparanase resulted in highly inhibitory conditioned medium, leading to almost complete inhibition of SMC growth in the proliferation assay ($3.3 \pm 1.5\%$ thymidine incorporation versus control, $p < 0.05$). These data indicate that endothelial expression of heparanase can serve as an effective mechanism to control endothelial inhibition of SMC proliferation.

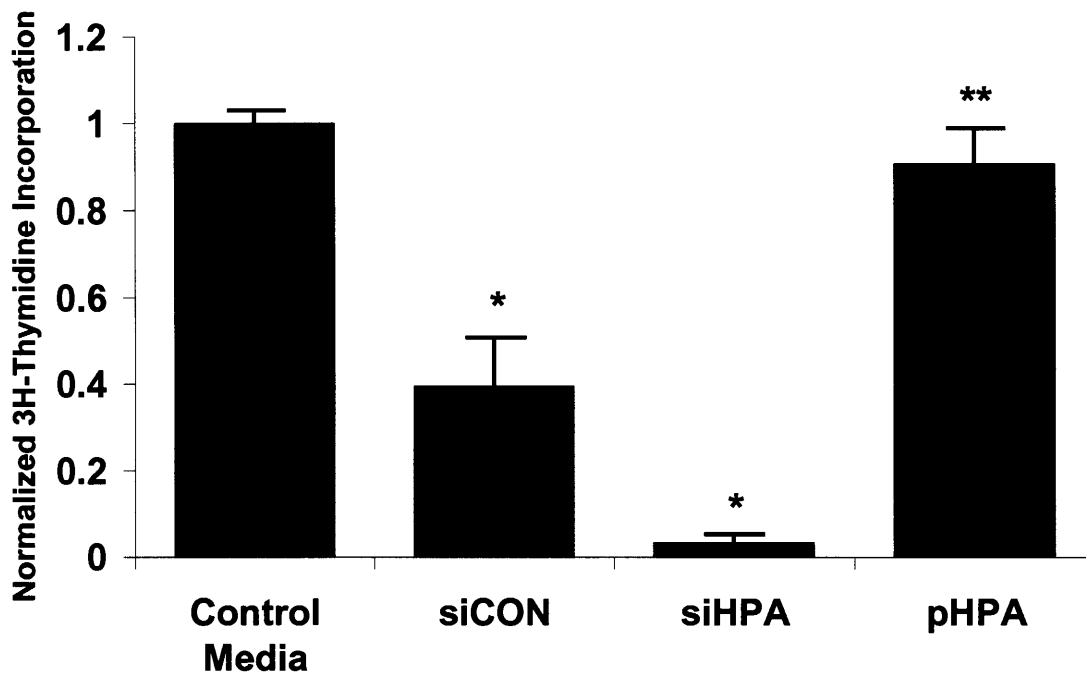


Figure 54. Vascular smooth muscle cell proliferation when exposed to endothelial cell conditioned medium from cells transfected with a control vector (siCON), a heparanase targeted siRNA vector (siHPA) or a heparanase expression vector (pHPA).

To further examine the mechanism of heparanase control of vSMC inhibition, endothelial cells were metabolically labeled with tritiated glucosamine and the conditioned media analyzed using ion exchange and size exclusion chromatography for glycosaminoglycan (GAG) expression (Figure 55 through Figure 58). Overexpression of heparanase led to a marked reduction in endothelial cell surface associated GAG and HSPG (Figure 58). Conversely, a reduction in heparanase produced an increase in cell surface GAG accumulation (Figure 58). The media GAG appeared to be less affected by heparanase expression, only showing a small decrease in total proteoglycan and HSPGs for heparanase overexpressing cells.

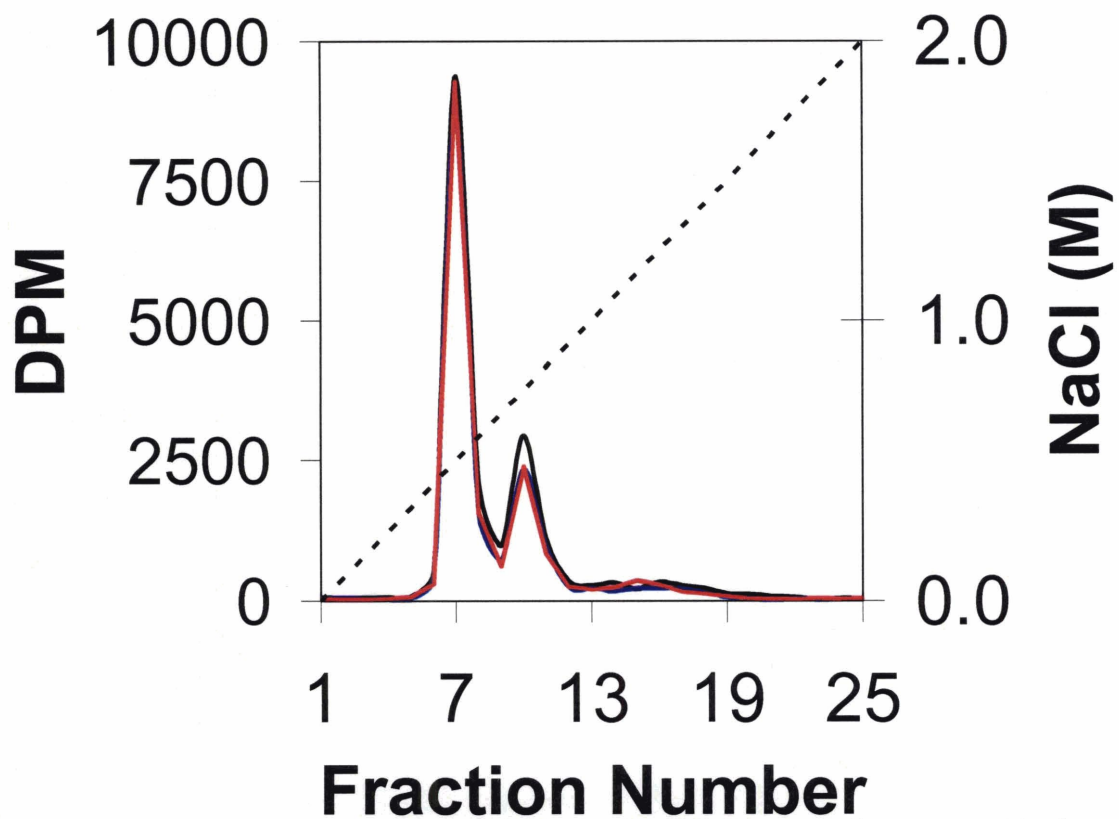


Figure 55. Total proteoglycans in endothelial cell conditioned media separated by ion exchange chromatography. Cells transfected with a control vector (black line), a heparanase targeted siRNA vector (blue line) or a heparanase expression vector (red line). The applied salt gradient (dotted line) on the second axis.

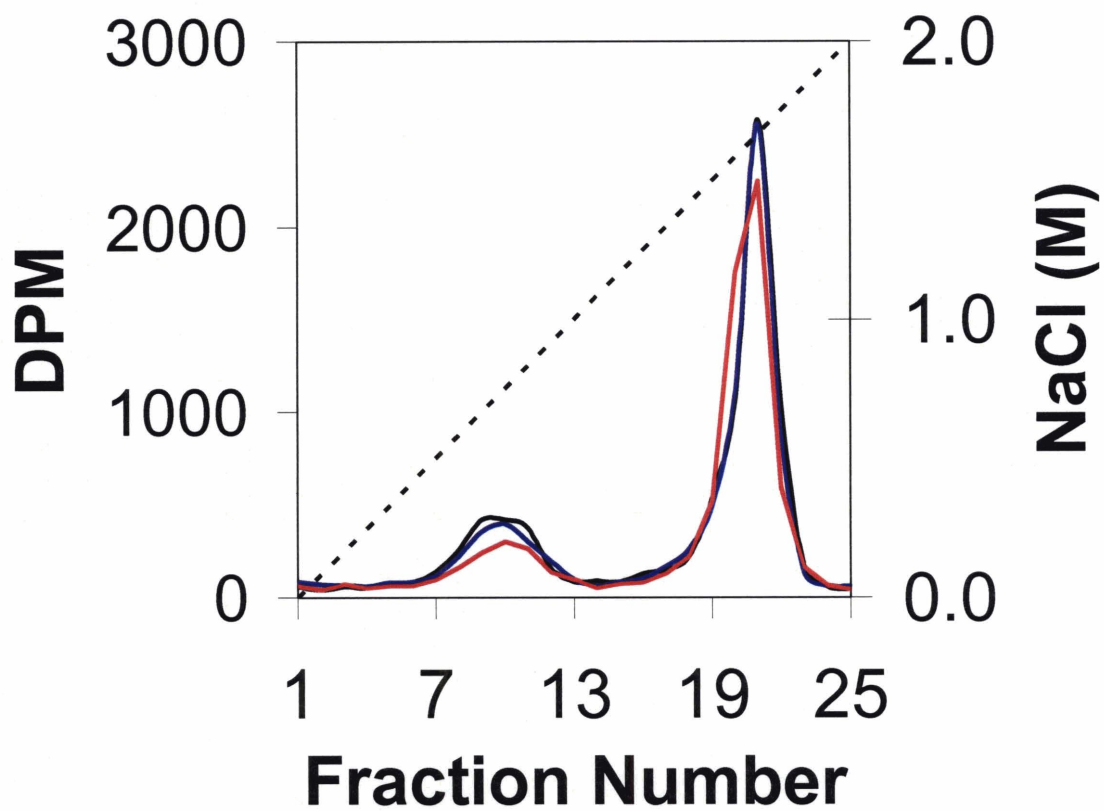


Figure 56. Heparan sulfate proteoglycans in endothelial cell conditioned media separated by ion exchange chromatography. Cells transfected with a control vector (black line), a heparanase targeted siRNA vector (blue line) or a heparanase expression vector (red line). The applied salt gradient (dotted line) on the second axis.

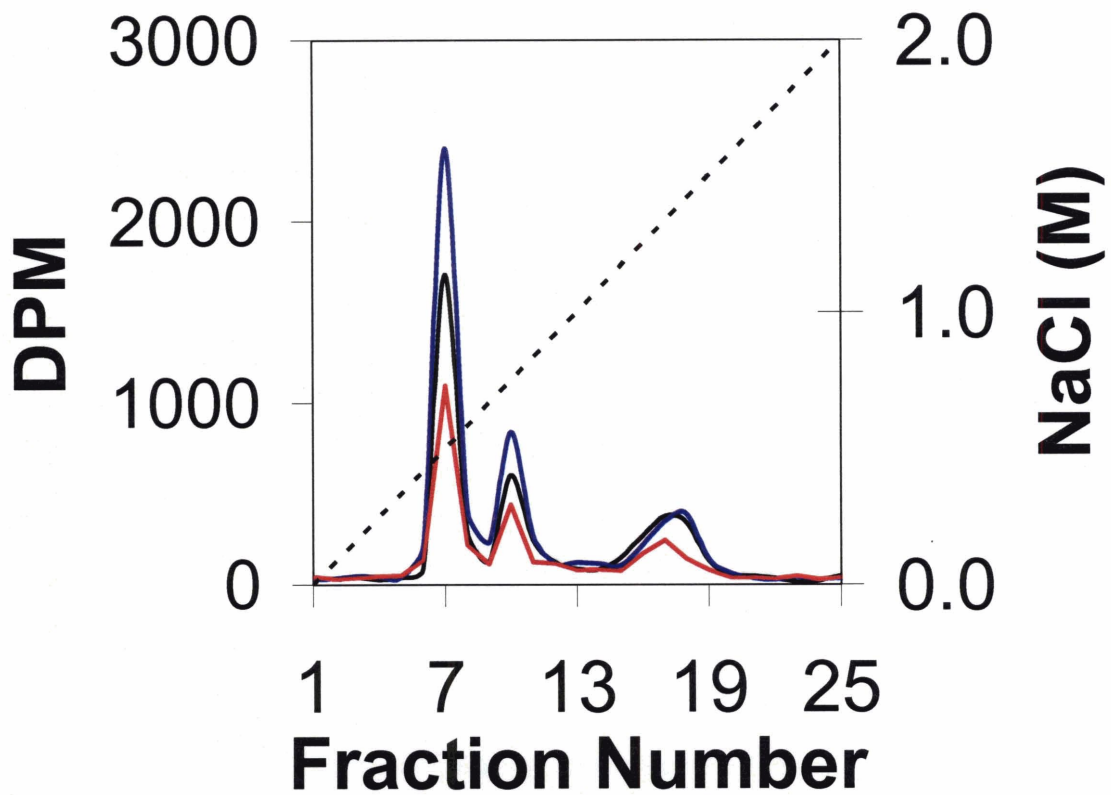


Figure 57. Total proteoglycans on the endothelial cell surface separated by ion exchange chromatography. Cells transfected with a control vector (black line), a heparanase targeted siRNA vector (blue line) or a heparanase expression vector (red line). The applied salt gradient (dotted line) on the second axis.

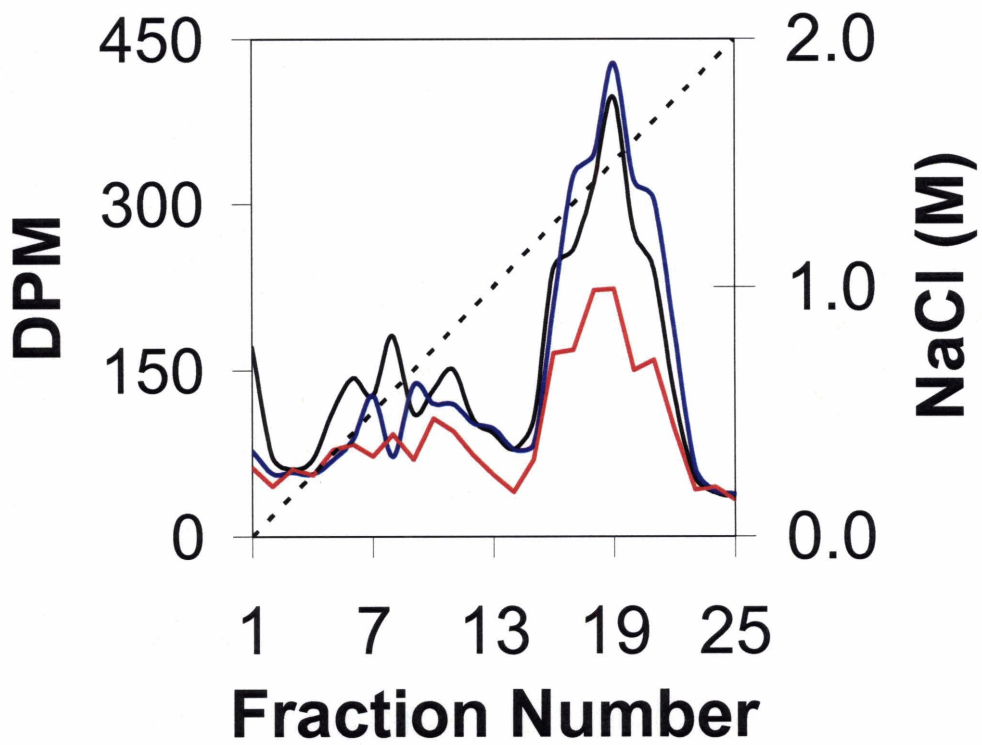


Figure 58. Heparan sulfate proteoglycans on the endothelial cell surface separated by ion exchange chromatography. Cells transfected with a control vector (black line), a heparanase targeted siRNA vector (blue line) or a heparanase expression vector (red line). The applied salt gradient (dotted line) on the second axis.

In addition to hypertension, percutaneous vascular intervention is another common mechanical stimulus for arterial remodeling. The effects of overexpression of heparanase on endothelial control of vSMC proliferation suggest that heparanase may also play a major role in modulating vascular response to injury. Platelets and inflammatory cells are known to express heparanase, providing a source of heparanase independent of the endothelium. We recently showed that vascular injury was exacerbated by the diabetic state in the Zucker rat model of type II diabetes[155]. To examine the role of heparanase in vascular injury we placed stents in the aortae of lean and fatty Zucker rats. Two weeks after stenting the animals were sacrificed and plastic embedded sections were prepared from the stented regions of the aortae.

Hematoxylin and eosin and van Geissen staining of aortae showed an increase in neointimal thickness comparing the fatty to lean Zucker rats (Figure 59 and Figure 60). Immunohistochemical staining for the expression of heparanase in the neointima of fatty rats showed intense staining for heparanase in the neointimal region surrounding the stent strut (Figure 61). A strong correlation was found between the lesion neointimal thickness and heparanase expression ($R = 0.749, p < 0.0005$, Figure 62).

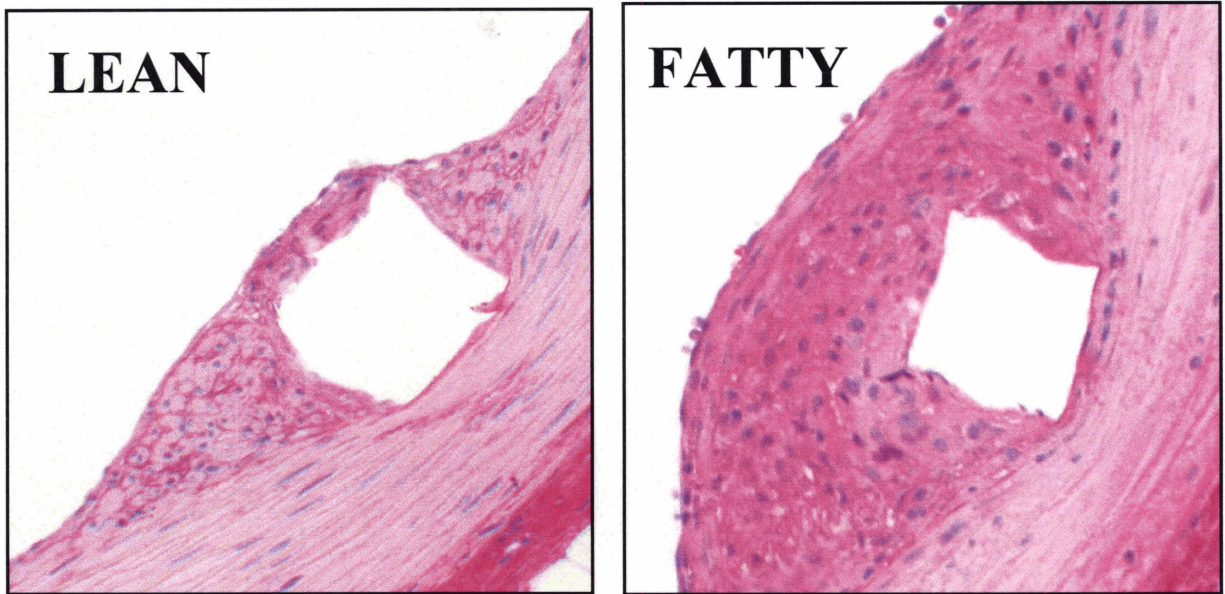


Figure 59. Hematoxylin and eosin staining of histological sections of the stented abdominal aorta.



Figure 60. Elastic fiber (Verhoff Van Geisen) staining of histological sections of the stented abdominal aorta.

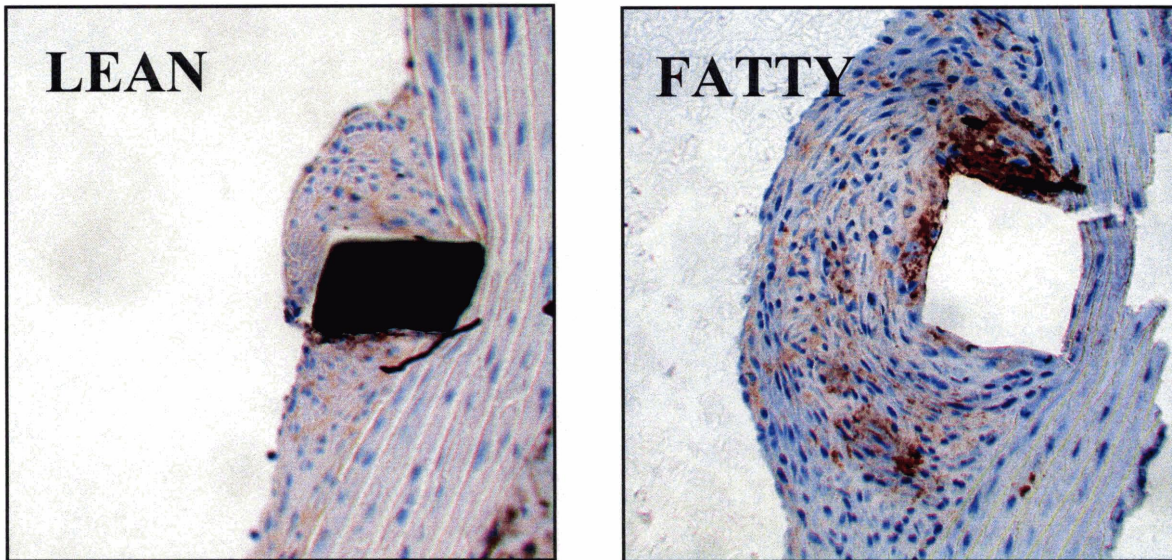


Figure 61. Immunohistochemical staining for heparanase of histological sections of the stented abdominal aorta.

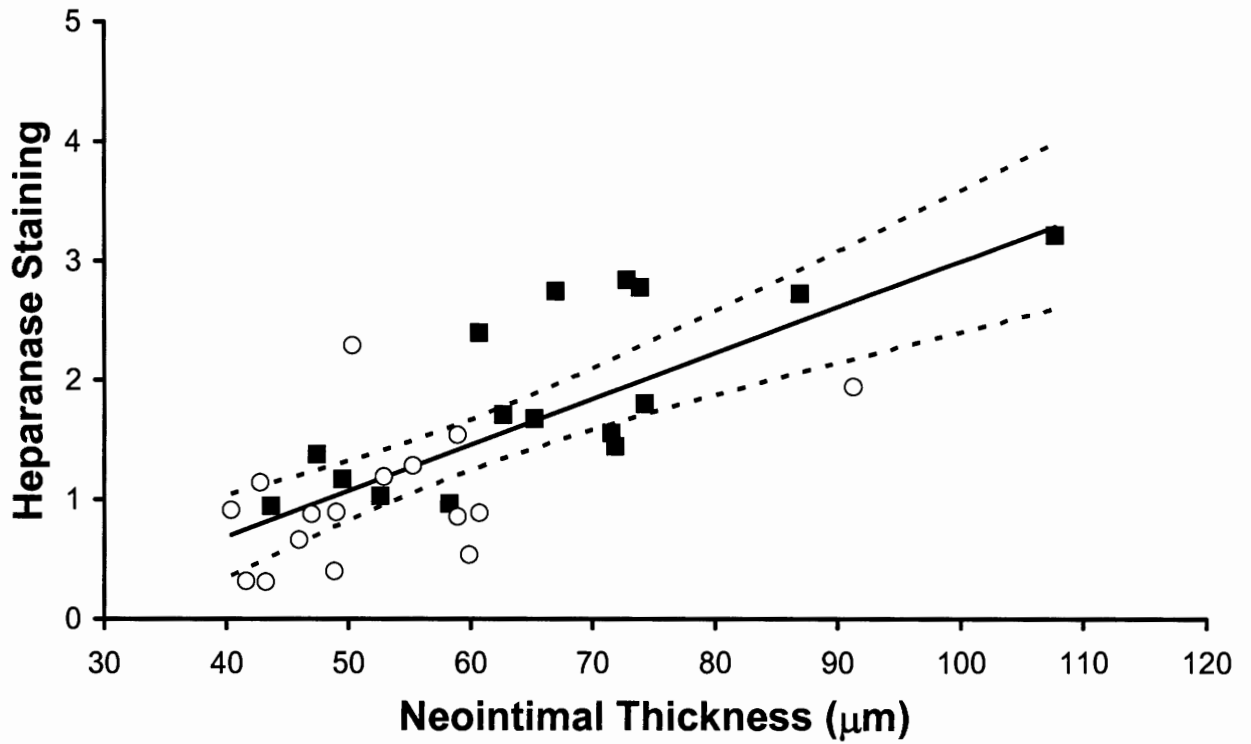


Figure 62. Correlation analysis comparing lesion thickness with heparanase staining. Correlation between medial thickening and endothelial heparanase expression in SHR (■) and WKY (□) rats.

Discussion

This study identifies endothelial heparanase as a regulator of vascular remodeling and provides evidence that altered heparanase expression may underlie the pathophysiology of common vascular disorders. Previous work on heparanase has focused primarily on its role in modulating tumor cell invasion and angiogenesis. Despite the discovery of heparanase expression in endothelial cells two decades ago, the functional role of this expression in arterial biology had not been explored. Our study shows that heparanase expression serves to counterbalance the expression of growth inhibitory heparan sulfate proteoglycans in endothelial cells, providing a feedback mechanism for endothelial cells to have fine control of vascular smooth muscle cell growth and proliferation.

Our studies show that gene silencing and enhancement of heparanase expression in endothelial cells leads to dramatic modulation of the conditioned media inhibitory properties towards vascular smooth muscle cell. Surprisingly, the silencing of heparanase expression resulted in almost complete inhibition of vascular smooth muscle cell growth. One potential mechanism of action of heparanase is to cleave extracellular matrix HSPG causing a release of matrix bound growth factors (particularly FGF-2). Heparanase isolated from platelets has been shown by others to release FGF-2 increasing the proliferation of vSMC [119]. While this mechanism may play a role in increasing proliferation in endothelial overexpression of heparanase, it is unlikely to explain the large increase in inhibition of vSMC growth observed in the heparanase silenced cells. It is also notable that the medium used for these experiments contained considerable amounts of FGF-2 in serum and as a supplement. Similar inhibition results were

obtained using the isolated proteoglycans as with full conditioned media, indicating that release of FGF-2 was not a major mechanism acting in this system. Heparanase appeared to act on endothelial cells by causing the cleavage of cell surface heparan sulfate proteoglycans. This result is consistent with prior work that found that heparanase did not cut heparan sulfate proteoglycans in conditioned media [156] and also that macrophage lysosomal lysates can digest cell surface heparan sulfate proteoglycan of smooth muscle cells [157].

Previous work has shown that heparanase does not completely digest heparan sulfate into disaccharides but rather it cuts infrequently to yield chains of 10-20 sugar units [158]. Studies examining the specific structural determinants of heparin's inhibitory properties have shown that a minimum length of a hexasaccharide was needed to get inhibitory properties but also revealed a dependence on sulfation [159]. A major question that arises is whether these short polysaccharides are more or less inhibitory than the original, longer heparan sulfate chain. Our work indicates that heparanase acts on cell surface heparan sulfate proteoglycan cutting them to make small fragments that increase vSMC proliferation. Cell surface heparan sulfate proteoglycans can serve as coreceptor facilitating FGF receptor signaling [82] thus these heparan sulfate proteoglycans, in particular, would be particularly effective in increasing vSMC proliferation when released from cells by heparanase. The released cell surface heparan sulfate proteoglycans serve to counterbalance the inhibitory properties of the secreted and matrix HSPG that endothelial cells produce.

In-vivo, an animal model of hypertension demonstrated an increase in heparanase, HPSG, and Sp1 in the endothelium of hypertensive rats. These results support that similar

processes that control the in-vitro response to mechanical load may be governing the vascular response to hypertension. Spontaneously hypertensive rats are known to have medial hypertrophy in the aorta due to their hypertension[154]. The strong correlation between the thickness of the aorta and the heparanase expression in the overlying endothelium illustrates that the balance between heparanase and HSPG plays a role in growth factor induced hyperplasia as well as proliferation.

Prior work has shown increased heparanase expression in the endothelium of apoE-null mice and in endothelial cells exposed to fatty acids [160]. We examined the effect of the mechanical injury of endovascular stenting on rats in the context of the Zucker rat model. Our studies revealed a strong correlation between neointimal heparanase expression and neointimal thickness. This work indicates that the increased fatty acids act in inflammatory cells in vascular injury, causing increased expression of heparanase and increased neointimal formation. A secondary mechanism may be the enhanced of heparanase expression in invading inflammatory cells. Heparin and PI-88 (a synthetic heparin analogue) have been used in animal models to reduce neointimal formation [161, 162]. Both of these compounds can inhibit heparanase activity but also have many other activities including growth factor binding and direct activity on vascular smooth muscle cell.

Taken together, our results define a new role for heparanase as a regulator of vascular remodeling. In this model heparanase serves as a control point allowing endothelial cells to modulate between inhibition and stimulation of vascular smooth muscle cells by utilizing one molecule. Further, these findings may have important implications in vascular disease progression. Aberrant heparanase may serve as a

common pathophysiological mechanism governing vascular remodeling under different pathological disease states. While specific small molecule inhibitors have long been sought after for the treatment of metastatic cancers, these results indicate that these molecules may also have a role in the treatment of postangioplasty restenosis, atherosclerosis, and hypertension.

Conclusions

In this chapter we have given evidence that endothelial heparanase expression causes decreased vascular smooth muscle cell inhibition. Further we have shown a strong correlation between the heparanase expression and neointimal thickness in an animal model of injury and diabetes. This work identifies heparanase as a major regulator of vascular remodeling. Heparanase inhibition is currently a major thrust of commercial research for cancer therapy. Our results imply that these therapeutics may be useful in controlling aberrant vascular remodeling as well.

Chapter 6: Conclusions and Future Directions

This thesis presents a body of work examining the fundamental biological mechanisms that govern vascular remodeling. In Chapter 3, we examined how endothelial cells change their control of vascular smooth muscle cells in response to mechanical environment. These changes were shown to be mediated, in part, by heparan sulfate proteoglycan. The changes in heparan sulfate proteoglycans were controlled by intracellular signaling pathways of MAPK and p38 MAPK, along with a TGF- β autocrine signaling. In Chapter 4, we found that the endothelium in hypertensive animals appeared to be similarly regulated by the increased mechanical strains. The hypertensive animals had increased endothelial heparanase expression that correlated with medial thickening. Finally, we examined the role of heparanase in modulating endothelial control over vascular smooth muscle cell proliferation and found that increasing endothelial heparanase expression caused a decreased vascular smooth muscle cell inhibition.

Future studies should be done to further examine the mechanotransduction pathway that was partially elucidated in this work. In particular it will be essential to identify the molecules responsible for the activation of TGF- β in response to load. A particularly appealing candidate group is the matrix metalloproteases (MMPs) some of which can activate TGF- β and have been modulated with other types of mechanical strain [163]. Another fascinating possibility is that the endothelial cell is activating the TGF- β through direct integrin-mediated pathway. Thrombospondin is known to bind to TGF- β and it has been proposed that certain integrins may be involved in activating TGF- β in

this state [54]. One potential theory is that the integrins could bind to TGF immobilized thrombospondin and mechanical force could serve as the activating factor.

A major portion of future work will focus on modulating the expression of heparanase to get in-vivo overexpression and underexpression. We recently created a lentiviral vector capable of in-vivo knockdown of heparanase. This tool can be used in several ways. The first is to give local delivery to arteries prior to vascular injury. In preliminary tests we delivered a GFP expressing virus in a rat model of carotid balloon injury. However, immunostaining for GFP showed that the virus did not penetrate the into the media of the artery.. Another approach is to use the virus to create transgenic animals. In this way we could study the affects of heparanase knockdown in hypertensive and diabetic Zucker rats. This method would likely be more effective than local delivery but requires a significant time investment. Another possibility that is being explored is to use small molecule inhibitors to heparanase as a means to knockdown heparanase activity. We recently started a collaboration with a research group that will provide us with a small molecule inhibitor towards heparanase. This methodology has great potent for clinical application. Drug eluting stents have been shown to work less effectively on diabetic patients. Combination therapy with a heparanase inhibitor and a currently used drug might create a stent specifically for use in these at risk patients.

References

1. Hacker, U., K. Nybakken, and N. Perrimon, *Heparan sulphate proteoglycans: the sweet side of development*. Nat Rev Mol Cell Biol, 2005. **6**(7): p. 530-41.
2. Laine, R.A., *A calculation of all possible oligosaccharide isomers both branched and linear yields 1.05×10^{12} structures for a reducing hexasaccharide: the Isomer Barrier to development of single-method saccharide sequencing or synthesis systems*. Glycobiology, 1994. **4**(6): p. 759-67.
3. Iozzo, R.V., *Basement membrane proteoglycans: from cellar to ceiling*. Nat Rev Mol Cell Biol, 2005. **6**(8): p. 646-56.
4. Whitelock, J.M. and R.V. Iozzo, *Heparan sulfate: a complex polymer charged with biological activity*. Chem Rev, 2005. **105**(7): p. 2745-64.
5. Nugent, M.A., et al., *Perlecan is required to inhibit thrombosis after deep vascular injury and contributes to endothelial cell-mediated inhibition of intimal hyperplasia*. Proc Natl Acad Sci U S A, 2000. **97**(12): p. 6722-7.
6. Ettenson, D.S., et al., *Endothelial heparan sulfate is necessary but not sufficient for control of vascular smooth muscle cell growth*. J Cell Physiol, 2000. **184**(1): p. 93-100.
7. Mertens, G., et al., *Cell surface heparan sulfate proteoglycans from human vascular endothelial cells. Core protein characterization and antithrombin III binding properties*. J Biol Chem, 1992. **267**(28): p. 20435-43.
8. Chua, C.C., et al., *Heparan sulfate proteoglycans function as receptors for fibroblast growth factor-2 activation of extracellular signal-regulated kinases 1 and 2*. Circ Res, 2004. **94**(3): p. 316-23.
9. Volk, R., et al., *The role of syndecan cytoplasmic domain in basic fibroblast growth factor-dependent signal transduction*. J Biol Chem, 1999. **274**(34): p. 24417-24.
10. Yayon, A., et al., *Cell surface, heparin-like molecules are required for binding of basic fibroblast growth factor to its high affinity receptor*. Cell, 1991. **64**(4): p. 841-8.
11. Tkachenko, E., J.M. Rhodes, and M. Simons, *Syndecans: new kids on the signaling block*. Circ Res, 2005. **96**(5): p. 488-500.
12. <http://owensboro.kctcs.edu/gcaplan/anat2/histology/Image206.gif>
13. Humphrey, J.D. and S. Na, *Elastodynamics and arterial wall stress*. Ann Biomed Eng, 2002. **30**(4): p. 509-23.

14. Gibbons, G.H. and V.J. Dzau, *The emerging concept of vascular remodeling*. N Engl J Med, 1994. **330**(20): p. 1431-8.
15. Lehoux, S., Y. Castier, and A. Tedgui, *Molecular mechanisms of the vascular responses to haemodynamic forces*. J Intern Med, 2006. **259**(4): p. 381-92.
16. Tronc, F., et al., *Role of NO in flow-induced remodeling of the rabbit common carotid artery*. Arterioscler Thromb Vasc Biol, 1996. **16**(10): p. 1256-62.
17. Duprez, D.A., et al., *Small and large artery elasticity indices in peripheral arterial occlusive disease (PAOD)*. Vasc Med, 2001. **6**(4): p. 211-4.
18. Faury, G., et al., *Developmental adaptation of the mouse cardiovascular system to elastin haploinsufficiency*. J Clin Invest, 2003. **112**(9): p. 1419-28.
19. Davies, P.F., *Flow-mediated endothelial mechanotransduction*. Physiol Rev, 1995. **75**(3): p. 519-60.
20. Critchley, D.R., *Cytoskeletal proteins talin and vinculin in integrin-mediated adhesion*. Biochem Soc Trans, 2004. **32**(Pt 5): p. 831-6.
21. Ishida, T., et al., *MAP kinase activation by flow in endothelial cells. Role of beta 1 integrins and tyrosine kinases*. Circ Res, 1996. **79**(2): p. 310-6.
22. Lehoux, S., et al., *Differential regulation of vascular focal adhesion kinase by steady stretch and pulsatility*. Circulation, 2005. **111**(5): p. 643-9.
23. Tanabe, Y., et al., *Mechanical stretch augments PDGF receptor beta expression and protein tyrosine phosphorylation in pulmonary artery tissue and smooth muscle cells*. Mol Cell Biochem, 2000. **215**(1-2): p. 103-13.
24. Schlaepfer, D.D. and T. Hunter, *Focal adhesion kinase overexpression enhances ras-dependent integrin signaling to ERK2/mitogen-activated protein kinase through interactions with and activation of c-Src*. J Biol Chem, 1997. **272**(20): p. 13189-95.
25. Bobak, D., et al., *Inactivation of the small GTPase Rho disrupts cellular attachment and induces adhesion-dependent and adhesion-independent apoptosis*. Oncogene, 1997. **15**(18): p. 2179-89.
26. Carbajal, J.M. and R.C. Schaeffer, Jr., *RhoA inactivation enhances endothelial barrier function*. Am J Physiol, 1999. **277**(5 Pt 1): p. C955-64.
27. Reusch, H.P., et al., *Activation of JNK/SAPK and ERK by mechanical strain in vascular smooth muscle cells depends on extracellular matrix composition*. Biochem Biophys Res Commun, 1997. **237**(2): p. 239-44.

28. Xu, Q., et al., *Acute hypertension activates mitogen-activated protein kinases in arterial wall*. J Clin Invest, 1996. **97**(2): p. 508-14.
29. Lehoux, S., et al., *Pulsatile stretch-induced extracellular signal-regulated kinase 1/2 activation in organ culture of rabbit aorta involves reactive oxygen species*. Arterioscler Thromb Vasc Biol, 2000. **20**(11): p. 2366-72.
30. Surapisitchat, J., et al., *Fluid shear stress inhibits TNF-alpha activation of JNK but not ERK1/2 or p38 in human umbilical vein endothelial cells: Inhibitory crosstalk among MAPK family members*. Proc Natl Acad Sci U S A, 2001. **98**(11): p. 6476-81.
31. Crespo, P., et al., *Ras-dependent activation of MAP kinase pathway mediated by G-protein beta gamma subunits*. Nature, 1994. **369**(6479): p. 418-20.
32. Iwasaki, H., et al., *Mechanical stretch stimulates growth of vascular smooth muscle cells via epidermal growth factor receptor*. Am J Physiol Heart Circ Physiol, 2000. **278**(2): p. H521-9.
33. Oeckler, R.A., P.M. Kaminski, and M.S. Wolin, *Stretch enhances contraction of bovine coronary arteries via an NAD(P)H oxidase-mediated activation of the extracellular signal-regulated kinase mitogen-activated protein kinase cascade*. Circ Res, 2003. **92**(1): p. 23-31.
34. Hajra, L., et al., *The NF-kappa B signal transduction pathway in aortic endothelial cells is primed for activation in regions predisposed to atherosclerotic lesion formation*. Proc Natl Acad Sci U S A, 2000. **97**(16): p. 9052-7.
35. Iiyama, K., et al., *Patterns of vascular cell adhesion molecule-1 and intercellular adhesion molecule-1 expression in rabbit and mouse atherosclerotic lesions and at sites predisposed to lesion formation*. Circ Res, 1999. **85**(2): p. 199-207.
36. Parmar, K.M., et al., *Integration of flow-dependent endothelial phenotypes by Kruppel-like factor 2*. J Clin Invest, 2006. **116**(1): p. 49-58.
37. Sen-Banerjee, S., et al., *Kruppel-like factor 2 as a novel mediator of statin effects in endothelial cells*. Circulation, 2005. **112**(5): p. 720-6.
38. Khachigian, L.M., et al., *Egr-1 is activated in endothelial cells exposed to fluid shear stress and interacts with a novel shear-stress-response element in the PDGF A-chain promoter*. Arterioscler Thromb Vasc Biol, 1997. **17**(10): p. 2280-6.
39. Lin, M.C., et al., *Shear stress induction of the tissue factor gene*. J Clin Invest, 1997. **99**(4): p. 737-44.
40. Resnick, N., et al., *Endothelial gene regulation by laminar shear stress*. Adv Exp Med Biol, 1997. **430**: p. 155-64.

41. Lan, Q., K.O. Mercurius, and P.F. Davies, *Stimulation of transcription factors NF kappa B and AP1 in endothelial cells subjected to shear stress*. *Biochem Biophys Res Commun*, 1994. **201**(2): p. 950-6.
42. Roberts, A.B. and M.B. Sporn, *Physiological actions and clinical applications of transforming growth factor-beta (TGF-beta)*. *Growth Factors*, 1993. **8**(1): p. 1-9.
43. Goumans, M.J., F. Lebrin, and G. Valdimarsdottir, *Controlling the angiogenic switch: a balance between two distinct TGF-b receptor signaling pathways*. *Trends Cardiovasc Med*, 2003. **13**(7): p. 301-7.
44. Pepper, M.S., *Transforming growth factor-beta: vasculogenesis, angiogenesis, and vessel wall integrity*. *Cytokine Growth Factor Rev*, 1997. **8**(1): p. 21-43.
45. Derynck, R., R.J. Akhurst, and A. Balmain, *TGF-beta signaling in tumor suppression and cancer progression*. *Nat Genet*, 2001. **29**(2): p. 117-29.
46. Roberts, A.B. and L.M. Wakefield, *The two faces of transforming growth factor beta in carcinogenesis*. *Proc Natl Acad Sci U S A*, 2003. **100**(15): p. 8621-3.
47. Blobel, G.C., W.P. Schiemann, and H.F. Lodish, *Role of transforming growth factor beta in human disease*. *N Engl J Med*, 2000. **342**(18): p. 1350-8.
48. Massague, J., S.W. Blain, and R.S. Lo, *TGFbeta signaling in growth control, cancer, and heritable disorders*. *Cell*, 2000. **103**(2): p. 295-309.
49. Johnson, D.W., et al., *Mutations in the activin receptor-like kinase 1 gene in hereditary haemorrhagic telangiectasia type 2*. *Nat Genet*, 1996. **13**(2): p. 189-95.
50. McAllister, K.A., et al., *Endoglin, a TGF-beta binding protein of endothelial cells, is the gene for hereditary haemorrhagic telangiectasia type 1*. *Nat Genet*, 1994. **8**(4): p. 345-51.
51. Sato, Y. and D.B. Rifkin, *Inhibition of endothelial cell movement by pericytes and smooth muscle cells: activation of a latent transforming growth factor-beta 1-like molecule by plasmin during co-culture*. *J Cell Biol*, 1989. **109**(1): p. 309-15.
52. Yu, Q. and I. Stamenkovic, *Cell surface-localized matrix metalloproteinase-9 proteolytically activates TGF-beta and promotes tumor invasion and angiogenesis*. *Genes Dev*, 2000. **14**(2): p. 163-76.
53. Schultz-Cherry, S. and J.E. Murphy-Ullrich, *Thrombospondin causes activation of latent transforming growth factor-beta secreted by endothelial cells by a novel mechanism*. *J Cell Biol*, 1993. **122**(4): p. 923-32.
54. Munger, J.S., et al., *The integrin alpha v beta 6 binds and activates latent TGF beta 1: a mechanism for regulating pulmonary inflammation and fibrosis*. *Cell*, 1999. **96**(3): p. 319-28.

55. Barcellos-Hoff, M.H., et al., *Transforming growth factor-beta activation in irradiated murine mammary gland*. J Clin Invest, 1994. **93**(2): p. 892-9.
56. Lyons, R.M., J. Keski-Oja, and H.L. Moses, *Proteolytic activation of latent transforming growth factor-beta from fibroblast-conditioned medium*. J Cell Biol, 1988. **106**(5): p. 1659-65.
57. Lyon, M., G. Rushton, and J.T. Gallagher, *The interaction of the transforming growth factor-betas with heparin/heparan sulfate is isoform-specific*. J Biol Chem, 1997. **272**(29): p. 18000-6.
58. Derynck, R. and Y.E. Zhang, *Smad-dependent and Smad-independent pathways in TGF-beta family signalling*. Nature, 2003. **425**(6958): p. 577-84.
59. Massague, J., *Integration of Smad and MAPK pathways: a link and a linker revisited*. Genes Dev, 2003. **17**(24): p. 2993-7.
60. Feng, X.H. and R. Derynck, *Specificity and versatility in tgf-beta signaling through Smads*. Annu Rev Cell Dev Biol, 2005. **21**: p. 659-93.
61. Shi, Y. and J. Massague, *Mechanisms of TGF-beta signaling from cell membrane to the nucleus*. Cell, 2003. **113**(6): p. 685-700.
62. Feng, X.H., X. Lin, and R. Derynck, *Smad2, Smad3 and Smad4 cooperate with Sp1 to induce p15(Ink4B) transcription in response to TGF-beta*. Embo J, 2000. **19**(19): p. 5178-93.
63. Qing, J., Y. Zhang, and R. Derynck, *Structural and functional characterization of the transforming growth factor-beta -induced Smad3/c-Jun transcriptional cooperativity*. J Biol Chem, 2000. **275**(49): p. 38802-12.
64. Yu, L., M.C. Hebert, and Y.E. Zhang, *TGF-beta receptor-activated p38 MAP kinase mediates Smad-independent TGF-beta responses*. Embo J, 2002. **21**(14): p. 3749-59.
65. Castellot, J.J., Jr., et al., *Cultured endothelial cells produce a heparinlike inhibitor of smooth muscle cell growth*. J Cell Biol, 1981. **90**(2): p. 372-9.
66. Dodge, A.B., X. Lu, and P.A. D'Amore, *Density-dependent endothelial cell production of an inhibitor of smooth muscle cell growth*. J Cell Biochem, 1993. **53**(1): p. 21-31.
67. Fillinger, M.F., et al., *The effect of endothelial cell coculture on smooth muscle cell proliferation*. J Vasc Surg, 1993. **17**(6): p. 1058-67; discussion 1067-8.
68. Nugent, M.A., M.J. Karnovsky, and E.R. Edelman, *Vascular cell-derived heparan sulfate shows coupled inhibition of basic fibroblast growth factor binding and mitogenesis in vascular smooth muscle cells*. Circ Res, 1993. **73**(6): p. 1051-60.

69. van Buul-Wortelboer, M.F., et al., *Reconstitution of the vascular wall in vitro. A novel model to study interactions between endothelial and smooth muscle cells.* Exp Cell Res, 1986. **162**(1): p. 151-8.
70. Clowes, A.W. and M.J. Karnovsky, *Suppression by heparin of injury-induced myointimal thickening.* J Surg Res, 1978. **24**(3): p. 161-8.
71. Edelman, E.R., M.A. Nugent, and M.J. Karnovsky, *Perivascular and intravenous administration of basic fibroblast growth factor: vascular and solid organ deposition.* Proc Natl Acad Sci U S A, 1993. **90**(4): p. 1513-7.
72. Guyton, J.R., et al., *Inhibition of rat arterial smooth muscle cell proliferation by heparin. In vivo studies with anticoagulant and nonanticoagulant heparin.* Circ Res, 1980. **46**(5): p. 625-34.
73. Hoover, R.L., et al., *Inhibition of rat arterial smooth muscle cell proliferation by heparin. II. In vitro studies.* Circ Res, 1980. **47**(4): p. 578-83.
74. Lindner, V., et al., *Inhibition of smooth muscle cell proliferation in injured rat arteries. Interaction of heparin with basic fibroblast growth factor.* J Clin Invest, 1992. **90**(5): p. 2044-9.
75. Volker, W., et al., *Inhibition of smooth muscle cell proliferation and neointimal growth by low-anticoagulant heparin.* Arzneimittelforschung, 1995. **45**(5): p. 546-50.
76. <http://www.med.unibs.it/~airc/hspgs.html>
77. Bernfield, M., et al., *Functions of cell surface heparan sulfate proteoglycans.* Annu Rev Biochem, 1999. **68**: p. 729-77.
78. Esko, J.D. and L. Zhang, *Influence of core protein sequence on glycosaminoglycan assembly.* Curr Opin Struct Biol, 1996. **6**(5): p. 663-70.
79. Rosenberg, R.D., et al., *Heparan sulfate proteoglycans of the cardiovascular system. Specific structures emerge but how is synthesis regulated?* J Clin Invest, 1997. **100**(11 Suppl): p. S67-75.
80. Noonan, D.M., et al., *The complete sequence of perlecan, a basement membrane heparan sulfate proteoglycan, reveals extensive similarity with laminin A chain, low density lipoprotein-receptor, and the neural cell adhesion molecule.* J Biol Chem, 1991. **266**(34): p. 22939-47.
81. Iozzo, R.V. and J.D. San Antonio, *Heparan sulfate proteoglycans: heavy hitters in the angiogenesis arena.* J Clin Invest, 2001. **108**(3): p. 349-55.
82. Nugent, M.A. and R.V. Iozzo, *Fibroblast growth factor-2.* Int J Biochem Cell Biol, 2000. **32**(2): p. 115-20.

83. Mali, M., et al., *Inhibition of basic fibroblast growth factor-induced growth promotion by overexpression of syndecan-1*. J Biol Chem, 1993. **268**(32): p. 24215-22.
84. Kato, M., et al., *Physiological degradation converts the soluble syndecan-1 ectodomain from an inhibitor to a potent activator of FGF-2*. Nat Med, 1998. **4**(6): p. 691-7.
85. Chen, L., C. Klass, and A. Woods, *Syndecan-2 regulates transforming growth factor-beta signaling*. J Biol Chem, 2004. **279**(16): p. 15715-8.
86. Sanderson, R.D., P. Lalor, and M. Bernfield, *B lymphocytes express and lose syndecan at specific stages of differentiation*. Cell Regul, 1989. **1**(1): p. 27-35.
87. Beauvais, D.M., B.J. Burbach, and A.C. Rapraeger, *The syndecan-1 ectodomain regulates alphavbeta3 integrin activity in human mammary carcinoma cells*. J Cell Biol, 2004. **167**(1): p. 171-81.
88. Beardsley, A., et al., *Loss of caveolin-1 polarity impedes endothelial cell polarization and directional movement*. J Biol Chem, 2005. **280**(5): p. 3541-7.
89. Borset, M., et al., *Syndecan-1 is targeted to the uropods of polarized myeloma cells where it promotes adhesion and sequesters heparin-binding proteins*. Blood, 2000. **96**(7): p. 2528-36.
90. Baciu, P.C. and P.F. Goetinck, *Protein kinase C regulates the recruitment of syndecan-4 into focal contacts*. Mol Biol Cell, 1995. **6**(11): p. 1503-13.
91. Wilcox-Adelman, S.A., F. Denhez, and P.F. Goetinck, *Syndecan-4 modulates focal adhesion kinase phosphorylation*. J Biol Chem, 2002. **277**(36): p. 32970-7.
92. Mukai, M., et al., *Sustained tyrosine-phosphorylation of FAK through Rho-dependent adhesion to fibronectin is essential for cancer cell migration*. Anticancer Res, 2002. **22**(6A): p. 3175-84.
93. Hsia, D.A., et al., *Differential regulation of cell motility and invasion by FAK*. J Cell Biol, 2003. **160**(5): p. 753-67.
94. Li, L. and E.L. Chaikof, *Mechanical stress regulates syndecan-4 expression and redistribution in vascular smooth muscle cells*. Arterioscler Thromb Vasc Biol, 2002. **22**(1): p. 61-8.
95. Cizmeci-Smith, G., et al., *Syndecan-4 is a primary-response gene induced by basic fibroblast growth factor and arterial injury in vascular smooth muscle cells*. Arterioscler Thromb Vasc Biol, 1997. **17**(1): p. 172-80.
96. Geary, R.L., et al., *Failure of heparin to inhibit intimal hyperplasia in injured baboon arteries. The role of heparin-sensitive and -insensitive pathways in the*

- stimulation of smooth muscle cell migration and proliferation. Circulation, 1995. 91(12): p. 2972-81.*
97. Li, J., et al., *Macrophage-dependent regulation of syndecan gene expression. Circ Res, 1997. 81(5): p. 785-96.*
 98. Halden, Y., et al., *Interleukin-8 binds to syndecan-2 on human endothelial cells. Biochem J, 2004. 377(Pt 2): p. 533-8.*
 99. Dobra, K., M. Nurminen, and A. Hjerpe, *Growth factors regulate the expression profile of their syndecan co-receptors and the differentiation of mesothelioma cells. Anticancer Res, 2003. 23(3B): p. 2435-44.*
 100. Vlodavsky, I., et al., *Mammalian heparanase: involvement in cancer metastasis, angiogenesis and normal development. Semin Cancer Biol, 2002. 12(2): p. 121-9.*
 101. Bitan, M., et al., *Heparanase expression in human leukemias is restricted to acute myeloid leukemias. Exp Hematol, 2002. 30(1): p. 34-41.*
 102. Elkin, M., et al., *Heparanase as mediator of angiogenesis: mode of action. Faseb J, 2001. 15(9): p. 1661-3.*
 103. Vlodavsky, I., et al., *Molecular properties and involvement of heparanase in cancer progression and normal development. Biochimie, 2001. 83(8): p. 831-9.*
 104. Hulett, M.D., et al., *Cloning of mammalian heparanase, an important enzyme in tumor invasion and metastasis. Nat Med, 1999. 5(7): p. 803-9.*
 105. Vlodavsky, I., et al., *Mammalian heparanase: gene cloning, expression and function in tumor progression and metastasis. Nat Med, 1999. 5(7): p. 793-802.*
 106. Fairbanks, M.B., et al., *Processing of the human heparanase precursor and evidence that the active enzyme is a heterodimer. J Biol Chem, 1999. 274(42): p. 29587-90.*
 107. Dempsey, L.A., G.J. Brunn, and J.L. Platt, *Heparanase, a potential regulator of cell-matrix interactions. Trends Biochem Sci, 2000. 25(8): p. 349-51.*
 108. Nakajima, M., T. Irimura, and G.L. Nicolson, *Heparanases and tumor metastasis. J Cell Biochem, 1988. 36(2): p. 157-67.*
 109. Parish, C.R., et al., *Evidence that sulphated polysaccharides inhibit tumour metastasis by blocking tumour-cell-derived heparanases. Int J Cancer, 1987. 40(4): p. 511-8.*
 110. Parish, C.R., et al., *Identification of sulfated oligosaccharide-based inhibitors of tumor growth and metastasis using novel in vitro assays for angiogenesis and heparanase activity. Cancer Res, 1999. 59(14): p. 3433-41.*

111. Parish, C.R., C. Freeman, and M.D. Hulett, *Heparanase: a key enzyme involved in cell invasion*. *Biochim Biophys Acta*, 2001. **1471**(3): p. M99-108.
112. Vlodavsky, I., et al., *Expression of heparanase by platelets and circulating cells of the immune system: possible involvement in diapedesis and extravasation*. *Invasion Metastasis*, 1992. **12**(2): p. 112-27.
113. Vlodavsky, I., et al., *Inhibition of tumor metastasis by heparanase inhibiting species of heparin*. *Invasion Metastasis*, 1994. **14**(1-6): p. 290-302.
114. Uno, F., et al., *Antisense-mediated suppression of human heparanase gene expression inhibits pleural dissemination of human cancer cells*. *Cancer Res*, 2001. **61**(21): p. 7855-60.
115. Miao, H.Q., et al., *Inhibition of heparanase activity and tumor metastasis by laminarin sulfate and synthetic phosphorothioate oligodeoxynucleotides*. *Int J Cancer*, 1999. **83**(3): p. 424-31.
116. Edovitsky, E., et al., *Heparanase gene silencing, tumor invasiveness, angiogenesis, and metastasis*. *J Natl Cancer Inst*, 2004. **96**(16): p. 1219-30.
117. Fitzgerald, M., et al., *Matrix metalloproteinase can facilitate the heparanase-induced promotion of phenotype change in vascular smooth muscle cells*. *Atherosclerosis*, 1999. **145**(1): p. 97-106.
118. Myler, H.A., et al., *Novel heparanase-inhibiting antibody reduces neointima formation*. *J Biochem (Tokyo)*, 2006. **139**(3): p. 339-45.
119. Myler, H.A. and J.L. West, *Heparanase and platelet factor-4 induce smooth muscle cell proliferation and migration via bFGF release from the ECM*. *J Biochem (Tokyo)*, 2002. **131**(6): p. 913-22.
120. Chobanian, A.V. and R.W. Alexander, *Exacerbation of atherosclerosis by hypertension. Potential mechanisms and clinical implications*. *Arch Intern Med*, 1996. **156**(17): p. 1952-6.
121. Malek, A.M., S.L. Alper, and S. Izumo, *Hemodynamic shear stress and its role in atherosclerosis*. *Jama*, 1999. **282**(21): p. 2035-42.
122. Dimmeler, S., et al., *Shear stress inhibits apoptosis of human endothelial cells*. *FEBS Lett*, 1996. **399**(1-2): p. 71-4.
123. Yamawaki, H., S. Lehoux, and B.C. Berk, *Chronic physiological shear stress inhibits tumor necrosis factor-induced proinflammatory responses in rabbit aorta perfused ex vivo*. *Circulation*, 2003. **108**(13): p. 1619-25.

124. Bao, X., C. Lu, and J.A. Frangos, *Temporal gradient in shear but not steady shear stress induces PDGF-A and MCP-1 expression in endothelial cells: role of NO, NF kappa B, and egr-1*. *Arterioscler Thromb Vasc Biol*, 1999. **19**(4): p. 996-1003.
125. Schaffer, J.L., et al., *Device for the application of a dynamic biaxially uniform and isotropic strain to a flexible cell culture membrane*. *J Orthop Res*, 1994. **12**(5): p. 709-19.
126. Gilbert, J.A., et al., *Strain profiles for circular cell culture plates containing flexible surfaces employed to mechanically deform cells in vitro*. *J Biomech*, 1994. **27**(9): p. 1169-77.
127. Cheng, G.C., et al., *Mechanical strain tightly controls fibroblast growth factor-2 release from cultured human vascular smooth muscle cells*. *Circ Res*, 1997. **80**(1): p. 28-36.
128. Rapraeger, A. and M. Bernfield, *Cell surface proteoglycan of mammary epithelial cells. Protease releases a heparan sulfate-rich ectodomain from a putative membrane-anchored domain*. *J Biol Chem*, 1985. **260**(7): p. 4103-9.
129. Zojer, N., A.V. Keck, and M. Pecherstorfer, *Comparative tolerability of drug therapies for hypercalcaemia of malignancy*. *Drug Saf*, 1999. **21**(5): p. 389-406.
130. Blume, S.W., et al., *Mithramycin inhibits SP1 binding and selectively inhibits transcriptional activity of the dihydrofolate reductase gene in vitro and in vivo*. *J Clin Invest*, 1991. **88**(5): p. 1613-21.
131. Eren, M., et al., *Relation between aortic stiffness and left ventricular diastolic function in patients with hypertension, diabetes, or both*. *Heart*, 2004. **90**(1): p. 37-43.
132. Cinthio, M., et al., *Longitudinal movements and resulting shear strain of the arterial wall*. *Am J Physiol Heart Circ Physiol*, 2006.
133. Vainio, S., et al., *Epithelial-mesenchymal interactions regulate the stage-specific expression of a cell surface proteoglycan, syndecan, in the developing kidney*. *Dev Biol*, 1989. **134**(2): p. 382-91.
134. Folkman, J., et al., *A heparin-binding angiogenic protein--basic fibroblast growth factor--is stored within basement membrane*. *Am J Pathol*, 1988. **130**(2): p. 393-400.
135. Tkachenko, E., et al., *Fibroblast growth factor 2 endocytosis in endothelial cells proceed via syndecan-4-dependent activation of Rac1 and a Cdc42-dependent macropinocytic pathway*. *J Cell Sci*, 2004. **117**(Pt 15): p. 3189-99.

136. Sotnikov, I., et al., *Enzymatically quiescent heparanase augments T cell interactions with VCAM-1 and extracellular matrix components under versatile dynamic contexts*. J Immunol, 2004. **172**(9): p. 5185-93.
137. Roberts, A.B., *Molecular and cell biology of TGF-beta*. Miner Electrolyte Metab, 1998. **24**(2-3): p. 111-9.
138. Schulick, A.H., et al., *Overexpression of transforming growth factor beta1 in arterial endothelium causes hyperplasia, apoptosis, and cartilaginous metaplasia*. Proc Natl Acad Sci U S A, 1998. **95**(12): p. 6983-8.
139. Endo, K., et al., *Cleavage of syndecan-1 by membrane type matrix metalloproteinase-1 stimulates cell migration*. J Biol Chem, 2003. **278**(42): p. 40764-70.
140. Jiang, P., et al., *Cloning and characterization of the human heparanase-1 (HPR1) gene promoter: role of GA-binding protein and Sp1 in regulating HPR1 basal promoter activity*. J Biol Chem, 2002. **277**(11): p. 8989-98.
141. Cohen, I.R., et al., *Structural characterization of the complete human perlecan gene and its promoter*. Proc Natl Acad Sci U S A, 1993. **90**(21): p. 10404-8.
142. Hinkes, M.T., et al., *Organization and promoter activity of the mouse syndecan-1 gene*. J Biol Chem, 1993. **268**(15): p. 11440-8.
143. Tsuzuki, S., et al., *Molecular cloning, genomic organization, promoter activity, and tissue-specific expression of the mouse ryudocan gene*. J Biochem (Tokyo), 1997. **122**(1): p. 17-24.
144. Yun, S., et al., *Transcription factor Sp1 phosphorylation induced by shear stress inhibits membrane type 1-matrix metalloproteinase expression in endothelium*. J Biol Chem, 2002. **277**(38): p. 34808-14.
145. Lomberk, G. and R. Urrutia, *The family feud: turning off Sp1 by Sp1-like KLF proteins*. Biochem J, 2005. **392**(Pt 1): p. 1-11.
146. Sakata, R., et al., *Mechanical stretch induces TGF-beta synthesis in hepatic stellate cells*. Eur J Clin Invest, 2004. **34**(2): p. 129-36.
147. Ma, Y.H., S. Ling, and H.E. Ives, *Mechanical strain increases PDGF-B and PDGF beta receptor expression in vascular smooth muscle cells*. Biochem Biophys Res Commun, 1999. **265**(2): p. 606-10.
148. Lee, R.T., et al., *Mechanical strain induces specific changes in the synthesis and organization of proteoglycans by vascular smooth muscle cells*. J Biol Chem, 2001. **276**(17): p. 13847-51.

149. Cherry, D.K., Woodwell, D.A., *National Ambulatory Medical Care Survey. Advance Data*, 2002. **328**.
150. Chobanian, A.V., *The Seventh Report of the Joint National Committee on Prevention, Detecton, Evaluation and Treatment of Hypertension*. 2003, NIH.
151. Lewington, S., et al., *Age-specific relevance of usual blood pressure to vascular mortality: a meta-analysis of individual data for one million adults in 61 prospective studies*. *Lancet*, 2002. **360**(9349): p. 1903-13.
152. Ruifrok, A.C. and D.A. Johnston, *Quantification of histochemical staining by color deconvolution*. *Anal Quant Cytol Histol*, 2001. **23**(4): p. 291-9.
153. Agrotis, A., N. Kalinina, and A. Bobik, *Transforming growth factor-beta, cell signaling and cardiovascular disorders*. *Curr Vasc Pharmacol*, 2005. **3**(1): p. 55-61.
154. Hadjiisky, P., et al., *Hypertensive arteriopathy: aortic histo-metabolic changes during postnatal ontogenesis in spontaneous hypertensive rats (Okamoto-Aoki strain)*. *Pathol Biol (Paris)*, 1976. **24**(6): p. 401-12.
155. Jonas, M., et al., *Vascular neointimal formation and signaling pathway activation in response to stent injury in insulin-resistant and diabetic animals*. *Circ Res*, 2005. **97**(7): p. 725-33.
156. Marchetti, D., et al., *Heparanase and a synthetic peptide of heparan sulfate-interacting protein recognize common sites on cell surface and extracellular matrix heparan sulfate*. *J Biol Chem*, 1997. **272**(25): p. 15891-7.
157. Campbell, J.H., et al., *Heparan sulfate-degrading enzymes induce modulation of smooth muscle phenotype*. *Exp Cell Res*, 1992. **200**(1): p. 156-67.
158. Pikas, D.S., et al., *Substrate specificity of heparanases from human hepatoma and platelets*. *J Biol Chem*, 1998. **273**(30): p. 18770-7.
159. Castellot, J.J., Jr., et al., *Structural determinants of the capacity of heparin to inhibit the proliferation of vascular smooth muscle cells*. *J Cell Physiol*, 1984. **120**(3): p. 315-20.
160. Chen, G., et al., *Inflammatory cytokines and fatty acids regulate endothelial cell heparanase expression*. *Biochemistry*, 2004. **43**(17): p. 4971-7.
161. Khachigian, L.M. and C.R. Parish, *Phosphomannopentaose sulfate (PI-88): heparan sulfate mimetic with clinical potential in multiple vascular pathologies*. *Cardiovasc Drug Rev*, 2004. **22**(1): p. 1-6.

162. Edelman, E.R., D.H. Adams, and M.J. Karnovsky, *Effect of controlled adventitial heparin delivery on smooth muscle cell proliferation following endothelial injury*. Proc Natl Acad Sci U S A, 1990. **87**(10): p. 3773-7.
163. Milkiewicz, M., et al., *Nitric oxide and p38 MAP kinase mediate shear stress-dependent inhibition of MMP-2 production in microvascular endothelial cells*. J Cell Physiol, 2006. **208**(1): p. 229-37.